THEORETICAL AND EXPERIMENTAL INVESTIGATION OF THIN-WALLED STRUCTURAL ELEMENTS UNDER VARIOUS LOAD ACTIONS.

A THESIS

PRESENTED TO THE UNIVERSITY OF GLASGOW

FOR THE DEGREE OF

DOCTOR OF PHILOSOPHY

FAROUK O. FAHMY, B.Sc., A.R.T.C.

NOVEMBER, 1955.

ProQuest LLC.
789 East Eisenhower Parkway
P.O. Box 1346
Ann Arbor, MI 48106 – 1346

A C K N O W L E D G E M E N T S.

The experimental work presented in the thesis was carried out in the Laboratories of the Department of Civil and Mechanical Engineering, Royal Technical College, Glasgow.

The author wishes to record his sense of indebtedness to Professor A.S.T. Thomson, D.Sc., Ph.D., A.R.T.C., M.I.Mech.E., and R.M. Kenedi, B.Sc., Ph.D., A.R.T.C., A.M.I.Mech.E., A.F.R.Ae.S., for their continued interest and encouragement.

I N D E X.

A B S T R A C T

Thin-walled structural forms exhibit in their behaviour under compressive actions, features normally suppressed by the heavy section outlines used in hot rolled constructions. Thus, over-all instability under a combination of torsion and flexure, is obtained in a much wider range than in hot rolled sections; and local instability, i.e., buckling of the plate components (flange or web), disregarded in hot rolled construction becomes one of the chief characteristics of thin-walled behaviour. The subject-matter of the thesis deals with these two forms of instability both theoretically and experimentally.

The contents of the thesis are divided into 4 main parts, each part being further subdivided into convenient sections.

Part I presents a critical review of published work relevant to:

(i) over-all instability in torsion-flexure, and

(ii) local instability of plate components of struts in flexure.

This reveals the absence of theoretical treatment of:

(i) mixed boundary conditions in torsional-flexural buckling, e.g., a hinged end strut with warping restraint, and

(ii) the determination of the critical stress in local buckling of plates subjected to linearly varying compressive load actions, applicable to the plate components of structural sections subjected to eccentric axial loading.

There also appears to be a scarcity of experimental investigations in this latter field.

The review is followed by the theoretical analysis presented in Part II. This develops an iterative method of general application to problems of instability. The method is first applied to the derivation of the torsional-flexural buckling load for mixed boundary conditions not hitherto solved, such as the combination of hinged ends with warping restraint. The second application of the iteration method is the derivation of the local buckling strength of plates elastically supported along one longitudinal edge and free along the other. The loading for these boundary conditions, not hitherto considered in published literature, is an axial compressive action linearly varying across the width of the plate. This is applied to assess the strength in local instability of eccentrically loaded thin-walled channel sections.

The experimental work described in Part III presents the results of some 190 strut tests to destruction. These consisted of equal and unequal angle and channel specimens of 65 S.W.P. Aluminium Alloy, 3 inches to 132 inches long. The tests were designed to investigate the effects on over-all and local buckling of the variation of load eccentricity, length, section profile and method of manufacture (cold formed versus extruded).

In Part IV the results obtained are analysed and compared with the theory showing good agreement.

The textual part of the thesis concludes with a Summary which draws attention to the main features of instability conditions investigated, as indicated by the theory and confirmed by the experimental work.

The thesis concludes with a Bibliography, followed by 7 Appendices in which the details of various aspects of the work are presented.

Certain portions of the theoretical and experimental work carried out by the author, are incorporated in a paper to be published by The Institution of Engineers and Shipbuilders in Scotland, in December, 1955 (42).

NOTATION.

The following symbols are used throughout the text. Any symbol not listed is defined where it first appears.

x, y, z - Rectangular co-ordinates.

u, v - Components of displacement in x- and y- directions.

φ - Angle of twist at any section.

ω - Deflection out of the plane of a plate.

m - Number of sinusoidal half waves.

A - Cross sectional area.

L - Length of a strut.

a, b, t - Length, breadth and thickness of a plate.

b_e - Effective width of a plate.

b_1 - Width of web of a channel section.

$H = \frac{b_1}{b}$ - Dimension ratio.

$D = \frac{E t^3}{12(1-\nu^2)}$ - Flexural rigidity of a plate.

r - Coefficient of edge fixity.

x_o, y_o - Co-ordinates of the shear centre.

r_x, r_y - Principal radii of gyration.

I_x, I_y - Principal moments of inertia.

I_p - Polar moment of inertia about the shear centre axis.

$r_o^2 = x_o^2 + y_o^2 + \frac{I_x + I_y}{A}$

K - Plate constant.

K_F - Channel constant referred to the flange plate.

e_x, e_y - Eccentricities in the x- and y- directions.

E - Young's Modulus.

G - Rigidity Modulus.

ν - Poisson's Ratio.

C - Torsional rigidity.

C_1 - Warping rigidity.

N_x, N_y, N_{xy} - Intensity of forces per unit length in the middle plane of a plate.

$(N_x)_{cr.}$ - Critical value of force.

P_1, P_2 - Euler buckling loads.

P_3 - Pure torsion buckling load.

$P_{cr.}$ - Critical load.

σ - Direct stress.

$\sigma_{cr.}$ - Critical stress.

σ_1, σ_2 - Euler buckling stress.

σ_y - Yield stress.

σ_p - Proof stress.

σ_u - Ultimate stress.

C O N T E N T S.

PART III.

EXPERIMENTAL INVESTIGATION.

PART IV.

ANALYSIS AND DISCUSSION OF EXPERIMENTAL RESULTS.

PART I.

CRITICAL REVIEW OF PUBLISHED WORK.

1. OVER-ALL INSTABILITY IN TORSION AND FLEXURE

   (i) Analytical Investigations.

   (ii) Experimental Investigations.

2. LOCAL INSTABILITY OF PLATE COMPONENTS OF STRUTS IN FLEXURE.

   (i) Analytical Investigations.

   (ii) Experimental Investigations.

1. OVER-ALL INSTABILITY OF STRUTS IN TORSION AND FLEXURE.

(i) Analytical Investigations.

Struts were first observed to fail by torsion when open thin-walled sections were used in aircraft design. Some torsionally weak struts have since been observed to fail by combined torsion and flexure.

Wagner(1,2) investigates torsional buckling of open thin-walled sections and introduces the concept of "unit warping" in his analysis. This is denoted by "w" , the warping of the cross section due to unit rate of twist about the shear centre and is given by the relation

$$w = \int_0^s r_t \, ds + r_n t \qquad \text{——————} (1)$$

where r_t and r_n are the lengths of the perpendiculars from the shear centre to the tangent and the normal at any particular point on the mean outline of the section respectively.

Wagner assumes that only torques act on the member at any section along the strut, and neglects the deformation due to the variation of normal stress along the length of the strut. He gives the load for an eccentrically loaded strut as

$$P_{cr.} = \frac{1}{r_1^2}\left(C + C_1 \frac{\pi^2}{L^2}\right) \qquad \text{——————} (2)$$

where $r_1^2 = r_o^2 + e\, i_\eta$

$i_\eta = \frac{1}{I_N} \int \eta r^2 dA$

η = distance of dA from the neutral axis,

and

r = distance of dA from the shear centre axis.

Wagner points out that for a centrally loaded strut there is no connection between Eulerian buckling and twisting, the section is to be computed either for buckling (Euler) or twisting, according to which phenomenon corresponds to the smallest buckling load.

Lundquist and Fligg(3) give an exact theory for the primary failure of centrally loaded struts with cross sections symmetrical about their principal axes. They assume that both torque and bending actions are present at any section along the strut, the combined effect of which is to cause the cross section to twist about an axis, other than the shear centre axis, parallel to the strut. The general equation for a centrally loaded strut is given by

$$\sigma_{cr.} = \frac{C}{I_p} + \frac{\overline{C}_1}{I_p} \frac{\pi^2}{L^2} \qquad (3)$$

where I_p is the polar moment of inertia of the cross section about the axis of rotation, and $\overline{C}_1$ is the torsion-bending constant (i.e., warping rigidity), depending upon the location of the axis of rotation.

Lundquist and Fligg extend the use of their proposed formulae to stresses beyond the limit of proportionality by the introduction of the effective moduli $\overline{E}$ and $\overline{G}$ in the values of C and $\overline{C}_1$.

Kappus(4) presents a theory for centrally loaded struts based upon Wagner's concept of unit warping. He employs the energy method and the calculus of variations to derive the differential equations for the strain quantities. Unlike Wagner, Kappus realises the possibility of buckling by simultaneous torsion and flexure. He considers the movement of the cross sections as pure rotations about certain axes of rotation, the location of which are defined in his analysis.

The critical value of the stress $\sigma_{cr.}$ is calculated from

$$\sigma^3 - \sigma^2(\sigma_1+\sigma_2+\sigma_3) + \sigma(\sigma_1\sigma_2+\sigma_2\sigma_3+\sigma_3\sigma_1-\rho_{xy}^2-\rho_x^2-\rho_y^2) - (\sigma_1\sigma_2\sigma_3+2\rho_{xy}\rho_x\rho_y-\rho_{xy}^2\sigma_3-\rho_y^2\sigma_2-\rho_x^2\sigma_1)=0 \quad \text{——} \quad (4)$$

where $\sigma_1 = \dfrac{\pi^2 E I_y}{L^2 A}$, $\sigma_2 = \dfrac{\pi^2 E I_x}{L^2 A}$, $\sigma_3 = \dfrac{C + \frac{\pi^2}{L^2} C_1}{I_p}$

$$\rho_x = \frac{\pi^2 E R_y}{L^2\sqrt{A I_p}} \ , \ \rho_y = \frac{\pi^2 E R_x}{L^2\sqrt{A I_p}} \ , \ \rho_{xy} = \frac{\pi^2 E I_{xy}}{L^2 A^2}$$

$$R_y = \int_A x w\, dA \ , \ R_x = \int_A y w\, dA \ .$$

Goodier(5,6) extending the ideas of Wagner and using the shear centre as the origin of the system of co-ordinates, presents a simplified theory. Complications, associated with the evaluation of constants for various centres of rotation, are avoided by considering the movement of the cross sections not as pure rotation, but as a translation and rotation about the shear centre.

The critical value of the load $P_{cr.}$ for a pin ended, eccentrically loaded strut is given by

$$r_o^2\left(1-\frac{P_1}{P}\right)\left(1-\frac{P_2}{P}\right)\left(1-\frac{P_3}{P}\right)+\left(1-\frac{P_1}{P}\right)\left(1-\frac{P_2}{P}\right)\left(\frac{e_x K_1}{I_y}+\frac{e_y K_2}{I_x}\right)$$
$$-\left(1-\frac{P_1}{P}\right)\left(e_x+x_o\right)^2-\left(1-\frac{P_2}{P}\right)\left(e_y+y_o\right)^2=0 \qquad (5)$$

where $K_1=\int x\left(x^2+y^2\right)dA - x_o A r_o^2$

$$K_2=\int y\left(x^2+y^2\right)dA - y_o A r_o^2$$

He also presents an alternative solution by the energy method, in a manner similar to that followed by Kappus, and shows that the critical load is again given by equation (5).

Timoshenko(7), taking the centroid as the origin of the system of co-ordinates, presents a general theory for centrally and eccentrically loaded struts. The method is essentially similar to that of Goodier's and leads to similar results.

The critical value of the load $P_{cr.}$ for a pin ended, eccentrically loaded strut is calculated from the cubic

$$r_o^2\left(P-P_1\right)\left(P-P_2\right)\left[P\left(1+\frac{e_y\beta_1+e_x\beta_2}{r_o^2}-P_3\right)\right]$$
$$-P^2\left(y_o-e_y\right)^2\left(P-P_2\right)-P^2\left(x_o-e_x\right)^2\left(P-P_1\right)=0$$

(6)

where $P_1 = \dfrac{\pi^2 E I_y}{L^2}$, $P_2 = \dfrac{\pi^2 E I_y}{L^2}$, $P_3 = \dfrac{1}{r_o^2}\left(C + C_1 \dfrac{\pi^2}{L^2}\right)$,

$$\beta_1 = \frac{\int_A y^3 dA + \int_A x^2 y \, dA}{I_x} - 2 y_o ,$$

$$\beta_2 = \frac{\int_A x^3 dA + \int_A x y^2 dA}{I_y} - 2 x_o .$$

F. Bleich(8) presents a theory for torsional buckling based upon the differential equations of bending and twisting of struts with open thin-walled polygonal cross sections. The method of approach is the same as presented in an earlier paper by F. and H. Bleich(9). The basic differential equations are developed without using Wagner's idea of unit warp. The assumption is made that Navier's hypothesis remains valid for each of the flat plate components of the strut. The centroid of the cross section is taken as the origin of the system of co-ordinates.

For a centrally loaded strut with symmetrical cross section about the y-axis, the critical stress $\sigma_{cr.}$ is given either by

$$\left.\begin{aligned} \sigma_{cr.} &= \frac{\pi^2 E}{\left(\frac{L}{r_x}\right)^2} \\ \text{or} \quad \sigma_{cr.} &= \frac{\pi^2 E}{\left(\frac{L}{r_e}\right)^2} \end{aligned}\right\} \qquad (7)$$

whichever is the smallest.

Where r_e is an equivalent radius of gyration to be calculated from

$$\left(1 - \frac{r_y^2}{r_e^2}\right)\left(1 - \frac{r_\beta^2}{r_e^2}\right) - \frac{A y_o^2}{I_p} = 0$$

and r_β is defined by

$$r_\beta = \sqrt{\frac{C_1}{EI_p} + \frac{L^2 C.}{\pi^2 E I_p}}$$

These equations also apply in the inelastic range by introducing the tangent moduli E_r and G_r in the calculations.

In all the investigations it is assumed that the cross sections warp but that their geometric shape does not change during buckling.

(ii) Experimental Investigations.

Wagner(2) conducted tests on thin-walled aluminium alloy struts to check his theoretical analysis of buckling due to twist. The struts were loaded both centrally and eccentrically, and were of plain and lipped angle section. There is quite close agreement between his experimental and theoretical results. Discrepances in the short strut results are attributed to the inaccuracy in calculating C_1. It can be proved that

$$C_1 = C_{1_u} + C_{1_n}$$

The constant C_{1_u} relates to the direct strain in the middle plane of the walls (arising from variation of warping of the cross section along the length, due to non-linear rate of twist about the shear centre). The constant C_{1_n} relates to the direct strain across the thickness of the

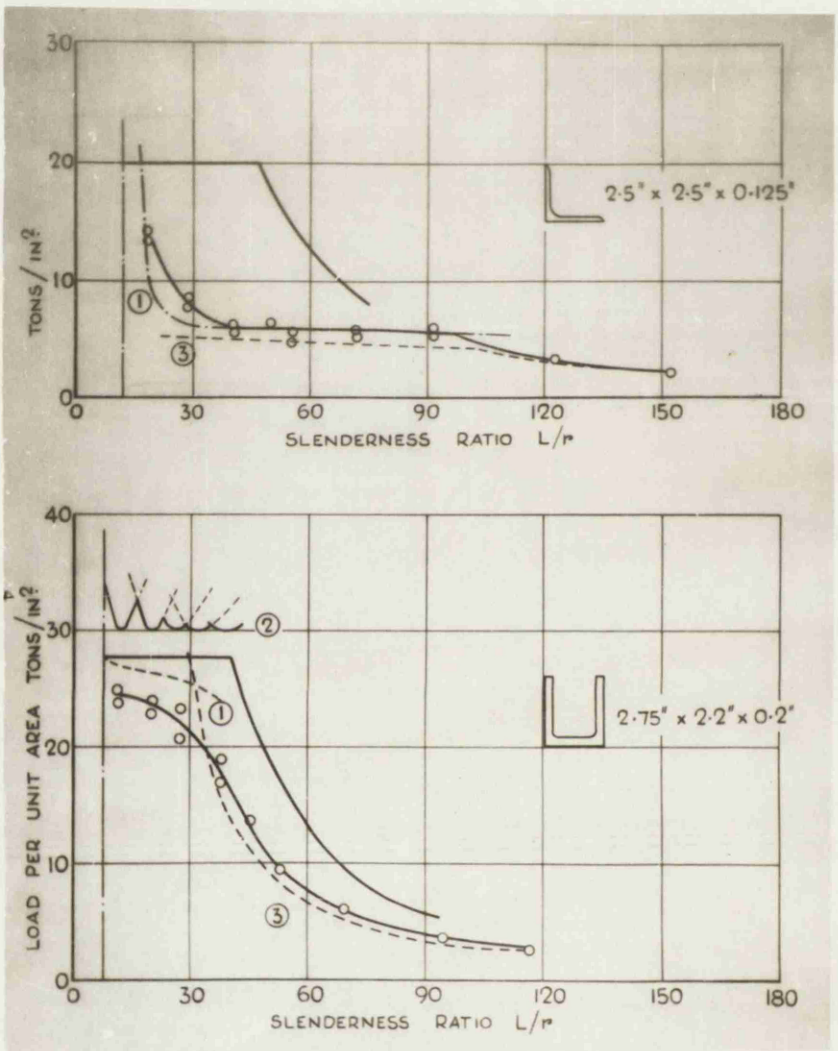
30
20
10
0
TONS/IN.²
0
30
60
90
120
150
180
SLENDERNESS RATIO L/r
2·5" x 2·5" x 0·125"
①
③
40
30
20
10
0
LOAD PER UNIT AREA TONS/IN.²
②
①
③
2·75" x 2·2" x 0·2"
SLENDERNESS RATIO L/r

FIG. 1.

walls (arising from variation of curvature of the walls along the length, due to non-linear rate of twist about the shear centre). As C_{1_n} is generally very small compared to C_{1_u}, Wagner neglects the value of C_{1_n} in calculating C_1. This approximation cannot be justified in cases such as angles for which C_{1_u} vanishes. Discrepancies are also caused by the unavoidable lateral deflections, especially in the eccentrically loaded struts, and the subsequent variable stress distribution over the length of the strut.

Baker and Roderick(10) carried out a comprehensive series of centrally loaded strut tests. The struts were made of various aluminium alloys and included angle, channel, T and I sections. The experimental failure stresses are presented in graphical form with theoretical values for convenient comparison, e.g., Figure 1. The theoretical curves represent:

(i) A modified form of the Perry formula,

(ii) Local buckling of outstanding plate components,

(iii) Torsional flexual buckling based on the general theory presented by Timoshenko(7).

The absence of a formula that takes into account restriction of warping at the ends is noted. Until this more accurate solution is available they suggest taking

$$P_1 = \frac{\pi^2 E I_y}{L^2} \quad , \quad P_2 = \frac{\pi^2 E I_x}{L^2} \quad ,$$

and assuming that the critical load for purely torsional buckling has the same value as for a strut with built in ends, i.e.,

$$P_3 = \frac{1}{r_o^2}\left(C + C_1 \frac{4\pi^2}{L^2}\right).$$

Satisfactory correspondence is shown when using these values in the general equation for buckling in torsion and flexure.

The values of critical loads given by the general theory are satisfactory for the higher values of slenderness ratio. For the lower values, where the breakdown of the material controls, no satisfactory solution is available.

Niles(11) carried out a series of tests to obtain an experimental verification of the theoretical formulae for torsional failure developed by Lundquist and his associates. The observed critical loads and twist-axis locations are sufficiently close to the values obtained by the formulae to establish the validity of the latter.

2. LOCAL INSTABILITY OF PLATE COMPONENTS OF STRUTS IN FLEXURE.

(i) Analytical Investigations.

The numerous investigations in this field are generally based on one of the two following methods of analysis:-

(a) Differential equation method.

The differential equation, Timoshenko(14), for the deflected surface of a plate with forces applied in the middle plane is

$$\frac{\partial^4\omega}{\partial x^4} + 2\frac{\partial^4\omega}{\partial x^2\partial y^2} + \frac{\partial^4\omega}{\partial y^4} = \frac{1}{D}\left(N_x\frac{\partial^2\omega}{\partial x^2} + N_y\frac{\partial^2\omega}{\partial y^2} + 2N_{xy}\frac{\partial^2\omega}{\partial x\partial y}\right) \qquad (8)$$

The plate is assumed to buckle slightly under the action of the applied forces. The magnitudes of the forces necessary to maintain this buckled shape are the required critical values.

(b) Energy method.

This method is useful in cases where a rigorous solution of equation (8) is unknown and only approximate values of the critical forces are required. Equating the energy of bending and twisting to the corresponding work done by the forces acting in the middle plane of the strut, Timoshenko(14), gives

$$\frac{1}{2}\iint\left[N_x\left(\frac{\partial\omega}{\partial x}\right)^2 + N_y\left(\frac{\partial\omega}{\partial y}\right)^2 + 2N_{xy}\frac{\partial\omega}{\partial x}\frac{\partial\omega}{\partial y}\right]dx\,dy$$
$$= \frac{D}{2}\iint\left\{\left(\frac{\partial^2\omega}{\partial x^2} + \frac{\partial^2\omega}{\partial y^2}\right)^2 - 2(1-\nu)\left[\frac{\partial^2\omega}{\partial x^2}\frac{\partial^2\omega}{\partial y^2} - \left(\frac{\partial^2\omega}{\partial x\partial y}\right)^2\right]\right\}dx\,dy \qquad (9)$$

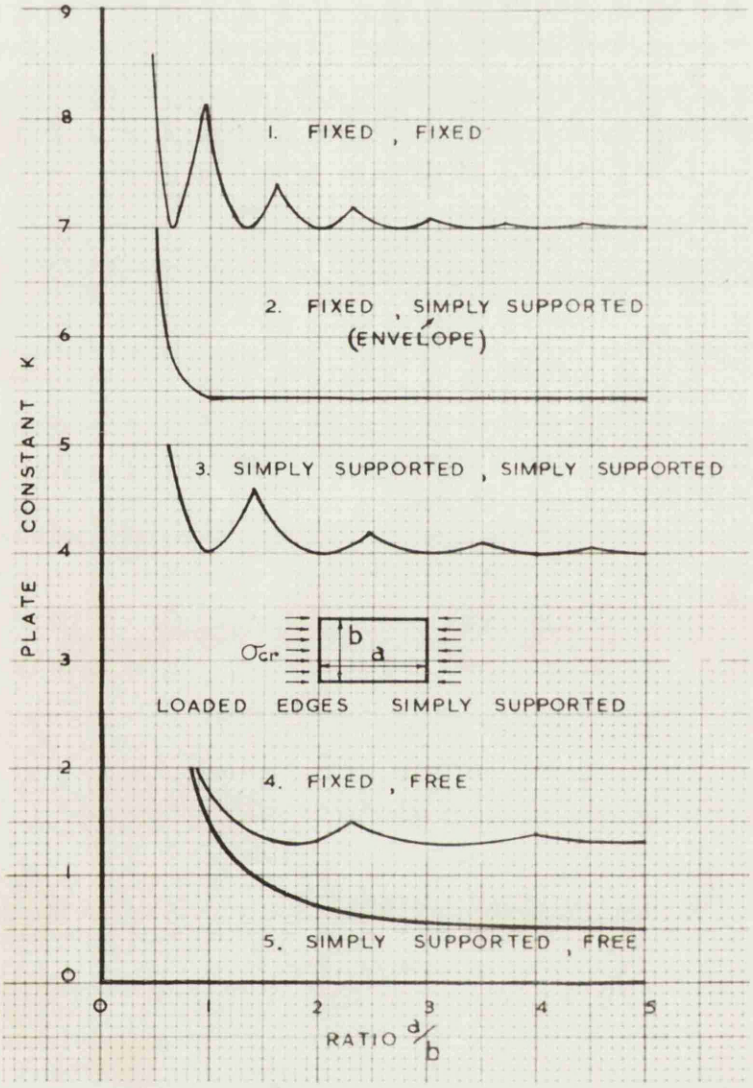
PLATE CONSTANT K
9
8
7
6
5
4
3
2
1
0
1. FIXED , FIXED
2. FIXED , SIMPLY SUPPORTED
(ENVELOPE)
3. SIMPLY SUPPORTED , SIMPLY SUPPORTED
σ_{cr}
b
a
LOADED EDGES SIMPLY SUPPORTED
4. FIXED , FREE
5. SIMPLY SUPPORTED , FREE
0
1
2
3
4
5
RATIO a/b

FIG. 2.

If the work done by the forces is smaller than the strain energy of bending and twisting for every possible shape of lateral buckling, the flat form of equilibrium of the plate is stable. If the same work done becomes larger than the energy of bending and twisting for any shape of lateral deflection, the plate is unstable and buckling occurs.

A development of the energy method, called the Lagrangian multiplier method, Budiansky and Pai(15,16), makes use of functions of ω which approximately satisfy the boundary conditions, to give conservative results.

In the following a summary covering a representative selection of contributions is presented.

Generally the buckling stress of a plate under compression can be represented, Timoshenko(14), in the form

$$\sigma_{cr.} = K \frac{\pi^2 E}{12(1-\nu^2)} \left(\frac{t}{b}\right)^2 \qquad (10)$$

where K is a numerical factor depending on the edge conditions and the length to breadth ratio of the plate.

Values of the plate constant K, for various edge support conditions, have been calculated for plates uniformly loaded along two opposite edges. In all cases the loaded edges were assumed to be simply supported.

Values of K (17 to 20), for free, simply supported and fixed edge conditions are shown in Figure 2. In most practical cases intermediate

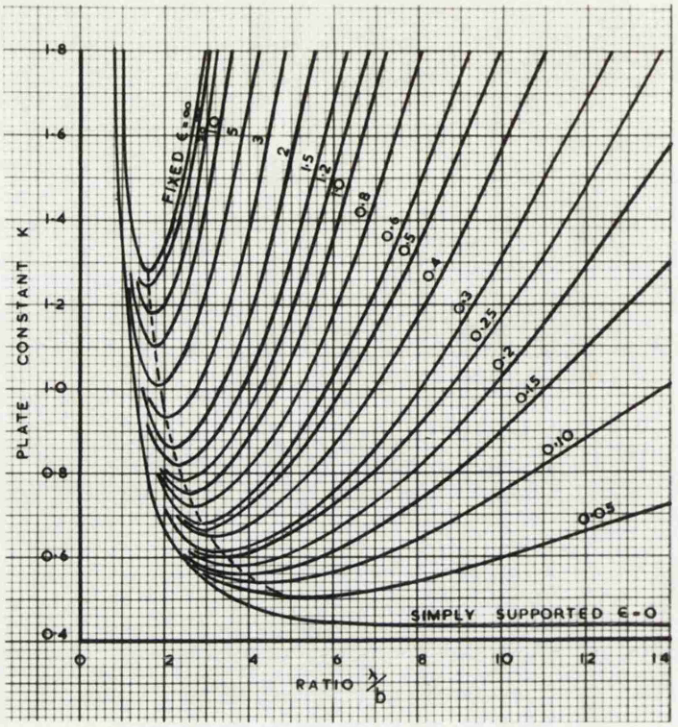
PLATE CONSTANT K
1·8
1·6
1·4
1·2
1·0
0·8
0·6
0·4
FIXED ε = ∞
100
50
30
20
15
12
10
8
5
3
2
1·5
1·2
1·0
0·8
0·6
0·5
0·4
0·3
0·25
0·2
0·15
0·10
0·05
SIMPLY SUPPORTED ε = 0
0
2
4
6
8
10
12
14
RATIO λ/b

FIG. 3.

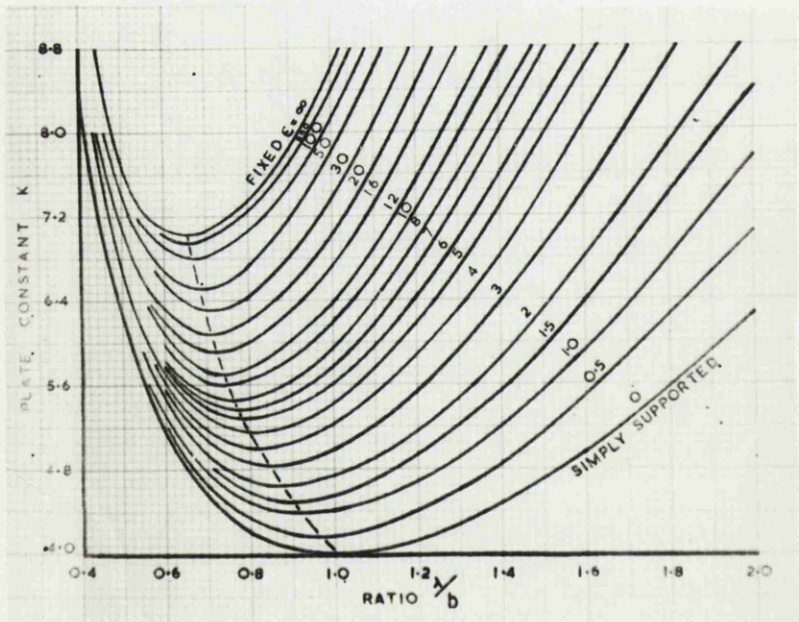
PLATE CONSTANT K
8·8
8·0
7·2
6·4
5·6
4·8
4·0
FIXED ε = ∞
100
50
30
20
16
12
10
8
7
6
5
4
3
2
1·5
1·0
0·5
0
SIMPLY SUPPORTED
0·4
0·6
0·8
1·0
1·2
1·4
1·6
1·8
2·0
RATIO λ/b

FIG 4.

degrees of elastic restraint against rotation exist along the unloaded edges. Values of K for a longitudinally compressed plate with one unloaded edge free and the other elastically restrained are given in Figure 3. The plate constant values for both unloaded edges elastically restrained against rotation are given in Figure 4. The values of K in Figures 3 and 4, Kroll(22), are given as functions of ϵ and λ, where ϵ is defined by

$$\epsilon = \frac{4 S_o}{D/b}$$

in which S_o is the stiffness of the elastic restraining medium assumed constant along the plate, and λ is the buckled half wave. For a given plate and a given restraining medium the minimum value of K is obtained by trial and error computations of mutually consistent ϵ and λ values.

The form of the critical stress can be extended to cover the case of an assembly of plates, i.e., a structural section, by evaluating the constant K appropriate to any particular section form. A representative selection of the numerous contributions in the field follows.

Tables prepared by Kroll(21) cam be used to evaluate the stiffness of elastic restraint provided between plate components of built up sections. The charts of figures 3 and 4 (22) can be applied if S_o the stiffness of the elastic edge restraint is constant along the edge. This necessitates the application of simusoidally varying moment along the straining medium.

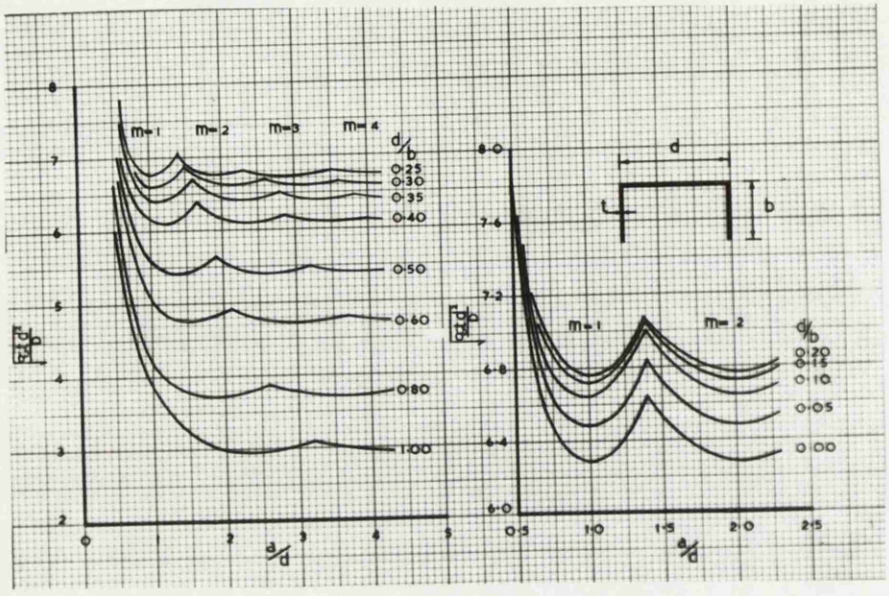
m=1
m=2
m=3
m=4
d/b
0·25
0·30
0·35
0·40
0·50
0·60
0·80
1·00
a/d
d
b
m=1
m=2
d/b
0·20
0·15
0·10
0·05
0·00

FIG. 5.

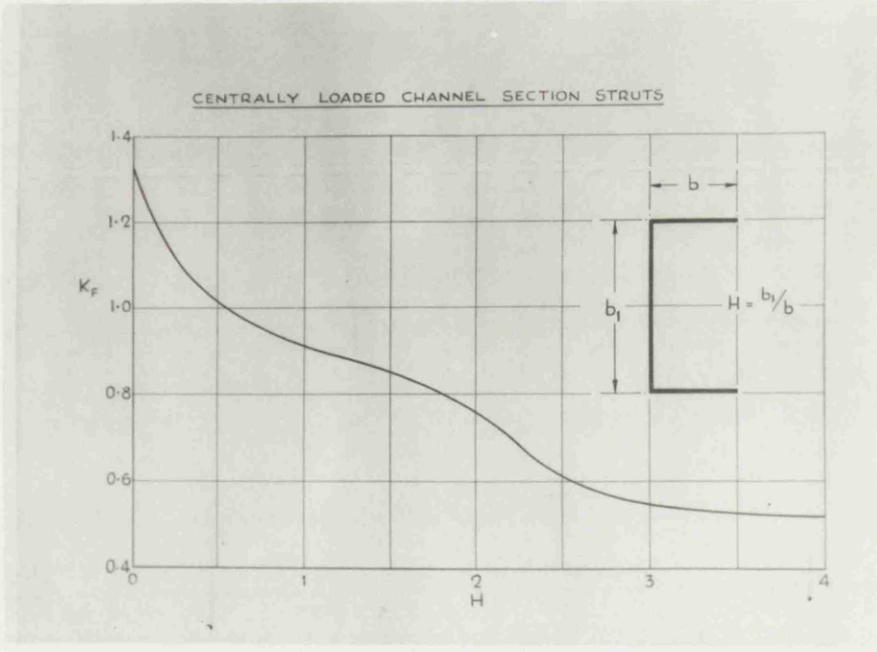
CENTRALLY LOADED CHANNEL SECTION STRUTS
K_F
H
b
b_1
$H = b_1/b$

FIG. 6.

Lundquist and Stowell(23) give a solution for the case of a plate supported by a "Sturdy Stiffener".

Chilver(24) gives a more direct solution for the case of a plain channel section. The buckling stress values obtained are shown in Figure 5.

Harvey(25) gives a complete analysis for the case of centrally loaded plain and lipped channel section struts. The values of K given in Figure 6 are based on the flange dimensions. The critical stress is given by

$$\sigma_{cr.} = K_F \frac{\pi^2 E}{12(1-\nu^2)} \left(\frac{t}{b}\right)^2 \qquad (11)$$

Davidson(26) gives buckling loads for a flat infinitely long elastic plate compressed in its own plane by thrusts which act parallel to the two opposite edges, and which vary linearly between them. One of these edges is assumed free, and the other fixed in position but elastically clamped. The method is applied to the case of an I-section under pure bending. The elastic support provided by the web is estimated from tables given by Kroll(21).

A plate after buckling may, in some cases, carry without failure a load many times larger than the critical load at which buckling begins. For reasons of safety and economy it is important to consider not only the critical load but also the ultimate load that a plate may carry before complete collapse.

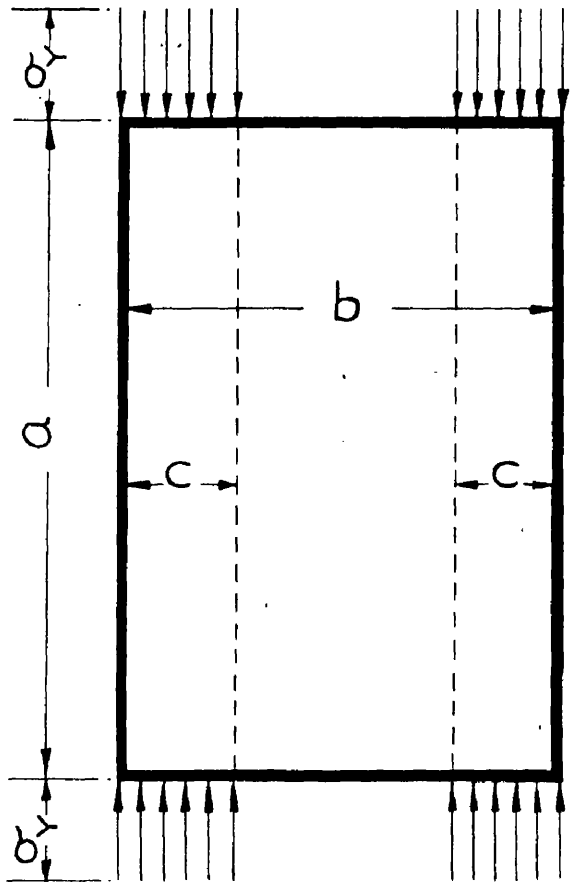

FIG. 7.

Stowell(27) presents an exact theory to calculate the ultimate load for the case of a plate with simply supported and free edge conditions. The theory takes into account large deflections and the inelastic behaviour of the material.

Kármán(28) gives an approximate solution for the case of a compressed rectangular plate with simply supported edges. It is assumed that the load transmitted to the plate is carried by two strips of width C, one on each side of the sheet, and that the load distribution is uniform across these strips, Figure 7. The ultimate load is then reached when the uniform stress in the edge strips becomes equal to the yield stress σ_y of the material. More recent investigations were carried out by Marguerre(29) and Levy(30), again assuming that the ultimate load is reached when the stress in the edge strips becomes equal to the yield stress and in addition assuming that the stress in the central strip remains equal to the buckling value.

Harvey(25), applying Kármán's assumption, gives the equivalent flange width of a centrally loaded channel strut as

$$b_e = \frac{\pi t \sqrt{K_F E}}{\sqrt{\sigma_y 12(1-\nu^2)}}$$

and the ultimate stress referred to the actual proportions of the flange by

$$\sigma_u = \frac{\pi t \sqrt{K_F E \sigma_y}}{b\sqrt{12(1-\nu^2)}} \qquad (12)$$

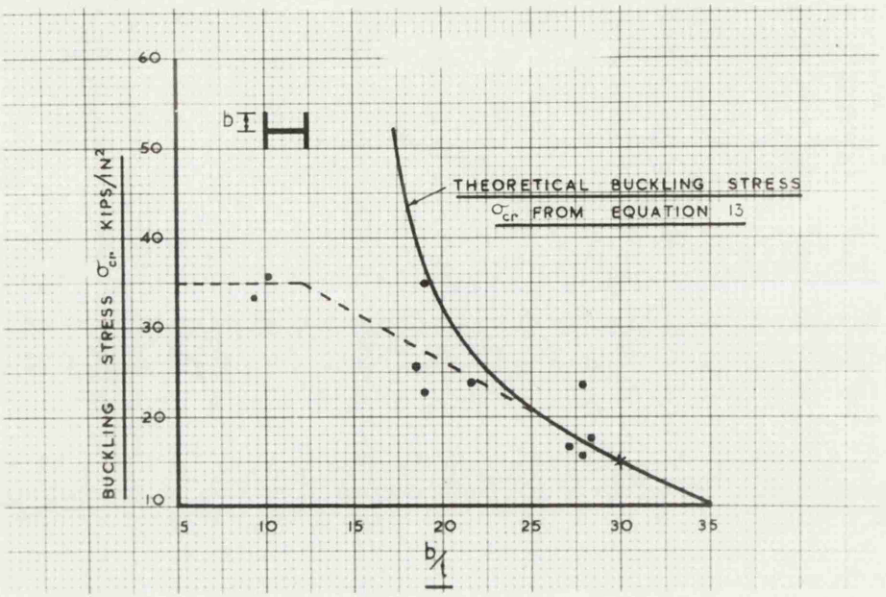
BUCKLING STRESS σ_{cr} KIPS/IN^2
60
50
40
30
20
10
5
10
15
20
25
30
35
b/t
b
t
THEORETICAL BUCKLING STRESS
σ_{cr} FROM EQUATION 13

FIG. 8

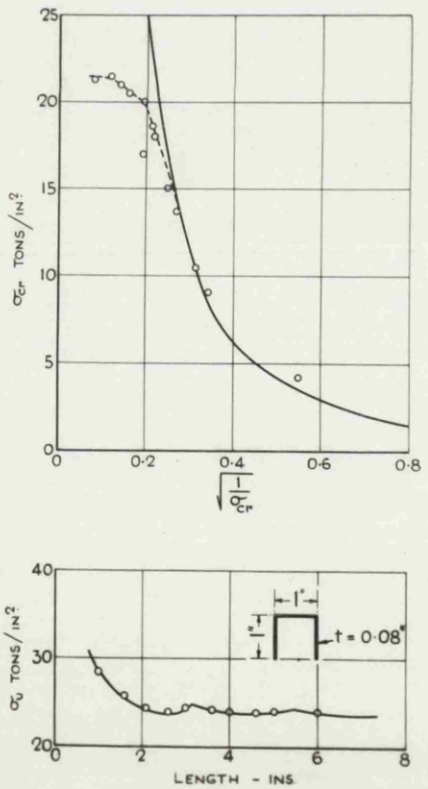
σ_{cr} TONS/IN.^{2}
25
20
15
10
5
0
0·2
0·4
0·6
0·8
$\sqrt{\frac{1}{\sigma_{cr}}}$
σ_u TONS/IN.^{2}
40
30
20
0
2
4
6
8
LENGTH - INS.
1"
1"
t = 0·08"

FIG. 9.

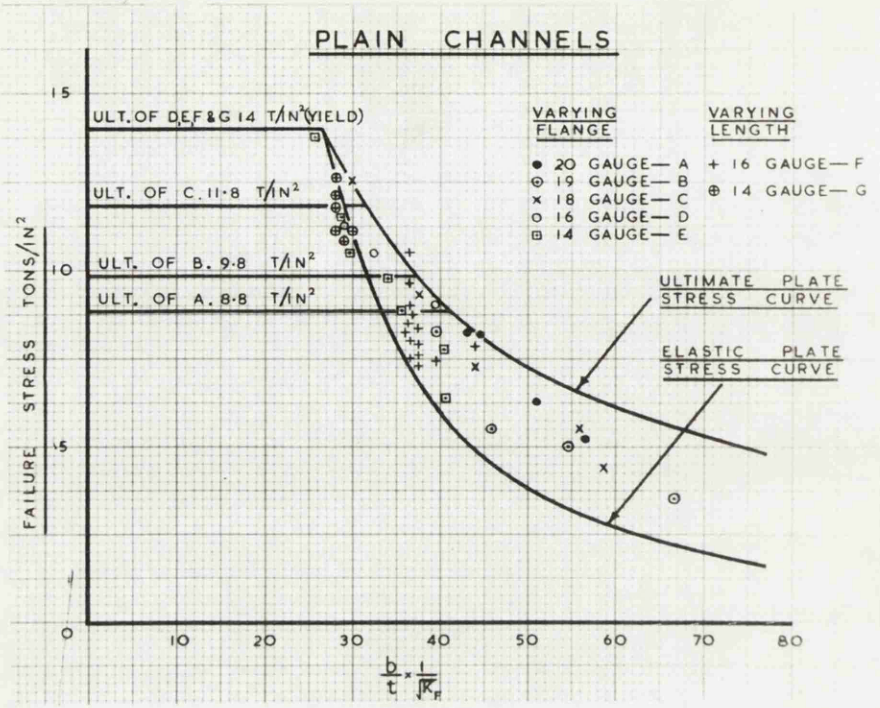
PLAIN CHANNELS
ULT. OF D,E,F & G 14 T/IN² (YIELD)
ULT. OF C. 11·8 T/IN²
ULT. OF B. 9·8 T/IN²
ULT. OF A. 8·8 T/IN²
VARYING FLANGE
● 20 GAUGE— A
⊙ 19 GAUGE— B
× 18 GAUGE— C
○ 16 GAUGE— D
⊡ 14 GAUGE— E
VARYING LENGTH
+ 16 GAUGE— F
⊕ 14 GAUGE— G
ULTIMATE PLATE STRESS CURVE
ELASTIC PLATE STRESS CURVE
FAILURE STRESS TONS/IN²
15
10
5
0
10
20
30
40
50
60
70
80
b/t × 1/√K_F

FIG. 10.

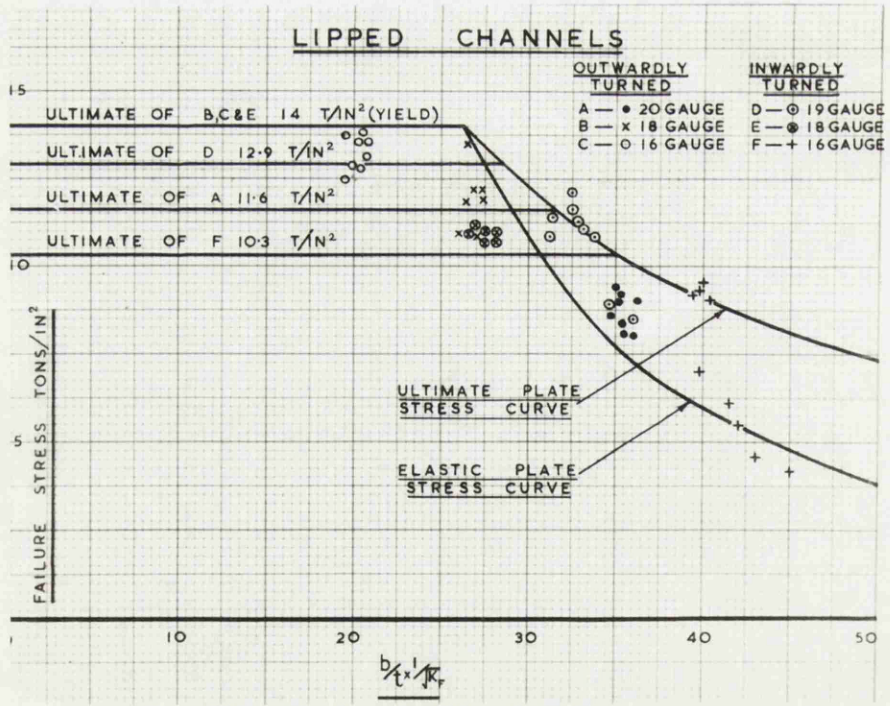
LIPPED CHANNELS
OUTWARDLY TURNED
A — ● 20 GAUGE
B — × 18 GAUGE
C — ○ 16 GAUGE
INWARDLY TURNED
D — ⊙ 19 GAUGE
E — ⊗ 18 GAUGE
F — + 16 GAUGE
ULTIMATE OF B,C & E 14 T/IN² (YIELD)
ULTIMATE OF D 12·9 T/IN²
ULTIMATE OF A 11·6 T/IN²
ULTIMATE OF F 10·3 T/IN²
ULTIMATE PLATE STRESS CURVE
ELASTIC PLATE STRESS CURVE
FAILURE STRESS TONS/IN²
15
10
5
10
20
30
40
50
b/t × 1/√K_F

FIG. 11

(ii) Experimental Investigations.

Winter(31) obtained the local buckling stresses from tests on a series of I-section struts. These together with the theoretical buckling stresses by the formula

$$\sigma_{cr.} = 0.5 \frac{\pi^2 E}{12\left(1-\nu^2\right)} \left(\frac{t}{b}\right)^2 \qquad (13)$$

are shown in Figure 8. Winter suggests an empirical curve shown dotted on the graph.

Chilver(24) tested cold-formed steel channels under concentric load. Some experimental results are compared with the theoretical stresses in Figure 9. There is a deviation from the elastic line in the high stress region where the sections are most prone to yielding of the material. The collapse loads for a number of struts all having the same cross sectional forms but of different lengths are shown in Figure 9. When the lengths of the sections are sufficient to develop more than one half wave the collapse loads are not appreciably effected by changes in length.

Harvey(25) carried out tests on plain and lipped steel channel struts. The experimental results are shown in Figures 10 and 11. The theoretical elastic and ultimate stress curves compare reasonably well with the experimental values.

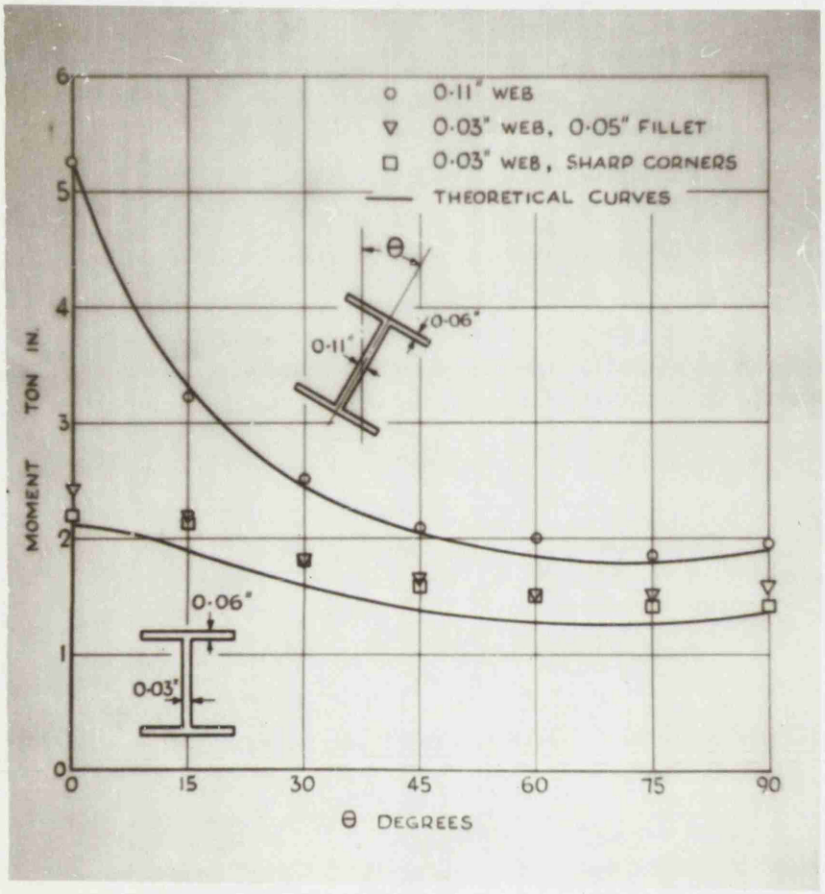
0·11" WEB
0·03" WEB, 0·05" FILLET
0·03" WEB, SHARP CORNERS
THEORETICAL CURVES
θ
0·06"
0·11"
0·06"
0·03"
MOMENT TON IN.
θ DEGREES
0
15
30
45
60
75
90
1
2
3
4
5
6

FIG. 12.

Davidson(26) describes tests carried out on I-section beams under pure bending. The theoretical and experimental results are shown in Figure 12. The theoretical buckling bending moments are obtained from tables prepared by Kroll(21). The experimental buckling moments are assessed by the Southwell plot method(32). The reason for the rather large differences between theory and experiment is attributed to the inaccuracy of the Southwell plot method. The results confirm the predictions of Pai, Lundquist and Batdorf(33), and Cox(34) in giving experimental critical values above the theoretical.

PART II.

THEORETICAL INVESTIGATION.

1. DEVELOPMENT OF THE ITERATIVE METHOD.

2. THE ITERATIVE METHOD APPLIED TO OVER-ALL INSTABILITY.

   (i) Concentrically Loaded Struts.

   (ii) Eccentrically Loaded Struts.

3. FLANGE PLATE INSTABILITY OF THIN-WALLED CHANNEL SECTIONS UNDER COMBINED BENDING AND COMPRESSION.

1. DEVELOPMENT OF THE ITERATIVE METHOD.

In the field of structural stability a number of cases obtain where due to certain combinations of boundary conditions or load distributions, rather more complex than usual, neither the equation method nor the energy method are capable of direct solution by classical means. In the following the principle of an iterative method is presented which has proved to be of general applicability both in the computation of over-all and local instability conditions. The method is generally that of assuming a form for the governing function satisfying the "important" boundary conditions. This converts the basic equation into a directly integreable form. The integration is then carried out yielding a new corrected form for the governing function as a second approximation. The process is then repeated and continued until the required degree of accuracy is achieved.

As an illustration, giving a comparison with the rigorously derived values, the case of a flat plate uniformly compressed in a longitudinal direction is presented.

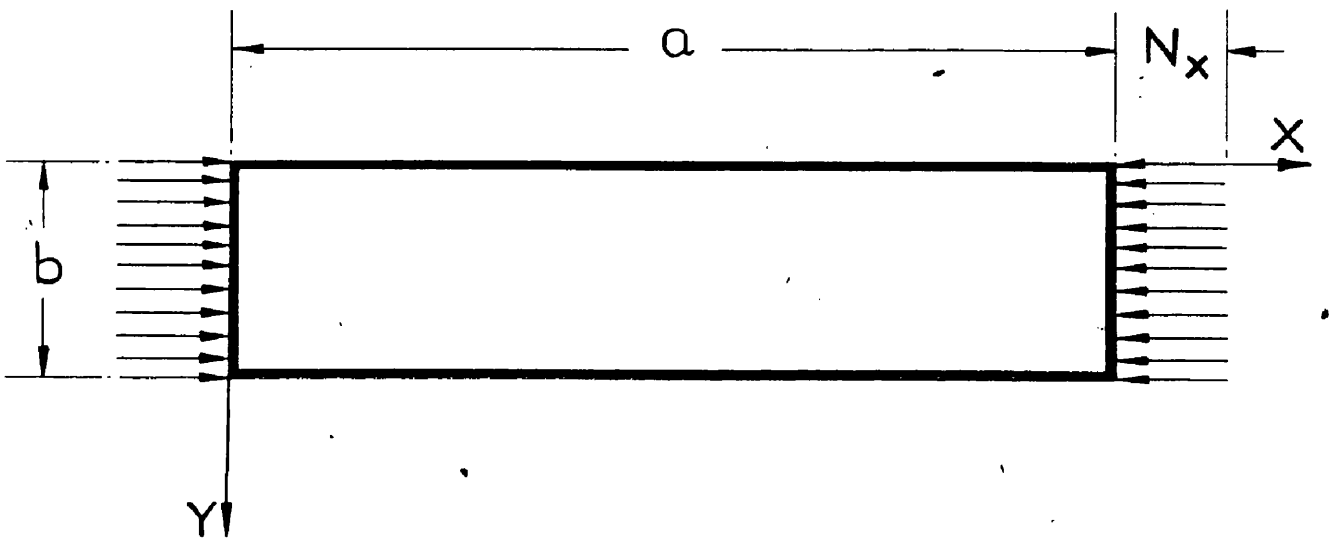

FIG. 13.

Buckling of Uniformly Compressed Rectangular Plates

The rectangular plate shown in Figure 13 is simply supported along the edges $x = o$ and $x = a$, elastically built in along the edge $y = o$ and free along the edge $y = b$. The plate is subjected to a uniform compressive force per unit length of magnitude N_x. The differential equation for the deflected form of a longitudinally compressed plate, with N_x positive for compression, is given by Timoshenko(14) as

$$\frac{\partial^4 \omega}{\partial x^4} + 2\frac{\partial^4 \omega}{\partial x^2 \partial y^2} + \frac{\partial^4 \omega}{\partial y^4} = -\frac{N_x}{D}\frac{\partial^2 \omega}{\partial x^2} \qquad (14)$$

The boundary conditions to be satisfied are

$$\left.\begin{aligned} \omega &= o \\ \frac{\partial^2 \omega}{\partial x^2} + \nu\frac{\partial^2 \omega}{\partial y^2} &= o \end{aligned}\right\} \text{for } x = o \text{ and } x = a \qquad (15)$$

$$\left.\begin{aligned} \omega &= o \\ \frac{\partial^2 \omega}{\partial y^2} - r\frac{\partial \omega}{\partial y} &= o \end{aligned}\right\} \text{for } y = o \qquad (16)$$

$$\left.\begin{aligned} \frac{\partial^2 \omega}{\partial y^2} + \nu\frac{\partial^2 \omega}{\partial x^2} &= o \\ \frac{\partial^3 \omega}{\partial y^3} + (2-\nu)\frac{\partial^3 \omega}{\partial x^2 \partial y} &= o \end{aligned}\right\} \text{for } y = b \qquad (17)$$

where r is the coefficient of edge fixity, Timoshenko(14).

The conditions at $x = 0$ and $x = a$ are satisfied by assuming that the plate buckles in m sinusoidal half waves, i.e., the solution of equation (14) can be written in the form

$$\omega = Y \sin \frac{m\pi x}{a} \qquad (18)$$

in which Y is a function of y only.

Substituting this in equation (14) gives

$$\frac{d^4Y}{dy^4} = \frac{2m^2\pi^2}{a^2}\frac{d^2Y}{dy^2} - \left(\frac{m^4\pi^4}{a^4} - \frac{m^2\pi^2}{a^2}\frac{N_x}{D}\right)Y$$

$$= A\frac{d^2Y}{dy^2} - BY \qquad (19)$$

where $A = \dfrac{2m^2\pi^2}{a^2}$

and $B = \left(\dfrac{m^4\pi^4}{a^4} - \dfrac{m^2\pi^2}{a^2}\dfrac{N_x}{D}\right)$

The appropriate boundary conditions in terms of Y and for $\nu = 0.25$, relevant to equation (19) are now

$$\left.\begin{aligned} Y &= 0 \\ \frac{d^2Y}{dy^2} - r\frac{dY}{dy} &= 0 \end{aligned}\right\} \text{ for } \quad y = 0 \qquad (20)$$

$$\left.\begin{aligned} \frac{d^2Y}{dy^2} - 2.467\ \frac{m^2}{a^2}\ Y &= 0 \\ \frac{d^3Y}{dy^3} - 17.27\ \frac{m^2}{a^2}\ \frac{dY}{dy} &= 0 \end{aligned}\right\} \text{for} \quad y = b \qquad (21)$$

For comparatively short plates the smallest value of N_x is obtained by taking $m=1$, i.e., by assuming that the plate buckles in one half wave in the direction of compression. The magnitude of the corresponding critical compressive load can be represented by the formula

$$(N_x)_{cr.} = K\frac{\pi^2 D}{b^2} \qquad (22)$$

in which K is a numerical factor depending on the magnitude of the ratio $\frac{a}{b}$ and the coefficient of fixity r.

Equation (19) is solved by the iterative method as follows.

The first approximation to the deflected form of the plate in the y - direction is assumed to be given by

$$Y_1 = \Omega\left(\frac{b^2y^2}{4} - \frac{by^3}{6} + \frac{y^3}{24} + \frac{b^3y}{2rb}\right) \qquad (23)$$

where Ω is a constant.

Substituting in the right hand side of equation (19) gives

$$\frac{d^4Y_2}{dy^4} = A\Omega\left(\frac{b^2}{2} - by + \frac{y^2}{2}\right) + B\Omega\left(-\frac{b^2y^2}{4} + \frac{by^3}{6} - \frac{y^4}{24} - \frac{b^3y}{2rb}\right) \qquad (24)$$

where Y_2 is the second approximation.

Successive integration of this equation leads to

$$Y_2 = A\Omega\left(\frac{b^2y^4}{48} - \frac{by^2}{120} + \frac{y^6}{720}\right) + B\Omega\left(-\frac{b^2y^6}{1440} + \frac{by^7}{5040} - \frac{y^8}{40320} - \frac{b^3y^5}{240rb}\right) + R\frac{y^3}{6} + S\frac{y^2}{2} + Ty + V \qquad (25)$$

where R, S, T and V are integration constants.

Using this form Y and the appropriate boundary conditions (20) and (21), the following equations for the four integration constants are obtained.

$$V = 0 \qquad (26)$$

$$T = \frac{S}{r} \qquad (27)$$

$$A\Omega\left(0.125\,b^4 - 0.03426\,\frac{b^6}{a^2}\right) + B\Omega\left(-0.01389\,b^6 + 0.001284\,\frac{b^8}{a^2} - 0.08333\,\frac{b^6}{rb} + 0.01028\,\frac{b^8}{a^2rb}\right) + R\left(b - 0.411\,\frac{b^3}{a^2}\right) + S\left(1 - 1.234\,\frac{b^2}{a^2} - 2.467\,\frac{b^2}{a^2rb}\right) = 0 \qquad (28)$$

$$A\Omega\left(0.1667\, b^3 - 0.8635\,\frac{b^5}{a^2}\right)$$
$$+B\Omega\left(-0.05\, b^5 + 0.0514\,\frac{b^7}{a^2} - 0.25\,\frac{b^5}{rb} + 0.3598\,\frac{b^7}{a^2 rb}\right)$$
$$+R\left(1 - 8.635\,\frac{b^2}{a^2}\right)$$
$$-17.27\, S\left(\frac{b}{a^2} + \frac{b}{a^2 rb}\right) = 0 \qquad \text{——————} (29)$$

Due to the bulkiness of symbolic computation it is convenient to evaluate the constants of integration for particular numerical cases.

For example, for the case of $rb=2$ and $\frac{a}{b}=1$, the constants of integration are

$$R = -0.1275\, A\Omega\, b^3 + 0.05121\, B\Omega\, b^5$$
$$S = 0.01069\, A\Omega\, b^4 - 0.01291\, B\Omega\, b^6$$
$$T = 0.005345\, A\Omega\, b^5 - 0.006455\, B\Omega\, b^7$$
$$V = 0$$

For the boundary conditions given the maximum deflection occurs at $y=b$. This gives

$$(Y_1)_{max.} = 0.375\,\Omega\, b^4 \qquad \text{——————} (30)$$

$$(Y_2)_{max.} = 0.003326\, A\Omega\, b^6 - 0.006979\, B\Omega\, b^6 \qquad \text{——————} (31)$$

TABLE 1.

$\frac{a}{b}$	1	1·5	1·8	2	2·3	2·5	2·7	3
$rb = 2$								
ITERATIVE	1·455	0·98		0·87		0·886		0·97
TIMOSHENKO	1·49	1·01		0·90		0·90		0·98
$rb = 8$								
ITERATIVE	1·563	1·143	1·097		1·167		1·296	
TIMOSHENKO	1·58	1·16	1·11		1·18		1·30	

after substituting the constants just calculated.

The first approximation to the critical load is obtained by equating $(Y_1)_{max.}$ to $(Y_2)_{max.}$. In the case quoted this reduces to

$$0.375 = 0.003326\, A b^2 - 0.000679\, B b^2 \qquad (32)$$

Noting that

$$A = \frac{2 m^2 \pi^2}{a^2}$$

and $$B = \left(\frac{m^4 \pi^4}{a^4} - K \frac{\pi^2}{b^2} \frac{m^2 \pi^2}{a^2} \right)$$

where $$(N_x)_{cr.} = K \frac{\pi^2 D}{b^2} \qquad (22)$$

Equation (32) finally gives

$$1 = 0.175 - 1.812 + 1.812\, K$$

hence $$K = 1.455$$

Similar calculations were made for $rb=2$ and $rb=8$ with several values of $\frac{a}{b}$. Values of K calculated by the iterative method and the corresponding values given by Timoshenko(14), using the classical equation method are given in Table 1.

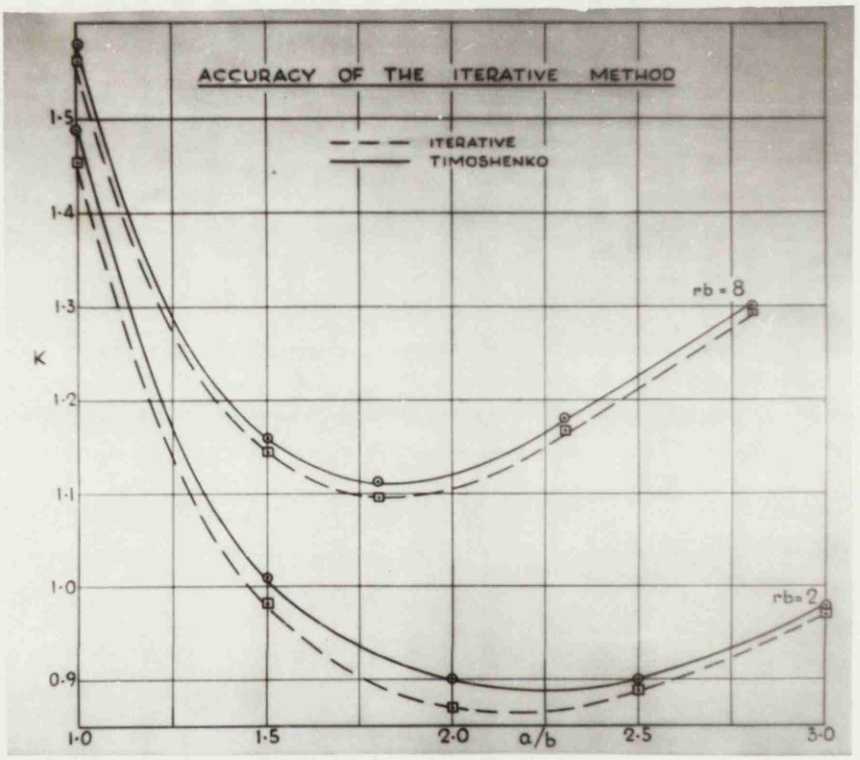
ACCURACY OF THE ITERATIVE METHOD
ITERATIVE
TIMOSHENKO
rb = 8
rb = 2
K
1·5
1·4
1·3
1·2
1·1
1·0
0·9
1·0
1·5
2·0
a/b
2·5
3·0

FIG. 14.

For a clearer comparison a graphical presentation of results is given in Figure 14. A maximum difference of 3·3% in the values of K, on the safe side, for $rb=2$ and $\frac{a}{b}=2$ is well within required engineering accuracy. Further correction by a second approximation is unnecessary.

It remains to be noted that the closer the assumed deflection form is to the actual case, the more accurate will be the results obtained. The ideal solution is that which requires one approximation to give the required degree of accuracy. A short critical discussion as regards the choice of a deflected form appropriate to the problem considered is given in Appendix 1, from which it is concluded that the accuracy of the iterative method as applied is governed by the accuracy of estimating the position of maximum deflection, rather than by choosing a particular deflected form.

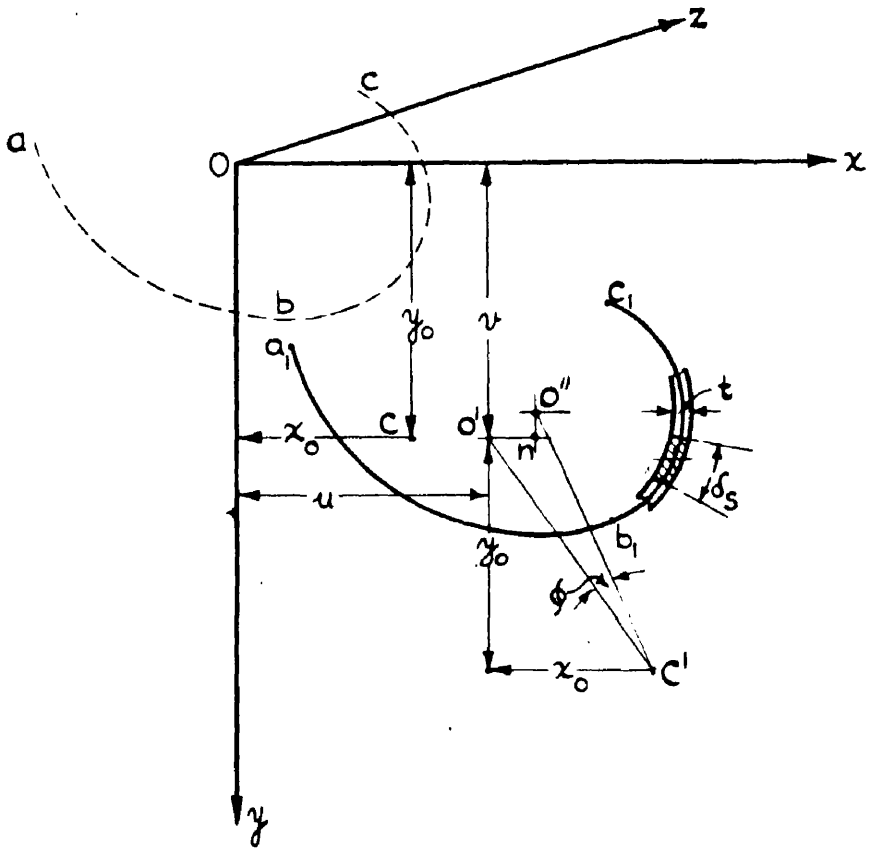

FIG. 15.

2. THE ITERATIVE METHOD APPLIED TO OVER-ALL INSTABILITY.

(i) Concentrically Loaded Struts.

The equations governing the behaviour of a concentrically loaded strut subjected to lateral deflection and cross-section rotation, Figure 15, are given by Timoshenko(7) as

$$E I_y \frac{d^2 u}{dz^2} = -P\left(u + y_o \varphi\right) \qquad (33)$$

$$E I_x \frac{d^2 v}{dz^2} = -P\left(v - x_o \varphi\right) \qquad (34)$$

$$C_1 \frac{d^4 \varphi}{dz^4} = \left(C - r_o^2 P\right)\frac{d^2 \varphi}{dz^2} + P\left(x_o \frac{d^2 v}{dz^2} - y_o \frac{d^2 u}{dz^2}\right) \qquad (35)$$

Timoshenko solves the three simultaneous equations for two particular cases of boundary conditions, namely,

$$\text{(i)} \quad \left.\begin{aligned} u = v = \varphi = 0 \\ u' = v' = \varphi' = 0 \end{aligned}\right\} \text{ for } z = 0 \text{ and } z = L \qquad (36)$$

$$\text{(ii)} \quad \left.\begin{aligned} u = v = \varphi = 0 \\ u'' = v'' = \varphi'' = 0 \end{aligned}\right\} \text{ for } z = 0 \text{ and } z = L \qquad (37)$$

No solution has so far been available for mixed boundary conditions.

The boundary conditions relevant to the experimental work carried out are; free rotation of the ends about the principal axes but fully restrained regarding twisting and warping, i.e.,

$$\left.\begin{aligned} u = v = \varphi = 0 \\ u'' = v'' = \varphi' = 0 \end{aligned}\right\} \text{for } z = 0 \text{ and } z = L \qquad (38)$$

These conditions are satisfied by

$$\left.\begin{aligned} u_1 &= A_1 \sin \frac{\pi z}{L} \\ v_1 &= A_2 \sin \frac{\pi z}{L} \\ \varphi_1 &= A_3 \left(1 - \cos \frac{2\pi z}{L}\right) \end{aligned}\right\} \qquad (39)$$

It should be noted that although the assumed solutions satisfy the boundary conditions they do not fully satisfy equations (33), (34) and (35). The following, therefore, is a first order approximation of the rigorous solution.

Putting $u = u_1$, and $\varphi = \varphi_1$ in the right hand side of equation (33) gives

$$EI_y \frac{d^2 u_2}{dz^2} = -P\left[A_1 \sin \frac{\pi z}{L} + y_o A_3 \left(1 - \cos \frac{2\pi z}{L}\right)\right] \qquad (40)$$

Integrating twice leads to

$$E I_y u_2 = -P\left[-A_1 \frac{\sin \frac{\pi z}{L}}{\left(\frac{\pi}{L}\right)^2} + y_0 A_3 \left(\frac{z^2}{2} + \frac{\cos \frac{2\pi z}{L}}{\left(\frac{2\pi}{L}\right)^2}\right)\right]$$

$$+ B z + C \qquad \text{(41)}$$

Using the appropriate boundary conditions (38) the integration constants are obtained as

$$B = P y_0 \frac{L}{2} A_3$$

$$C = P y_0 \left(\frac{L}{2\pi}\right) A_3$$

Substituting for B and C in equation (41) and putting $u_2 = u_1$ at $z = \frac{L}{2}$ gives

$$E I_y A_1 = P\left(\frac{L}{\pi}\right)^2 A_1 + P y_0 \frac{L^2}{8} A_3 + 2 P y_0 \left(\frac{L}{2\pi}\right)^2 A_3$$

Multiplying both sides by $\left(\frac{\pi}{L}\right)^2$ and grouping terms

$$\left(P - E I_y \frac{\pi^2}{L^2}\right) A_1 + 1.733\, P y_0 A_3 = 0 \qquad \text{(42)}$$

Similarly, putting $v = v_1$ and $\varphi = \varphi_1$, in the right hand side of equation (34) gives

$$E I_x \frac{d^2 v_2}{dz^2} = -P\left[A_2 \sin \frac{\pi z}{L} - x_0 A_3 \left(1 - \cos \frac{2\pi z}{L}\right)\right] \qquad \text{(43)}$$

Integrating twice leads to

$$E I_x v_2 = -P\left[-A_2 \frac{\sin \frac{\pi z}{L}}{\left(\frac{\pi}{L}\right)^2} - x_0 A_3 \left(\frac{z^2}{2} + \frac{\cos \frac{2\pi z}{L}}{\left(\frac{2\pi}{L}\right)^2}\right)\right] + Dz + E \qquad (44)$$

Using the appropriate boundary conditions (38) the integration constants are obtained as

$$D = -P x_0 \frac{L}{2} A_3$$

$$E = -P x_0 \left(\frac{L}{2\pi}\right)^2 A_3$$

Substituting for D and E in equation (44) and putting $v_2 = v_1$, at $z = \frac{L}{2}$ gives

$$E I_x A_2 = P\left(\frac{L}{\pi}\right)^2 A_2 - P x_0 \frac{L^2}{8} A_3 - 2P x_0 \left(\frac{L}{2\pi}\right)^2 A_3$$

Multiplying both sides by $\left(\frac{\pi}{L}\right)^2$ and grouping terms

$$\left(P - E I_x \frac{\pi^2}{L^2}\right) A_2 - 1.733\, P x_0 A_3 = 0 \qquad (45)$$

Putting $\frac{d^2u}{dz^2} = \frac{d^2u_1}{dz^2}$, $\frac{d^2v}{dz^2} = \frac{d^2v_1}{dz^2}$ and $\frac{d^2\varphi}{dz^2} = \frac{d^2\varphi_1}{dz^2}$ in the right hand side of equation (33) gives

$$C_1 \frac{d^4\varphi_2}{dz^4} = R_1 \cos \frac{2\pi z}{L} + R_2 \sin \frac{\pi z}{L} \qquad (46)$$

where $R_1 = \left(C - r_0^2 P\right)\left(\frac{2\pi}{L}\right)^2 A_3$

and $R_2 = P\left[-x_0 \left(\frac{\pi}{L}\right)^2 A_3 + y_0 \left(\frac{\pi}{L}\right)^2 A_1\right]$

successive integration leads to

$$C_1 \varphi_2 = R_1 \frac{\cos \frac{2\pi z}{L}}{\left(\frac{2\pi}{L}\right)^4} + R_2 \frac{\sin \frac{\pi z}{L}}{\left(\frac{\pi}{L}\right)^4} + F \frac{z^3}{6} + G \frac{z^2}{2} + H z + K \qquad (47)$$

To evaluate the constants of integration, the boundary conditions used are

$$\left.\begin{aligned} \varphi &= A_3 \left(1 - \cos \frac{2\pi z}{L}\right) = 0 \\ \varphi' &= A_3 \left(\frac{2\pi}{L}\right) \sin \frac{2\pi z}{L} = 0 \end{aligned}\right\} \text{for } z = 0 \qquad (38)$$

$$\left.\begin{aligned} \varphi' &= A_3 \left(\frac{2\pi}{L}\right) \sin \frac{2\pi z}{L} = 0 \\ \varphi''' &= -A_3 \left(\frac{2\pi}{L}\right)^3 \sin \frac{2\pi z}{L} = 0 \end{aligned}\right\} \text{for } z = \frac{L}{2} \qquad (48)$$

The additional boundary conditions (48) are selected to conform to the conditions which prevail in the experimental work. The constants of integration are obtained as

$$F = 0$$

$$H = -R_2 \left(\frac{L}{\pi}\right)^3$$

$$G = R_2 \frac{2}{L} \left(\frac{L}{\pi}\right)^3$$

$$K = -R_1 \left(\frac{L}{2\pi}\right)^4$$

Equation (47) now can be rewritten

$$C_1 \varphi_2 = R_1 \frac{\cos \frac{2\pi z}{L}}{\left(\frac{2\pi}{L}\right)^4} + R_2 \frac{\sin \frac{\pi z}{L}}{\left(\frac{\pi}{L}\right)^4} + R_2 \frac{1}{L}\left(\frac{L}{\pi}\right)^3 z^2$$

$$- R_2 \left(\frac{L}{\pi}\right)^3 z - R_1 \left(\frac{L}{2\pi}\right)^4 \qquad (49)$$

Putting $\varphi_2 = \varphi_1$ at $z = \frac{L}{2}$ in equation (49) and collecting terms

$$2 C_1 A_3 = -2 R_1 \left(\frac{L}{2\pi}\right)^4 - R_2 \left(\frac{L}{4}\right)\left(\frac{L}{\pi}\right)^3 + R_3 \left(\frac{L}{\pi}\right)^4$$

substituting for R_1 and R_2

$$2 C_1 A_3 = -2 \left(C - r_0^2 P\right)\left(\frac{L}{2\pi}\right)^2 A_3 + P x_0 \frac{L}{4}\left(\frac{L}{\pi}\right) A_2 - P y_0 A_1 \left(\frac{L}{4}\right)\left(\frac{L}{\pi}\right)$$

$$- P x_0 \left(\frac{L}{4}\right)\left(\frac{L}{\pi}\right) A_1 + P y_0 \left(\frac{L}{\pi}\right)^2 A_1$$

Multiplying both sides by $\left(\frac{\pi}{L}\right)^2$ and collecting terms

$$0.215 P y_0 A_1 - 0.215 P x_0 A_2 + \left[-2 C_1 \left(\frac{\pi}{L}\right)^2 - \frac{1}{2} C + \frac{1}{2} r_0^2 P\right] A_3 = 0 \qquad (50)$$

To simplify the writing the following notations are introduced:

$$P_1 = E I_y \frac{\pi^2}{L^2}, \quad P_2 = E I_x \frac{\pi^2}{L^2}, \quad P_3 = \frac{1}{r_0^2}\left(C + C_1 \frac{4\pi^2}{L^2}\right) \qquad (51)$$

Equations (42), (45) and (50) can be rewritten

$$(P - P_1) A_1 + 1.733\, P y_o A_3 = 0 \qquad (52)$$

$$(P - P_2) A_2 - 1.733\, P x_o A_3 = 0 \qquad (53)$$

$$0.215\, P y_o A_1 - 0.215\, P x_o A_2 + 0.5\, r_o^2 (P - P_3) A_3 = 0 \qquad (54)$$

Equating to zero the determinant of equations (52), (53) and (54),

$$\begin{vmatrix} (P - P_1) & 0 & 1.733\, P y_o \\ 0 & (P - P_2) & -1.733\, P x_o \\ 0.215\, P y_o & -0.215\, P x_o & -0.5\, r_o^2 (P - P_3) \end{vmatrix} = 0$$

which after evaluation, gives the following cubic equation for calculating the critical value of P

$$r_o^2 (P - P_1)(P - P_2)(P - P_3) - 0.744 P^2 y_o^2 (P - P_2) - 0.744 P^2 x_o^2 (P - P_1) = 0 \qquad (55)$$

If the x-axis of a cross section is an axis of symmetry, then $y_o = 0$ and the general equation (55) reduces to

$$(P-P_1)\left[r_o^2\,(P-P_2)(P-P_3) - 0.744\,P^2 x_o^2\right] = 0 \qquad (56)$$

One of the roots of equation (56) is $P = P_1$, the other roots are given by the quadratic

$$r_o^2\,(P-P_2)(P-P_3) - 0.744\,P^2 x_o^2 = 0 \qquad (57)$$

If the cross section is symmetrical about both axes the general equation (55) reduces to

$$(P-P_1)(P-P_2)(P-P_3) = 0 \qquad (58)$$

In all cases the smallest root gives the critical value of P.

The second order approximation in which the initial values of u_2, v_2 and φ_2 are assumed as follows:

$$u_2 = -\frac{P}{EI_y}\left[-A_1\frac{\sin\frac{\pi z}{L}}{\left(\frac{\pi}{L}\right)^2} + y_o A_3\frac{\cos\frac{2\pi z}{L}}{\left(\frac{2\pi}{L}\right)^2} + y_o A_3\frac{z^2}{2} - y_o A_3 L\frac{z}{2} - y_o A_3\left(\frac{L}{2\pi}\right)^2\right] \qquad (59)$$

$$v_2 = -\frac{P}{EI_x}\left[-A_2\frac{\sin\frac{\pi z}{L}}{\left(\frac{\pi}{L}\right)^2} - x_o A_3\frac{\cos\frac{2\pi z}{L}}{\left(\frac{2\pi}{L}\right)^2} - x_o A_3\frac{z^2}{2} + x_o A_3 L\frac{z}{2} + x_o A_3\left(\frac{L}{2\pi}\right)^2\right] \qquad (60)$$

$$\varphi_2 = \frac{R_1}{C_1}\frac{\cos\frac{2\pi z}{L}}{\left(\frac{2\pi}{L}\right)^4} + \frac{R_2}{C_1}\frac{\sin\frac{\pi z}{L}}{\left(\frac{\pi}{L}\right)^4} + \frac{R_2}{C_1}\frac{1}{L}\left(\frac{L}{\pi}\right)^3 z^2 - \frac{R_2}{C_1}\left(\frac{L}{\pi}\right)^3 z - \frac{R_1}{C_1}\left(\frac{L}{2\pi}\right)^4 \qquad (61)$$

is given in Appendix 2.

Applying the first and second approximations, to the calculation of the critical load of a concentrically loaded, 40 inch long, aluminium strut of 2·5" x 2·5" x 10G. angle cross section, it is seen that the second approximation does not change the value significantly, indicating that the value given by the first approximation is sufficiently accurate.

(ii) . Eccentrically Loaded Struts.

Timoshenko(7) gives the following equations for an eccentrically loaded strut

$$EI_y \frac{d^4u}{dz^4} = -P\frac{d^2u}{dz^2} - P(y_o - e_y)\frac{d^2\varphi}{dz^2} \qquad (62)$$

$$EI_x \frac{d^4v}{dz^4} = -P\frac{d^2v}{dz^2} + P(x_o - e_x)\frac{d^2\varphi}{dz^2} \qquad (63)$$

$$C_1 \frac{d^4\varphi}{dz^4} = \left(C - Pe_y\beta_1 - Pe_x\beta_2 - Pr_o^2\right)\frac{d^2\varphi}{dz^2} - P(y_o - e_y)\frac{d^2u}{dz^2} + P(x_o - e_x)\frac{d^2v}{dz^2} \qquad (64)$$

where $$\beta_1 = \frac{\int_A y^3 dA + \int_A x^2 y\, dA}{I_x} - 2y_o$$

and $$\beta_2 = \frac{\int_A x^3 dA + \int_A x y^2 dA}{I_y} - 2x_o$$

As in the case of concentric thrust the assumed end conditions are

$$\left.\begin{aligned} u = v = \varphi = 0 \\ u'' = v'' = \varphi' = 0 \end{aligned}\right\} \text{for } z = 0 \text{ and } z = L \qquad (38)$$

These conditions are satisfied by

$$\left.\begin{aligned} u_1 &= A_1 \sin \frac{\pi z}{L} \\ v_1 &= A_2 \sin \frac{\pi z}{L} \\ \varphi_1 &= A_3 \left(1 - \cos \frac{2\pi z}{L}\right) \end{aligned}\right\} \qquad (39)$$

Hence, following the same procedure as in the concentrically loaded case (made considerably more complex by the fact that all three equations are of the fourth order, see Appendix 3), the following three equations are obtained:

$$(P - P_1) A_1 + 1.733 P (y_0 - e_y) A_3 = 0 \qquad (65)$$

$$(P - P_2) A_2 - 1.733 P (x_0 - e_x) A_3 = 0 \qquad (66)$$

$$0.215 P (y_0 - e_y) A_1 - 0.215 P (x_0 - e_x) A_2 + 0.5 r_0^2 \left[P\left(1 + \frac{e_y \beta_1 + e_x \beta_2}{r_0^2}\right) - P_3\right] A_3 = 0 \qquad (67)$$

As for concentrically loaded struts P_1, P_2 and P_3 are given by (51).

Equating to zero the determinant of equations (65), (66) and (67)

$$\begin{vmatrix} (P - P_1) & 0 & 1.733 P (y_0 - e_y) \\ 0 & (P - P_2) & -1.733 P (x_0 - e_x) \\ 0.215 P (y_0 - e_y) & -0.215 P (x_0 - e_x) & 0.5 r_0^2 \left[P\left(1 + \frac{e_y \beta_1 + e_x \beta_2}{r_0^2}\right) - P_3\right] \end{vmatrix} = 0$$

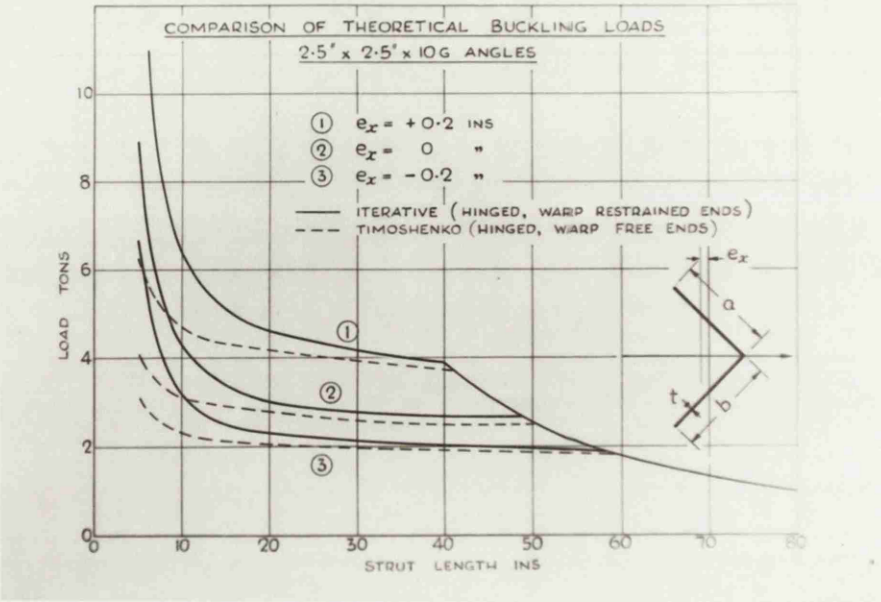
COMPARISON OF THEORETICAL BUCKLING LOADS
2·5" x 2·5" x 10G ANGLES
① e_x = +0·2 INS
② e_x = 0 "
③ e_x = −0·2 "
ITERATIVE (HINGED, WARP RESTRAINED ENDS)
TIMOSHENKO (HINGED, WARP FREE ENDS)
LOAD TONS
STRUT LENGTH INS
e_x
a
b
t

FIG. 16.

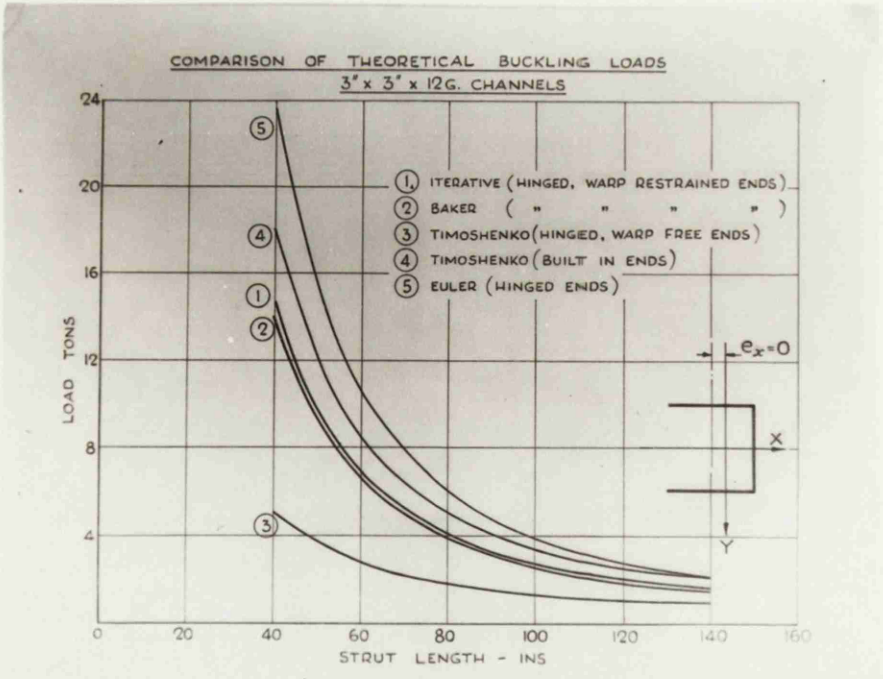
COMPARISON OF THEORETICAL BUCKLING LOADS
3" x 3" x 12G. CHANNELS
① ITERATIVE (HINGED, WARP RESTRAINED ENDS)
② BAKER (" " " ")
③ TIMOSHENKO (HINGED, WARP FREE ENDS)
④ TIMOSHENKO (BUILT IN ENDS)
⑤ EULER (HINGED ENDS)
LOAD TONS
STRUT LENGTH - INS
e_x=0
X
Y

FIG. 17.

which, after evaluation, gives the following cubic equation for calculating the critical value of P

$$r_o^2 (P-P_1)(P-P_2)\left[P\left(1 + \frac{e_y \beta_1 + e_x \beta_2}{r_o^2} - P_3\right]\right.$$
$$- 0.744 P^2 (y_o - e_y)^2 (P-P_2) - 0.744 P^2 (x_o - e_x)^2 (P-P_1) = 0 \qquad (68)$$

If the xz - plane is a plane of symmetry and the thrust P acts in that plane the general equation (68) reduces to

$$(P-P_1)\left\{r_o^2 (P-P_2)\left[P\left(1 + \frac{e_x \beta_2}{r_o^2}\right) - P_3\right] - 0.744 P^2 (x_o - e_x)^2\right\} = 0 \qquad (69)$$

As in the case of concentric struts it appears to be unnecessary to solve for higher orders of approximation.

To give a comparison of the effects of the end conditions on the critical strength of angle and channel section struts, indicated by the theoretical treatment presented in (i) and (ii), Figures 16 and 17 were prepared. From Figure 16 it can be seen that the effect of warping restraint becomes very appreciable in the shorter lengths. The theoretical buckling loads for the channel struts, Figure 17, exhibit the same characteristics. The most interesting feature is the close agreement obtained between Baker's proposed formula and the iterative method.

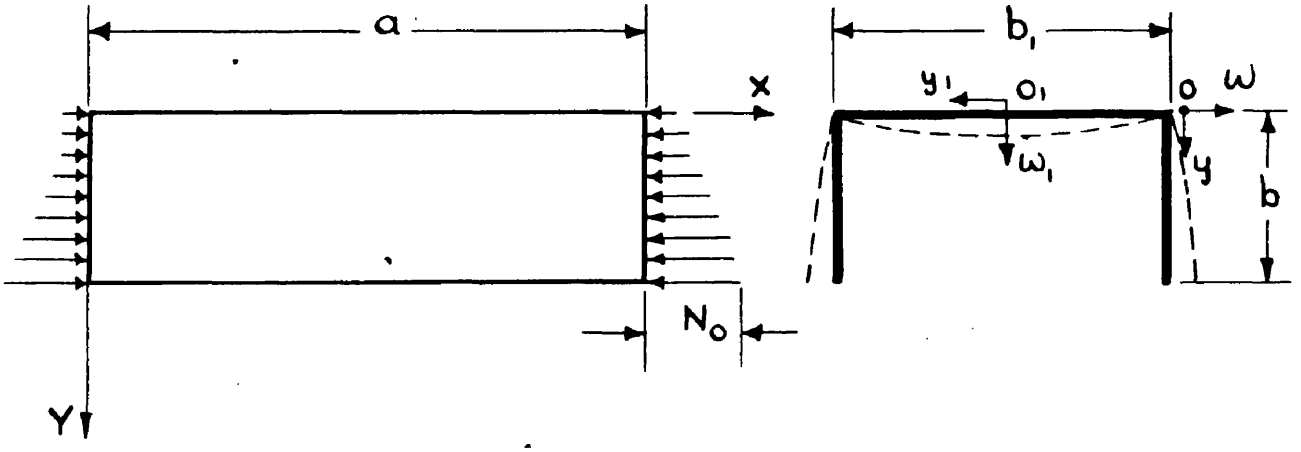

FIG. 18.

3. FLANGE PLATE INSTABILITY OF THIN-WALLED CHANNEL SECTIONS UNDER COMBINED BENDING AND COMPRESSION.

One aspect of this problem is presented, namely, the flange plate instability of thin-walled channel struts under eccentric load. The load is applied in the plane of symmetry of the channel such that the maximum intensity of load is at the free edge of the flange.

The flange is considered as a flat plate, compressed by thrusts of uniformly varying intensity in its own plane and parallel to the longitudinal edges, Figure 18. The edges $y = b$ and $y = b$ are free and elastically built in respectively, the edges $x = o$ and $x = a$ are assumed to be simply supported. The intensity of the applied load is given by

$$N_x = N_o \left(\frac{1}{\alpha} + \left(1 - \frac{1}{\alpha} \right) \frac{y}{b} \right) \qquad (70)$$

where N_o is the intensity of the applied load at the edge $y = b$ and α is the ratio of the stress at the free edge to the stress at the elastically built in edge.

The solution of the particular case when the stress ratio in the flange equals 4 is presented. The intensity of compressive load is then given by equation (70) taking $\alpha = 4$

$$N_x = \frac{1}{4} N_o \left(1 + \frac{3y}{b} \right) \qquad (71)$$

The differential equation for the deflected form of the flange is again given by equation (14), substituting for N_x from (71) gives

$$\frac{\partial^4 w}{\partial x^4} + 2\frac{\partial^4 w}{\partial x^2 \partial y^2} + \frac{\partial^4 w}{\partial y^4} = -\frac{1}{D}\frac{1}{4} N_o \left(1 + \frac{3y}{b}\right) \frac{\partial^2 w}{\partial x^2} \qquad (72)$$

The boundary conditions to be satisfied are

$$\left.\begin{aligned} w &= 0 \\ \frac{\partial^2 w}{\partial x^2} + \nu \frac{\partial^2 w}{\partial y^2} &= 0 \end{aligned}\right\} \text{ for } x = 0 \text{ and } x = a \qquad (15)$$

$$\left.\begin{aligned} w &= 0 \\ \frac{\partial^2 w}{\partial y^2} - r\frac{\partial w}{\partial y} &= 0 \end{aligned}\right\} \text{ for } y = 0 \qquad (16)$$

$$\left.\begin{aligned} \frac{\partial^2 w}{\partial y^2} + \nu \frac{\partial^2 w}{\partial x^2} &= 0 \\ \frac{\partial^3 w}{\partial y^3} + (2-\nu)\frac{\partial^3 w}{\partial x^2 \partial y} &= 0 \end{aligned}\right\} \text{ for } y = b \qquad (17)$$

Assuming that the flange buckles in m sinusoidal half waves, the solution can be written in the form

$$w = Y \sin \frac{m\pi x}{a} \qquad (18)$$

in which Y is a function of y only. This satisfies the boundary conditions along the simply supported edges $x=0$ and $x=a$.

Substituting in equation (72) gives

$$\frac{d^4Y}{dy^4} = 2\frac{m^2\pi^2}{a^2}\frac{d^2Y}{dy^2} - \left[\frac{m^4\pi^4}{a^4} - \frac{m^2\pi^2}{a^2}\frac{N_0}{4D}\left(1+\frac{3y}{b}\right)\right]Y$$

$$= A\frac{d^2Y}{dy^2} + BY + CyY \qquad (73)$$

where $A = \dfrac{2m^2\pi^2}{a^2}$

$$B = -\left(\frac{m^4\pi^4}{a^4} - \frac{m^2\pi^2}{a^2}\frac{N_0}{4D}\right)$$

$$C = \frac{m^2\pi^2}{a^2}\frac{N_0}{4D}\frac{3}{b}$$

The appropriate boundary conditions in terms of Y and for $\nu = 0.32$, relevant to equation (73) are now

$$\left.\begin{aligned} Y &= 0 \\ \frac{d^2Y}{dy^2} - r\frac{dY}{dy} &= 0 \end{aligned}\right\} \text{ for } y = 0 \qquad (20)$$

$$\left.\begin{aligned} \frac{d^2Y}{dy^2} - 3.157\,\frac{m^2}{a^2}\,Y &= 0 \\ \frac{d^3Y}{dy^3} - 16.58\,\frac{m^2}{a^2}\,\frac{dY}{dy} &= 0 \end{aligned}\right\} \text{for } y = b \qquad (21)a$$

For comparatively short channels the flange buckles in one half wave in the direction of compression, i.e., the smallest value of $(N_o)_{cr.}$ is obtained by taking $m=1$ in the calculations. The magnitude of the corresponding critical compressive load can be represented by

$$(N_o)_{cr.} = K_F\,\frac{\pi^2 D}{b^2} \qquad (74)$$

The first approximation to the deflected form of the flange in the y-direction is assumed to be given by

$$Y_1 = \Omega\left(\frac{3b^3y^2}{2} - \frac{5b^2y^3}{6} + \frac{by^4}{12} + \frac{y^5}{20} + \frac{3b^4y}{rb}\right) \qquad (75)$$

where Ω is a constant.

Substituting in the right hand side of equation (73) gives

$$\begin{aligned} \frac{d^4Y_2}{dy^4} = {} & A\Omega\left(3b^3 - 5b^2y + by^2 + y^3\right) \\ & + B\Omega\left(\frac{3b^3y^2}{2} - \frac{5b^2y^3}{6} + \frac{by^4}{12} + \frac{y^5}{20} + \frac{3b^4y}{rb}\right) \\ & + C\Omega\left(\frac{3b^3y^3}{2} - \frac{5b^2y^4}{6} + \frac{by^5}{12} + \frac{y^6}{20} + \frac{3b^4y^2}{rb}\right) \end{aligned} \qquad (76)$$

where Y_2 is the second approximation.

Successive integration of this equation leads to

$$Y_2 = A\Omega\left(\frac{b^3y^4}{8} - \frac{b^2y^5}{24} + \frac{by^6}{360} + \frac{y^7}{840}\right)$$
$$+ B\Omega\left(\frac{b^3y^6}{240} - \frac{b^2y^7}{1008} + \frac{by^8}{20160} + \frac{y^9}{60480} + \frac{b^4y^5}{40rb}\right)$$
$$+ C\Omega\left(\frac{b^3y^7}{560} - \frac{b^2y^8}{2016} + \frac{by^9}{36288} + \frac{y^{10}}{100800} + \frac{b^4y^6}{120rb}\right)$$
$$+ R\frac{y^3}{6} + S\frac{y^2}{2} + Ty + V \qquad (77)$$

Using this form of Y and the appropriate boundary conditions (20) and (21)a, the following equations for the four integration constants are obtained:

$$V = 0 \qquad (78)$$

$$T = \frac{S}{r} \qquad (79)$$

$$A\Omega b^5\left(0.8-0.2756\frac{b^2}{a^2}\right)+B\Omega b^7\left[\left(0.0873+\frac{0.5}{rb}\right)-\frac{b^2}{a^2}\left(0.01023+\frac{0.07893}{rb}\right)\right]$$

$$+C\Omega b^8\left[\left(0.0501+\frac{0.25}{rb}\right)-\frac{b^2}{a^2}\left(0.004183+\frac{0.0263}{rb}\right)\right]+Rb\left(1-0.526\frac{b^2}{a^2}\right)$$

$$+S\left[1-\frac{b^2}{a^2}\left(1.578+\frac{3.157}{rb}\right)\right]=0 \qquad \text{(80)}$$

$$A\Omega b^4\left(1.083-5.248\frac{b^2}{a^2}\right)+B\Omega b^6\left[\left(0.3166+\frac{1.5}{rb}\right)-\frac{b^2}{a^2}\left(0.3083+\frac{2.073}{rb}\right)\right]$$

$$+C\Omega b^7\left[\left(0.2294+\frac{1}{rb}\right)-\frac{b^2}{a^2}\left(0.1472+\frac{0.829}{rb}\right)\right]+R\left(1-8.29\frac{b^2}{a^2}\right)$$

$$-16.58\,S\frac{b}{a^2}\left(1+\frac{1}{rb}\right)=0 \qquad \text{(81)}$$

For the case of $rb=8$ and $\frac{a}{b}=1$ the constants of integration are

$$R=-0.87A\Omega b^4-0.156B\Omega b^6-0.0803C\Omega b^7$$

$$S=0.115A\Omega b^5+0.0574B\Omega b^7+0.0369C\Omega b^8$$

$$T=0.01438A\Omega b^6+0.007175B\Omega b^8+0.004613C\Omega b^9$$

$$V=0$$

For the boundary conditions given the maximum deflection occurs at $y = b$. This gives

$$(Y_1)_{max.} = 1.175\ \Omega b^5 \qquad (82)$$

$$(Y_2)_{max.} = 0.0142\ A\Omega b^7 + 0.01616\ B\Omega b^9 + 0.01204\ C\Omega b^{10} \qquad (83)$$

The first approximation to the critical load is obtained by equating $(Y_1)_{max.}$ to $(Y_2)_{max.}$. This reduces to

$$1.175 = 0.0142\ A b^2 + 0.01616\ B b^4 + 0.01204\ C b^5 \qquad (84)$$

Noting that

$$A = \frac{2m^2\pi^2}{a^2}$$

$$B = -\left(\frac{m^4\pi^4}{a^4} - K_F \frac{\pi^2}{4b^2}\ \frac{m^2\pi^2}{a^2}\right)$$

and $$C = K_F \frac{3\pi^2}{4b^3}\ \frac{m^2\pi^2}{a^2}$$

where $$(N_0)_{cr.} = K_F \frac{\pi^2 D}{b^2} \qquad (74)$$

Equation (84) finally gives

$$1.175 = 0.2802 - 1.574 + 0.3934\ K_F + 0.8788\ K_F$$

ECCENTRICALLY LOADED CHANNEL SECTION STRUTS

STRESS RATIO ACROSS FLANGE $\alpha = 4$

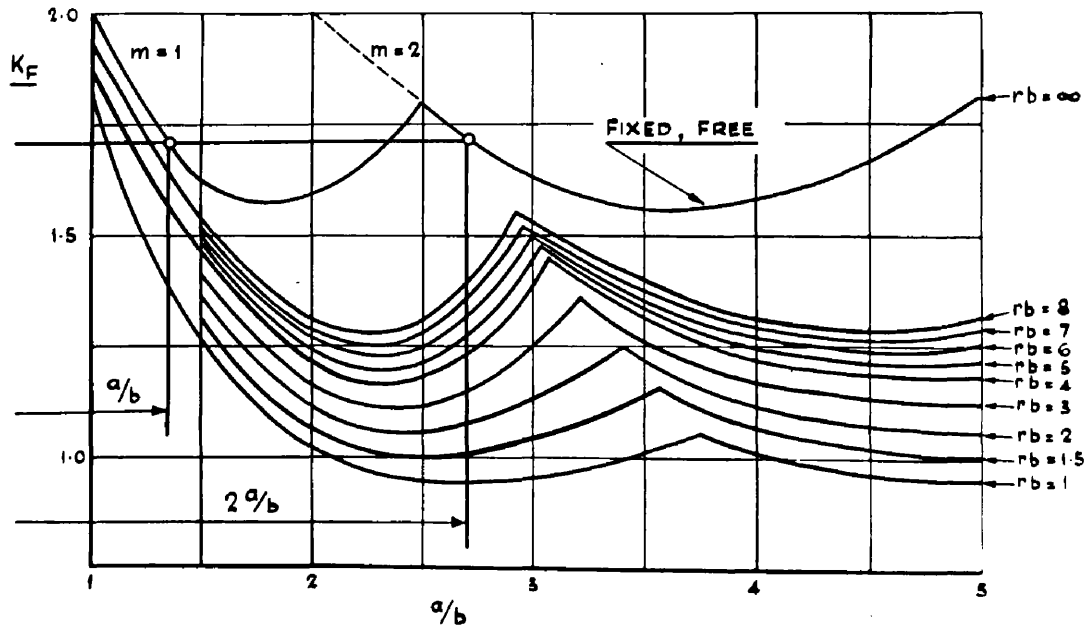

FIG. 19.

hence $K_F = 1.939$

The results of calculations made for various values of $r\,b$ and for $\nu = 0.32$ are given in Figure 19. Curves for $m = 2, 3$, etc., may be obtained by keeping the K_F ordinates the same but multiplying the corresponding $\frac{a}{b}$ ordinates by the value of m. The construction is indicated in Figure 19.

The elastic edge restraint provided by the web plate of a concentrically loaded channel section strut is obtained as follows, Harvey(25) :

The deflected form of the uniformly compressed web and flange plates is given by

$$\frac{\partial^4 \omega}{\partial x^4} + 2\frac{\partial^4 \omega}{\partial x^2 \partial y^2} + \frac{\partial^4 \omega}{\partial y^4} = -\frac{N_x}{D}\frac{\partial^2 \omega}{\partial x^2} \qquad (14)$$

The general solution of this equation can be presented in the form

$$\omega = \left(C_1 e^{-\alpha y} + C_2 e^{\alpha y} + C_3 \cos \beta y + C_4 \sin \beta y\right) \sin \frac{m\pi x}{a} \qquad (85)$$

where $$\alpha^2 = \frac{m^2\pi^2}{a^2} + \left[\left(\frac{N_x}{D}\right)\left(\frac{m^2\pi^2}{a^2}\right)\right]^{\frac{1}{2}}$$

$$\beta^2 = -\frac{m^2\pi^2}{a^2} + \left[\left(\frac{N_x}{D}\right)\left(\frac{m^2\pi^2}{a^2}\right)\right]^{\frac{1}{2}}$$

Considering first the supporting plate, in this case, the web

$$\omega_1 = \left(C_1' e^{-\alpha_1 y_1} + C_2' e^{\alpha_2 y_2} + C_3' \cos\beta_1 y_1 + C_4' \sin\beta_1 y_1\right) \sin\frac{m\pi x}{a} \qquad (86)$$

The boundary conditions are

$$\omega_1 = 0 \quad \text{for} \quad y_1 = -\frac{b}{2} \qquad (87)$$

$$\omega_1 = 0 \quad \text{for} \quad y_1 = \frac{b_1}{2} \qquad (88)$$

$$\frac{\partial\omega_1}{\partial y_1} = 0 \quad \text{for} \quad y_1 = 0 \qquad (89)$$

the origin being taken at the centre of the web plate, Figure 18.

The fourth necessary condition is obtained by assuming that the bending moment at the edge connecting the web and flange varies in a sinusoidal fashion along the length of the plate, i.e.,

$$M_{y_1} = M \sin\frac{m\pi x}{a} \qquad (90)$$

where M is the bending moment at the connecting edge at the centre of a longitudinal half wave.

Substituting these boundary conditions in equation (86), the values of the constants are obtained as

$$\left.\begin{aligned} C_1' = C_2' &= -\frac{M}{\left(2 D_1 \cosh \alpha_1 \frac{b_1}{2}\right)\left(\alpha_1^2 + \beta_1^2\right)} \\ C_3' &= \frac{M}{\left(D_1 \cos \beta_1 \frac{b_1}{2}\right)\left(\alpha_1^2 + \beta_1^2\right)} \\ C_4' &= 0 \end{aligned}\right\} \quad (91)$$

Considering now the buckling plate, in this case, the flange

$$\omega = \left(C_1 e^{-\alpha y} + C_2 e^{\alpha y} + C_3 \cos \beta y + C_4 \sin \beta y\right) \sin \frac{m \pi x}{a} \quad (85)$$

The boundary conditions are

$$\omega = 0 \qquad \text{for} \quad y = 0 \quad (92)$$

$$\frac{\partial^2 \omega}{\partial y^2} + \sigma \frac{\partial^2 \omega}{\partial x^2} = 0 \qquad \text{for} \quad y = b \quad (93)$$

$$\frac{\partial^3 \omega}{\partial y^3} + (2 - \nu) \frac{\partial^3 \omega}{\partial x^2 \partial y} = 0 \qquad \text{for} \quad y = b \quad (94)$$

the origin being taken at the edge of the flange plate, Figure 18.

The fourth necessary condition is obtained from the web. By substituting the values of the constants given in (91) in equation (86) and differentiating, the slope at the connecting edge, i.e., for $y_1 = \frac{b_1}{2}$ is

$$\frac{\partial w_1}{\partial y_1} = -M \sin \frac{m\pi x}{a} \left\{ \frac{\alpha_1 \tanh \alpha_1 \frac{b}{2} + \beta_1 \tan \beta_1 \frac{b_1}{2}}{D_1 (\alpha_1^2 + \beta_1^2)} \right\}$$

$$= -M y_1 \frac{1}{r D_1} \qquad (95)$$

where r is the coefficient of edge fixity and

$$r = \frac{\alpha_1^2 + \beta_1^2}{\alpha_1 \tanh \alpha_1 \frac{b_1}{2} + \beta_1 \tan \beta_1 \frac{b_1}{2}}$$

or

$$r = \frac{\alpha_1^2 + \beta_1^2}{\alpha_1 \tanh H\alpha_1 \frac{b}{2} + \beta_1 \tan H\beta_1 \frac{b}{2}} \qquad (96)$$

where $H = \frac{b_1}{b}$

It should be noted that the nature of the load carried by the web, in the case of the eccentric loading analysed, is the same as in the concentric case. For the eccentric loading of the type considered expression (96) is applicable substituting $\frac{N_0}{4}$ for N_x in the values of α_1^2 and β_1^2.

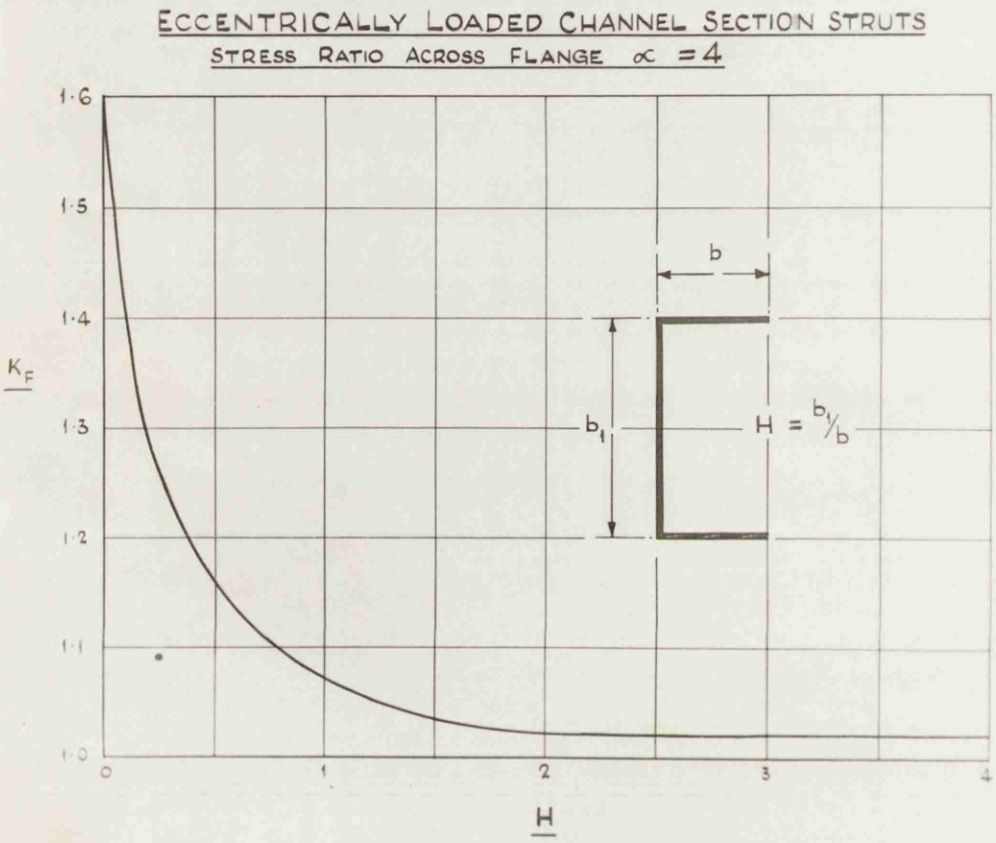
ECCENTRICALLY LOADED CHANNEL SECTION STRUTS
STRESS RATIO ACROSS FLANGE ∝ = 4
1·6
1·5
1·4
1·3
1·2
1·1
1·0
K_F
0
1
2
3
4
H
b
b1
H = b1/b

FIG. 20.

For any value of r_b the ratio $\frac{a}{b}$ at which K_F is a minimum, can be obtained from Figure 19. Using these values the corresponding value of H is then obtained from equation (96). The results of these calculations are shown in Figure 20. A typical example of the method is presented in Appendix 4.

PART III.

EXPERIMENTAL INVESTIGATION.

1. EXPERIMENTAL APPLIANCES.
   - (i) Testing Machines.
   - (ii) Universal End Clamps.
   - (iii) Strain Gauge Bridge.
   - (iv) Measuring Devices.

2. METHOD OF TESTING.
   - (i) Load Capacity Tests.
   - (ii) Stress Distribution Tests.
   - (iii) Tensile Tests.

3. EXPERIMENTAL RESULTS.
   - (i) Angle Section Struts.
   - (ii) Channel Section Struts.

The experimental work was planned to investigate over-all failure in torsion-flexure and local plate failure in flexure of thin-walled angle and channel section struts. The loading conditions included concentric and eccentric axial loads. The following variables were investigated - eccentricity of load, section profile, length and method of manufacture.

The specimens were cold formed from sheet or extruded, in 65 S.W.P. Aluminium Alloy. A complete list of some 190 specimens is given in Appendix 5. Tensile tests to determine the material characteristics were carried out, as described in Appendix 6.

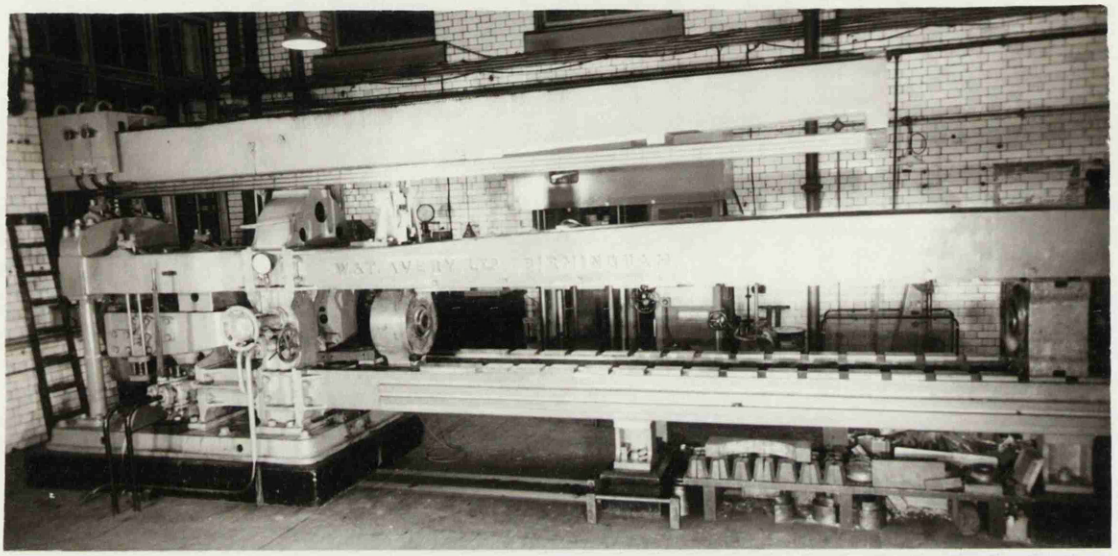

FIG. 21.

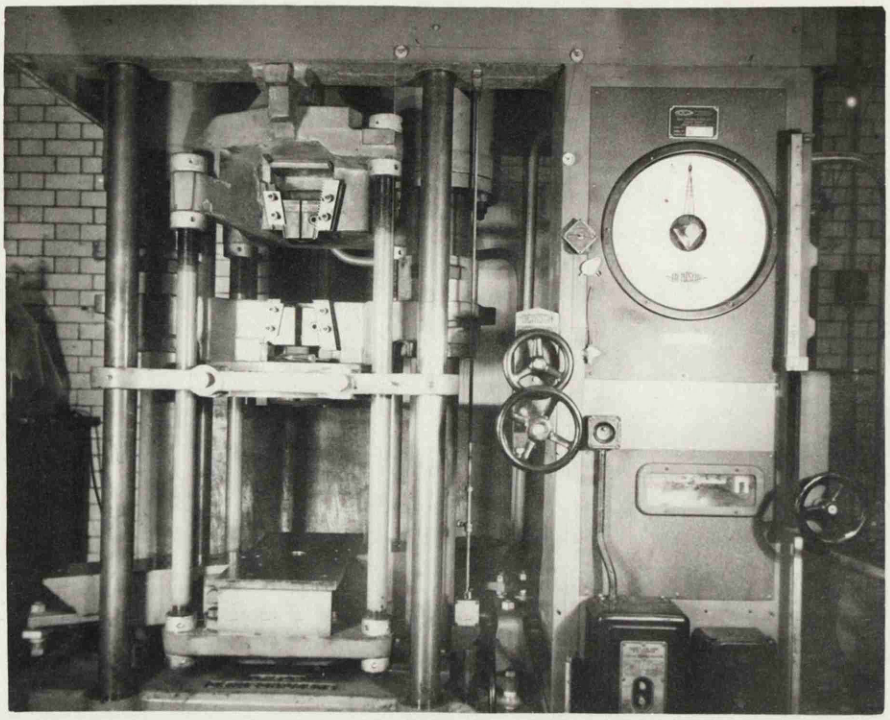

FIG. 22

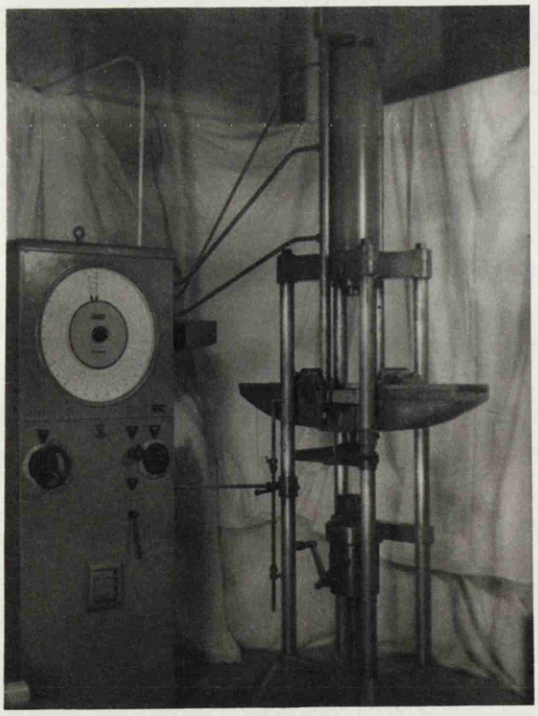

FIG. 23.

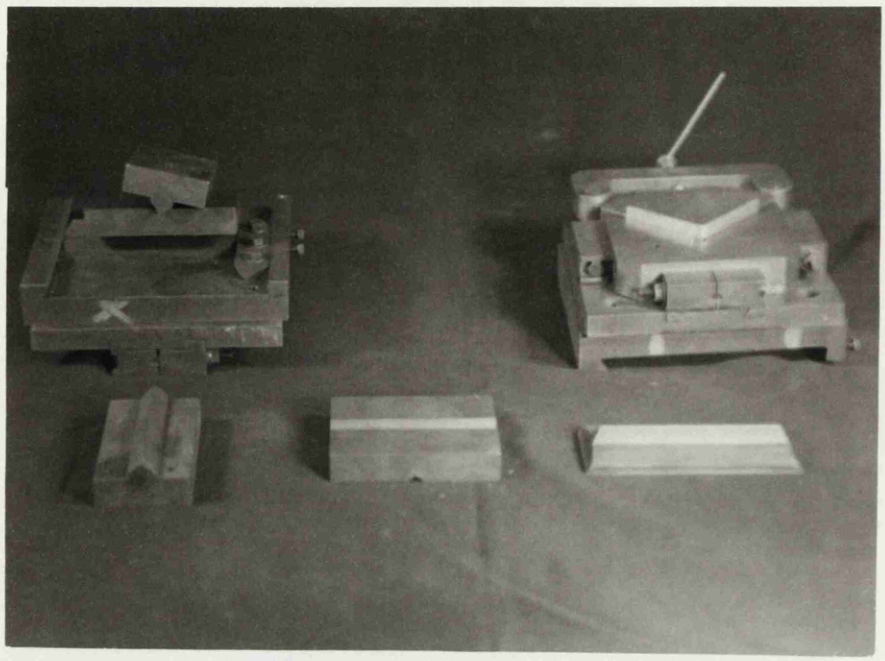

FIG. 24.

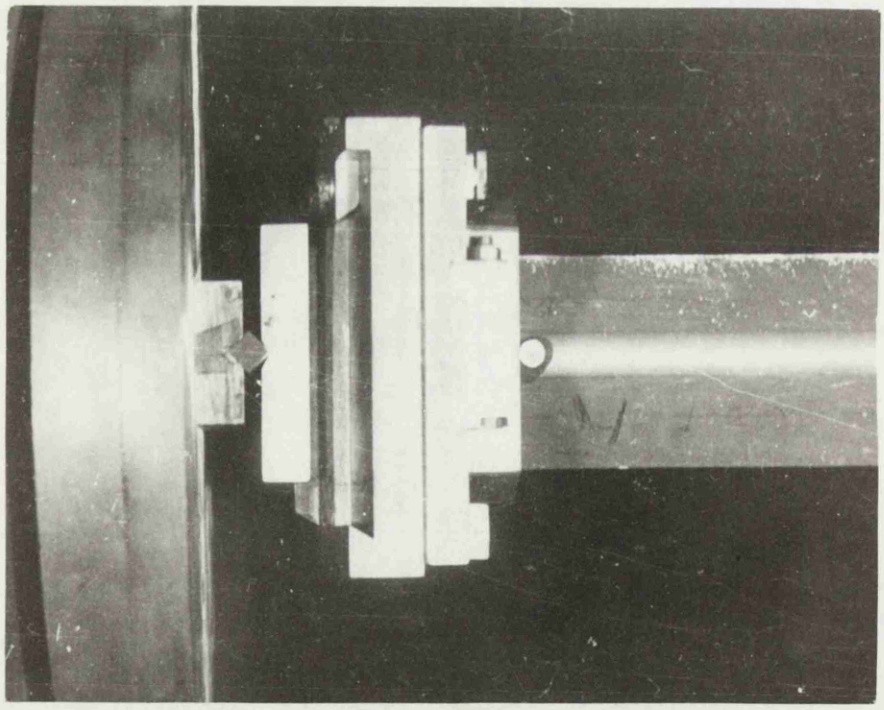

FIG. 25.

1. EXPERIMENTAL APPLIANCES.

(i) Testing Machines.

Most of the strut specimens were tested in a horizontal 100 ton Avery Testing Machine, Figure 21. All the 12 inches long channels were tested in a vertical 50 ton Denison Testing Machine, Figure 22. A 30 ton Avery Universal Testing Machine, Figure 23, was used for the tensile tests carried out to determine the material constants. All three machines are hydraulically operated.

(ii) Universal End Clamps.

Special end clamps, Figure 24, were designed to insure loading of the strut with pin-end conditions. One set of clamps were used for all the specimens tested. These could also be used for other sections of similar over-all cross sectional dimensions. Special distance pieces were made to clamp the different sections in position, such that the centroids of the sections are always in line with the centres of the clamps. Provision was made so that loads could be applied concentrically or eccentrically, in either of the two principal directions to within 1/100th of an inch.

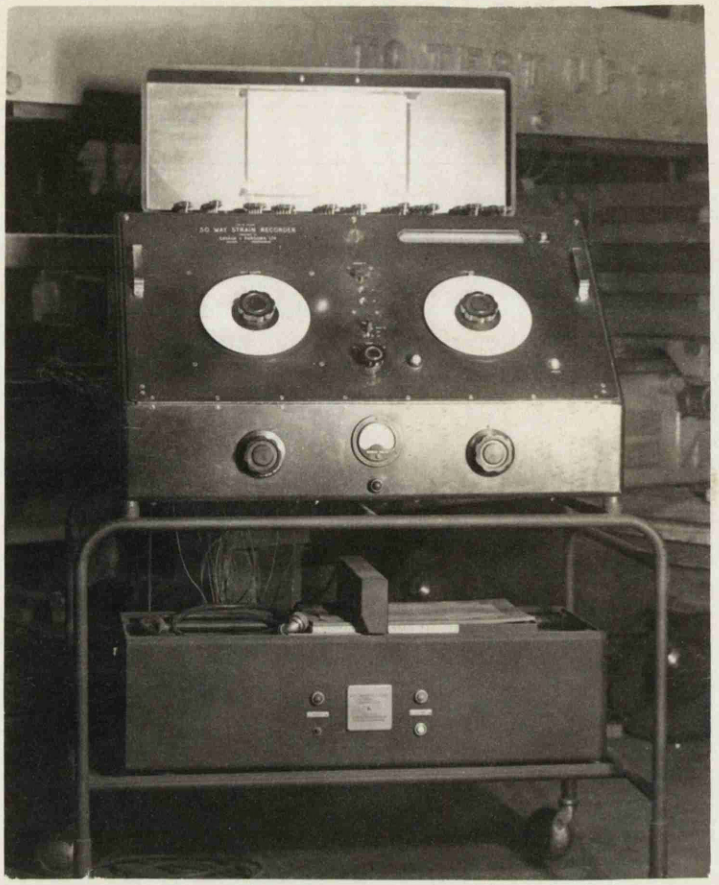

FIG. 26.

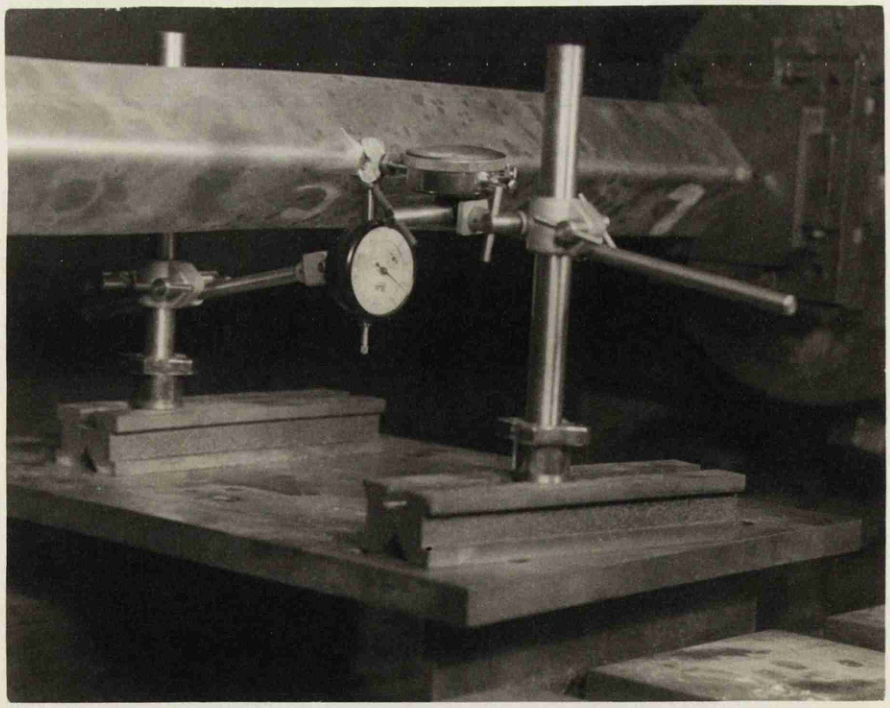

FIG. 27.

Either crossed-knife edges or ball ends could be used as required. Crossed-knife edges were adopted in preference to ball ends due to their small frictional torque and to the fact that they prevent relative twisting of the strut ends. Figure 25 shows a clamp with crossed-knife edges in position during a test.

All parts were made of mild steel with the exception of the base plate which was of hardened ground flat stock steel. The distance pieces were case hardened and ground to size.

(iii) Strain Gauge Bridge.

A Savage and Parsons, 50 gauge capacity strain gauge bridge, Figure 26, was used for the stress analysis and in connection with the tensile tests to determine Poisson's Ratio.

(iv) Measuring Devices.

Vertical and horizontal deflections of the shear centre were measured by means of Baty dial gauge comparators. Small cast iron discs, with one quarter cut out, were attached in the manner shown in Figure 27 to facilitate deflection measurements. A small surface plate, placed conveniently in position under the strut in the 100 ton machine, served as a datum plane for these measurements.

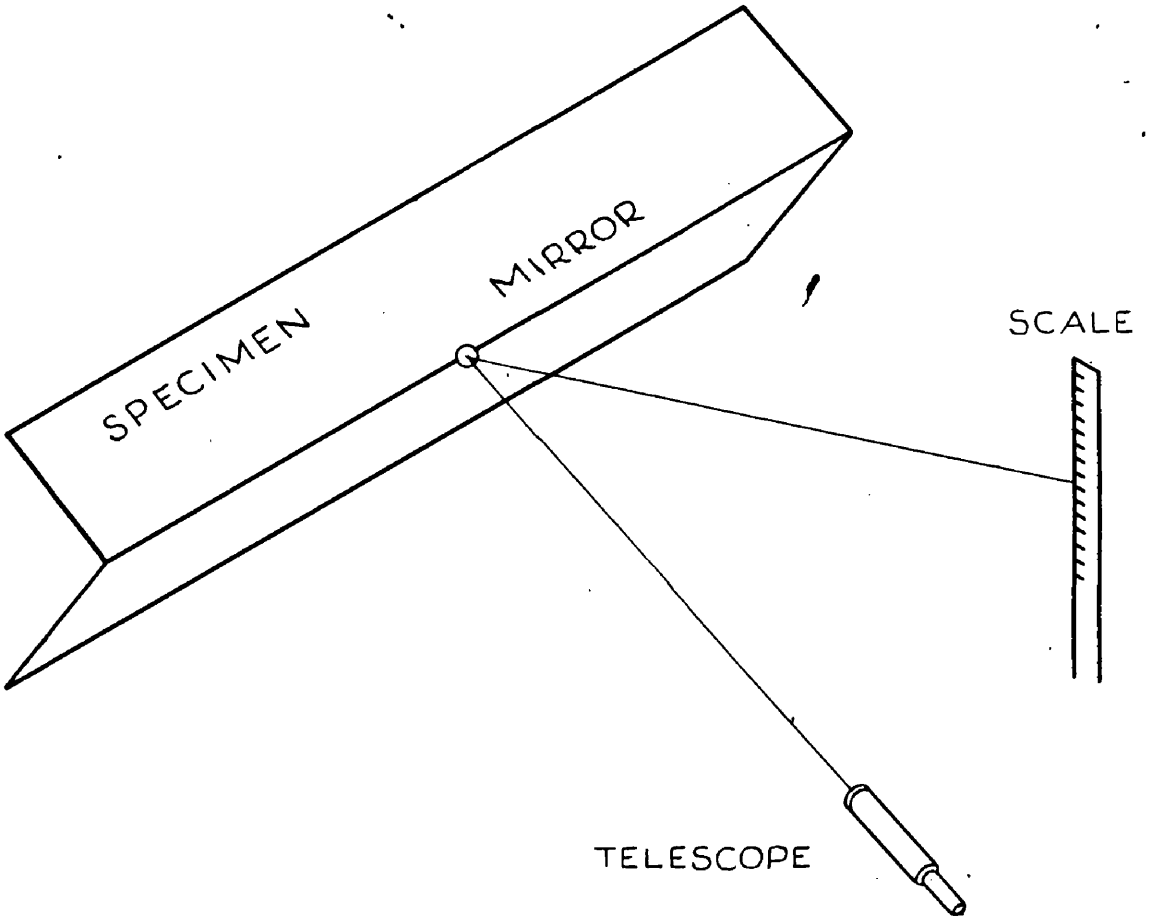

FIG. 28.

Angles of twist were measured at the two ends and centre of the strut by means of optical lever twist metres. These consist of galvanometer mirrors placed conveniently at the shear centre and telescopes and scales placed in line with the mirrors. This set-up is shown in Figure 28.

Other measuring instruments included inside and outside micrometers and a Hounsfield extensometer for the tensile tests.

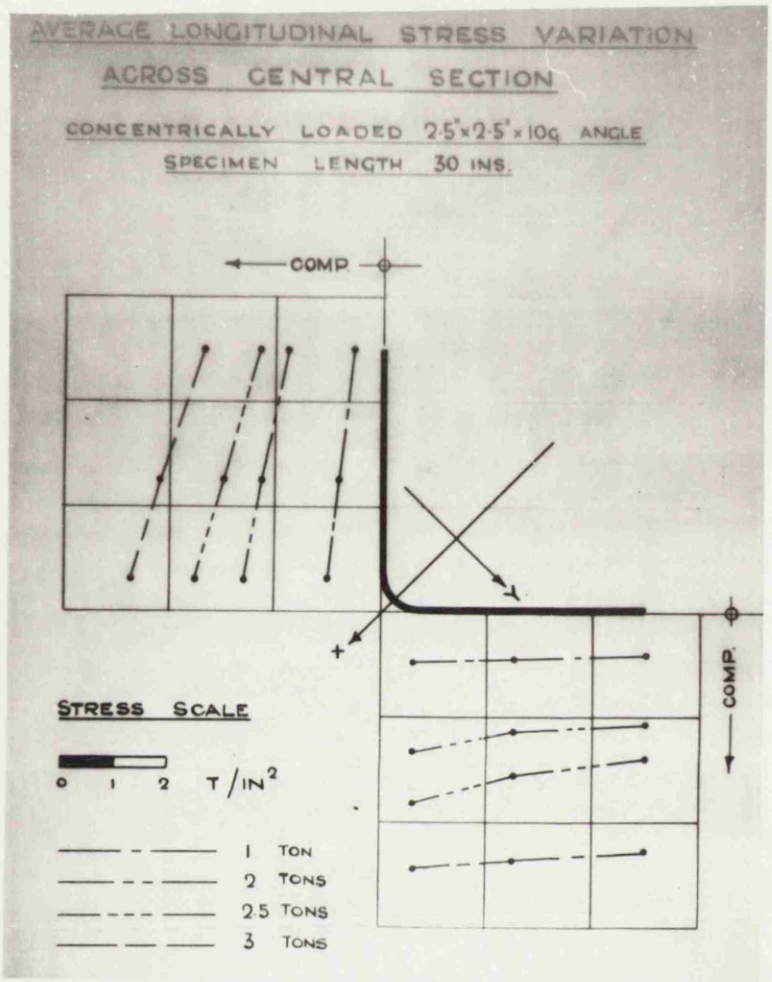
AVERAGE LONGITUDINAL STRESS VARIATION
ACROSS CENTRAL SECTION
CONCENTRICALLY LOADED 2·5"×2·5"×10G ANGLE
SPECIMEN LENGTH 30 INS.
COMP.
COMP.
+
STRESS SCALE
0 1 2 T/IN²
1 TON
2 TONS
2·5 TONS
3 TONS

FIG. 29.

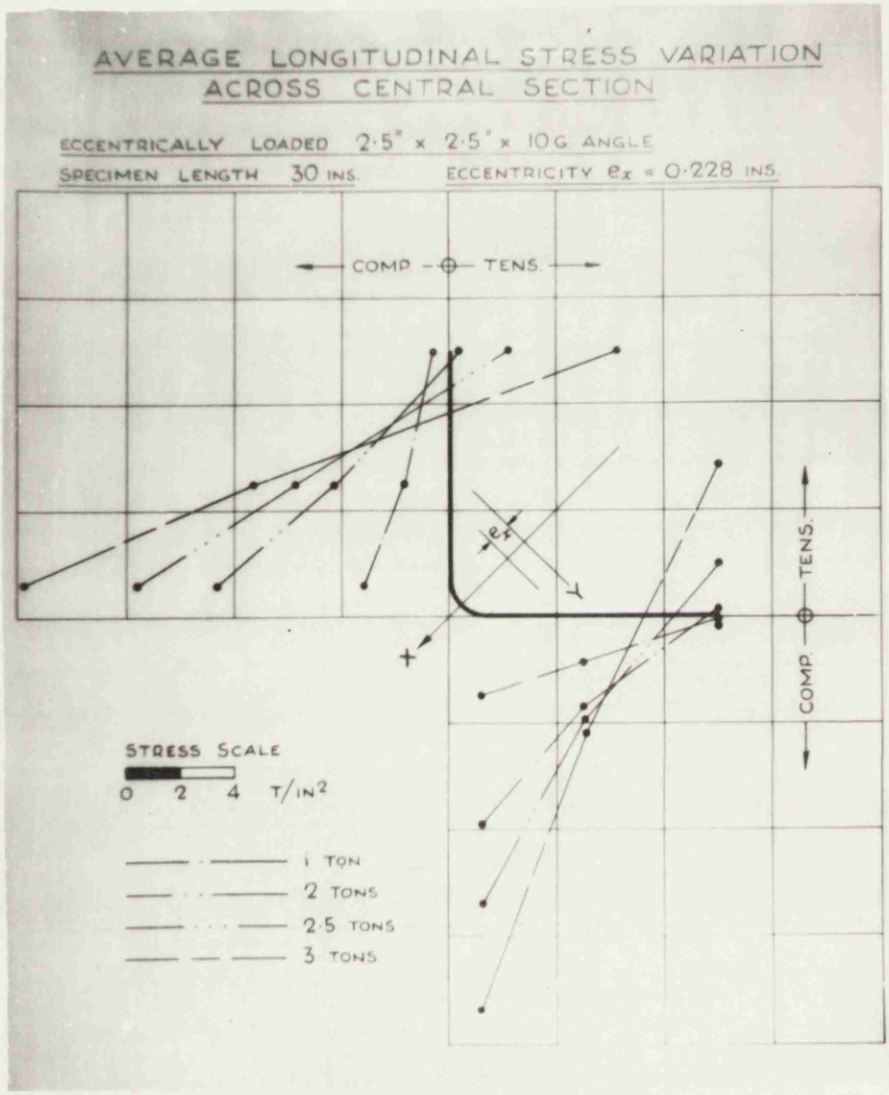
AVERAGE LONGITUDINAL STRESS VARIATION
ACROSS CENTRAL SECTION
ECCENTRICALLY LOADED 2·5" x 2·5" x 10G ANGLE
SPECIMEN LENGTH 30 INS.
ECCENTRICITY e_x = 0·228 INS.
COMP. TENS.
e_x
y
+
TENS.
COMP.
STRESS SCALE
0 2 4 T/IN²
1 TON
2 TONS
2·5 TONS
3 TONS

FIG. 30.

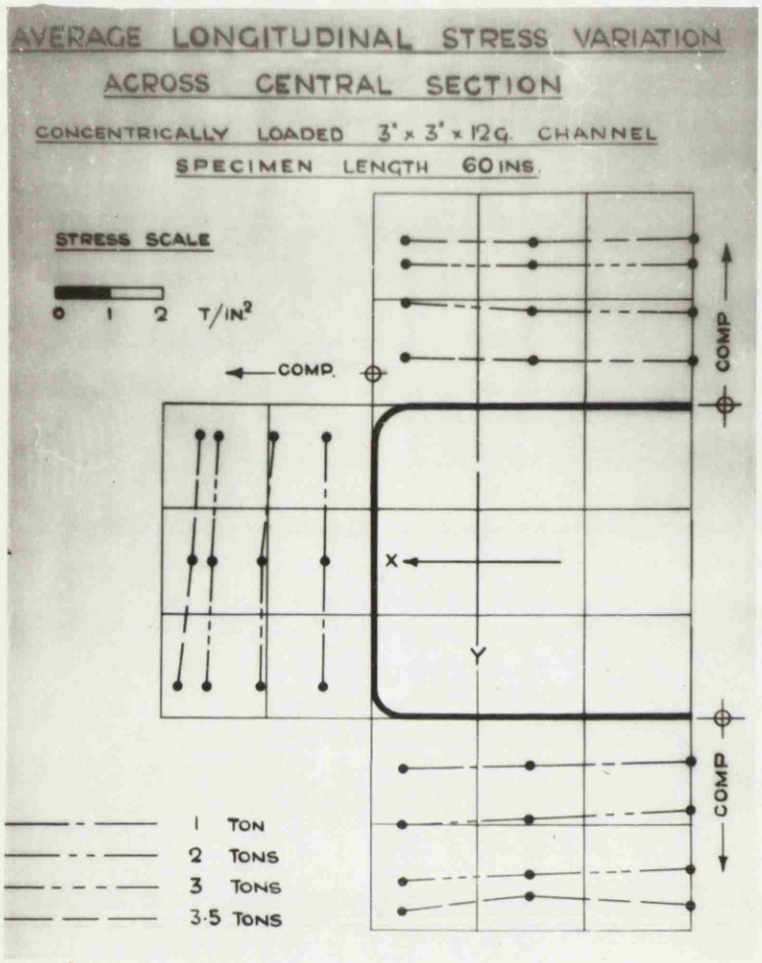
AVERAGE LONGITUDINAL STRESS VARIATION
ACROSS CENTRAL SECTION
CONCENTRICALLY LOADED 3" x 3" x 12G. CHANNEL
SPECIMEN LENGTH 60 INS.
STRESS SCALE
0 1 2 T/IN.²
COMP.
COMP.
COMP.
X
Y
1 TON
2 TONS
3 TONS
3·5 TONS

FIG. 31.

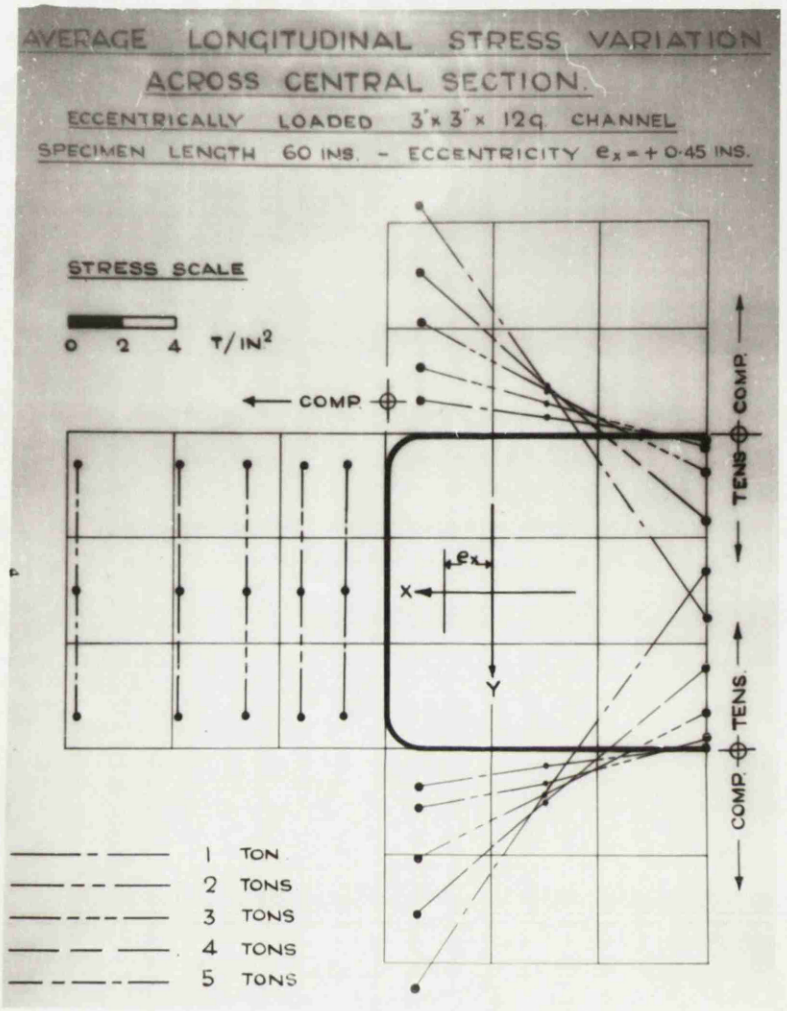
AVERAGE LONGITUDINAL STRESS VARIATION
ACROSS CENTRAL SECTION.
ECCENTRICALLY LOADED 3"x3"x 12g. CHANNEL
SPECIMEN LENGTH 60 INS. - ECCENTRICITY e_x = + 0·45 INS.
STRESS SCALE
0 2 4 T/IN²
COMP.
TENS.
COMP.
e_x
X
Y
COMP.
TENS.
1 TON
2 TONS
3 TONS
4 TONS
5 TONS

FIG. 32.

2. METHOD OF TESTING.

(i) Load Capacity Tests.

All the specimens were measured and mean values of thickness and width of plate components recorded. The clamps were adjusted for the required eccentricity and a specimen fitted into the clamps. The strut was then placed in position in the testing machine. The load was applied gradually and zero values of deflection and angles of twist were recorded. This procedure was repeated for each load setting till failure. The general behaviour of the specimen was carefully observed, the failure load recorded and the observed mode of failure noted for comparison with the theoretical work.

(ii) Stress Distribution Tests.

The longitudinal stresses at the central section of four specimens were recorded by means of electrical resistance strain gauges as a feature of general interest, and as a check on the concentricity and eccentricity of the loads applied. The stress distributions are shown in Figures 29 to 32. It can be seen that in the case of the concentrically loaded angle strut there is a slight tendency towards a stress increase in the region of the heel, due to the effect of the gradually developing twist.

In the case of the eccentrically loaded struts the distributions correspond to the eccentricities applied.

(iii) Tensile Tests.

Strips suitable for tensile tests were cut from a number of representative specimens. The procedure and results of the tensile tests are given in Appendix 6.

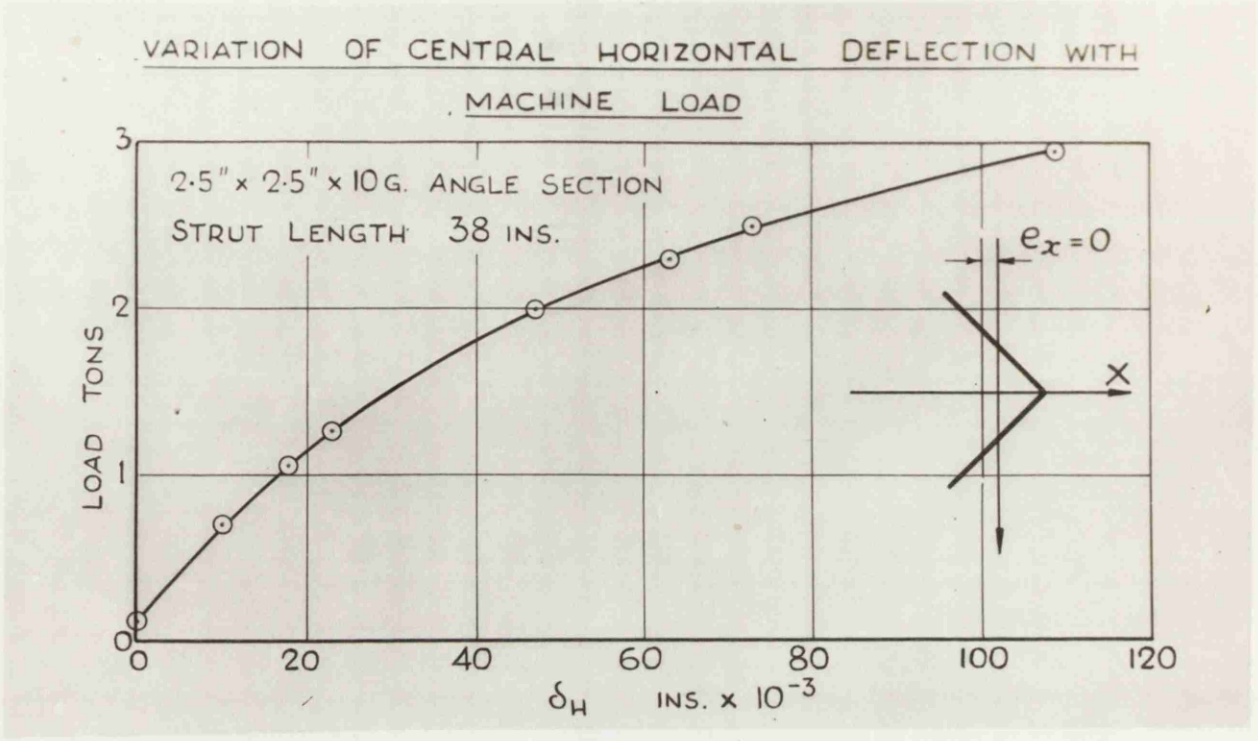
VARIATION OF CENTRAL HORIZONTAL DEFLECTION WITH MACHINE LOAD
2·5" x 2·5" x 10G. ANGLE SECTION
STRUT LENGTH 38 INS.
$e_x = 0$
X
LOAD TONS
0
1
2
3
0
20
40
60
80
100
120
δ_H INS. x 10^{-3}

FIG. 33.

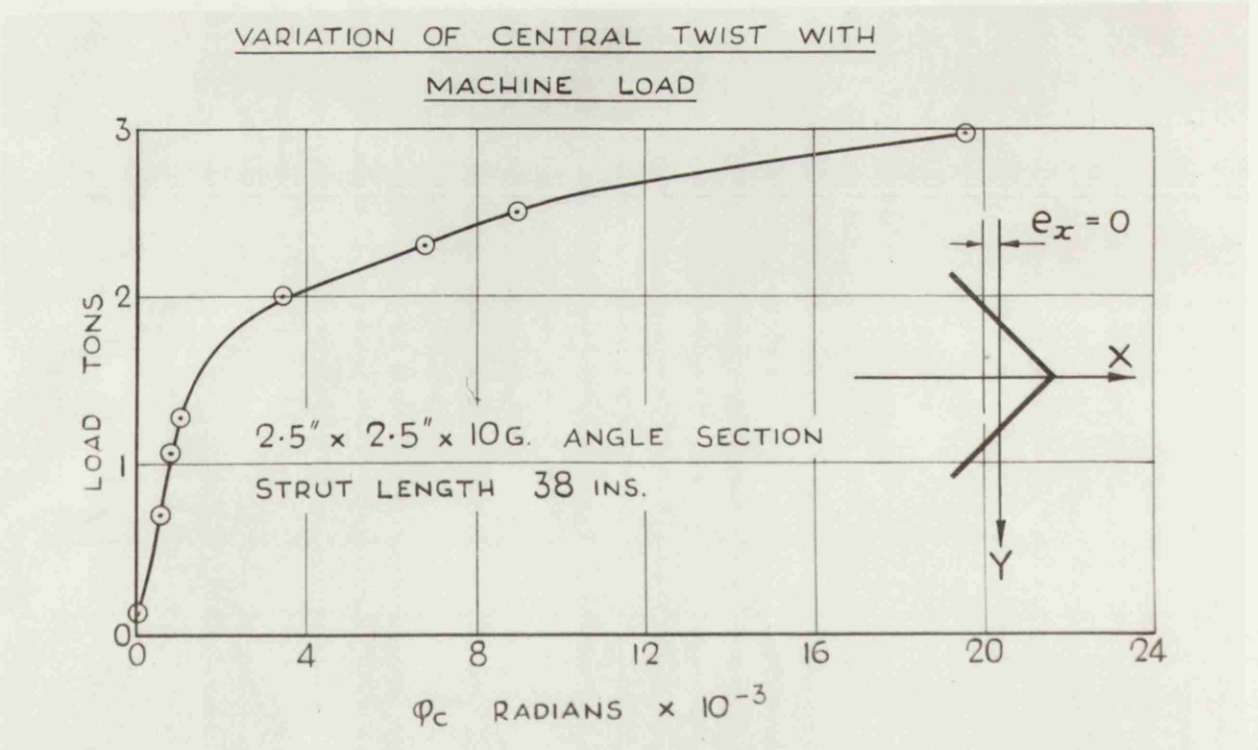
VARIATION OF CENTRAL TWIST WITH MACHINE LOAD
2·5" x 2·5" x 10G. ANGLE SECTION
STRUT LENGTH 38 INS.
$e_x = 0$
X
Y
LOAD TONS
0
1
2
3
0
4
8
12
16
20
24
φ_c RADIANS x 10^{-3}

FIG. 34.

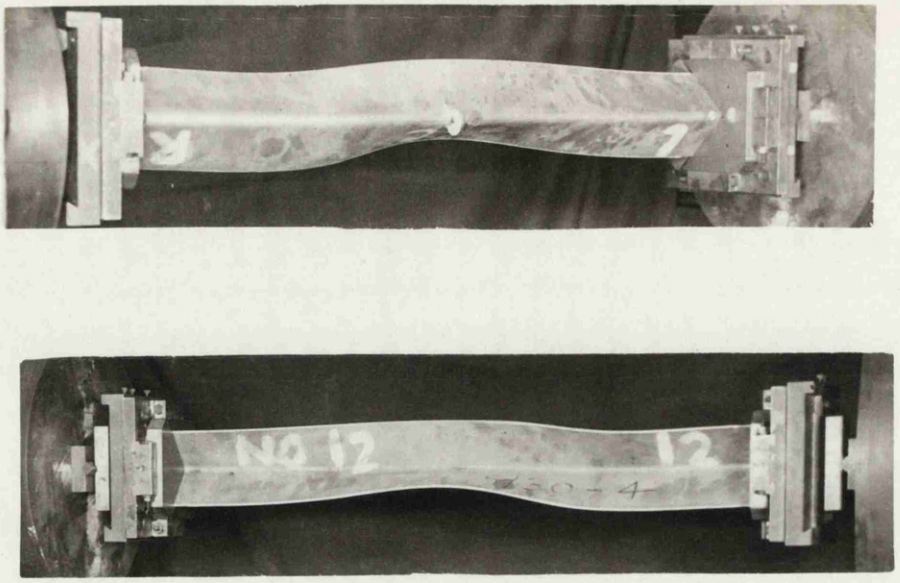

FIG. 35.

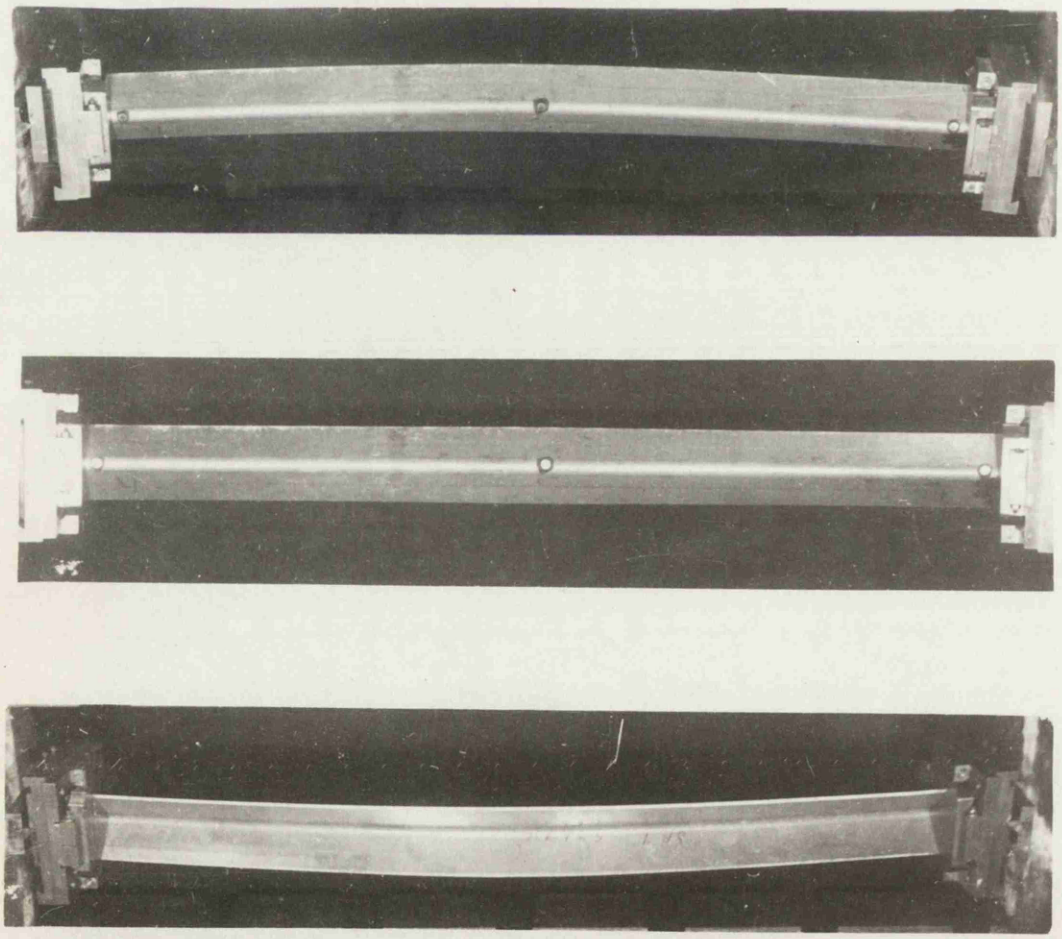

FIG. 36.

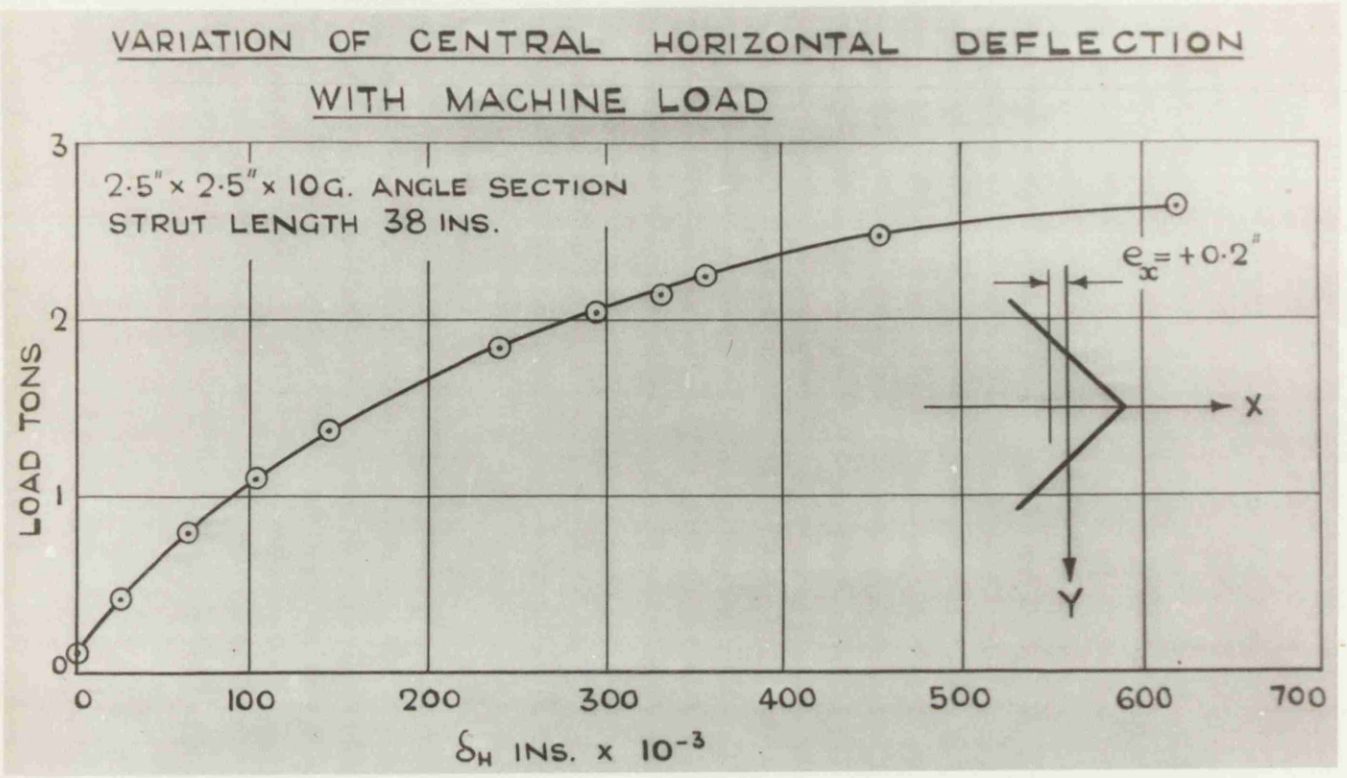
VARIATION OF CENTRAL HORIZONTAL DEFLECTION
WITH MACHINE LOAD
2·5" x 2·5" x 10G. ANGLE SECTION
STRUT LENGTH 38 INS.
e_x = +0·2"
X
Y
LOAD TONS
0
1
2
3
0
100
200
300
400
500
600
700
δ_H INS. x 10^{-3}

FIG. 37.

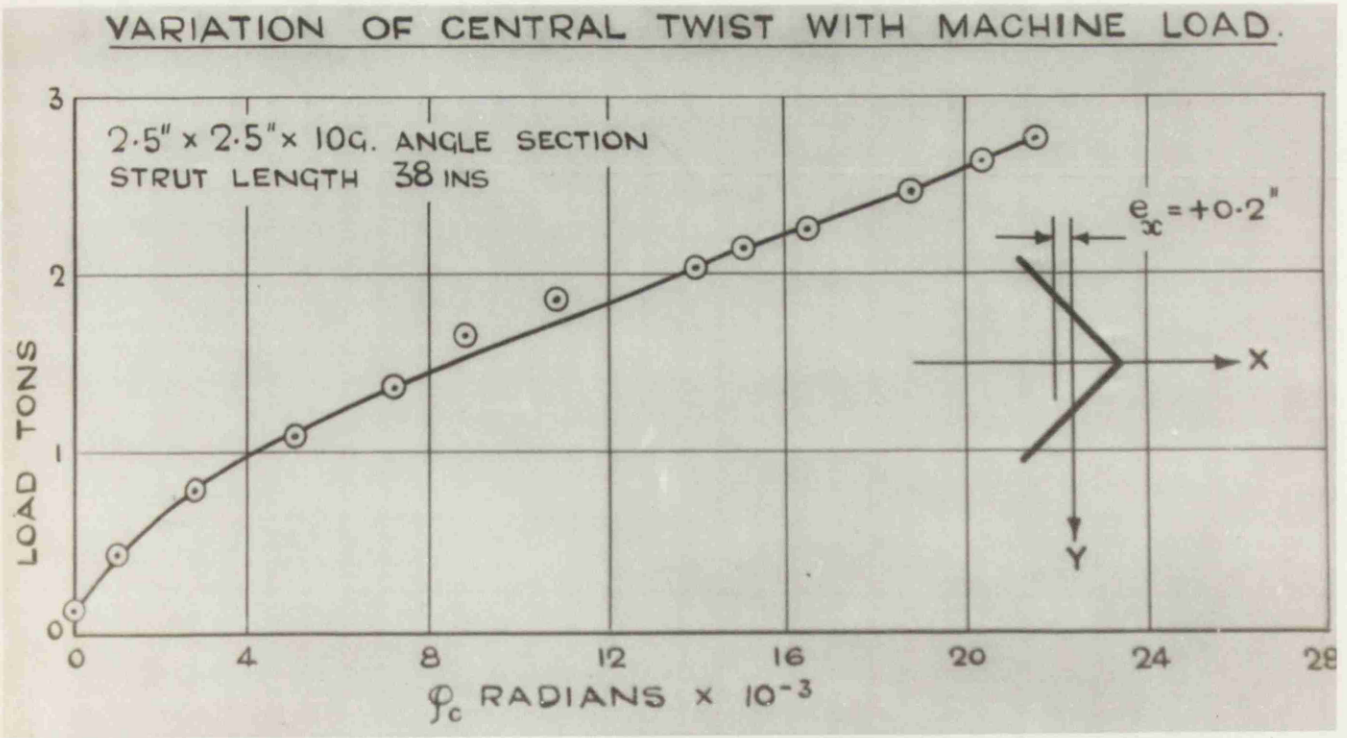
VARIATION OF CENTRAL TWIST WITH MACHINE LOAD.
2·5" x 2·5" x 10G. ANGLE SECTION
STRUT LENGTH 38 INS
e_x = +0·2"
X
Y
LOAD TONS
0
1
2
3
0
4
8
12
16
20
24
φ_c RADIANS x 10^{-3}

FIG. 38.

3. EXPERIMENTAL RESULTS.

(i) Angle Section Struts.

Three typical modes of failure were observed, torsional-flexural, purely flexural and material failure. Torsional-flexural failure was denoted by a gradual increase of central deflection and twist as the load approached the failure load, then by a sudden increase of twist at failure. Figures 33, 34, 29 and 30 show typical deflection, twist and stress distribution values respectively. Figure 35 shows a typical example of this mode of failure. Pure flexural failure was characterised by a sudden collapse of the specimen due to bending or bowing in the shorter specimens, or a gradual bending action in the longer specimens, with little or no twist. Figures 37 and 38 show typical deflection and twist values. Figure 36 shows a concentrically loaded equal angle strut after failure by pure flexure. Material failure occurred in some of the shorter specimens.

(ii) Channel Section Struts.

The three typical modes of failure observed were torsional-flexural, purely flexural and plate component failure. Torsional-flexural and purely flexural failure were denoted by similar characteristics as for angle struts; typical deflection and twist values are shown in Figures

VARIATION OF CENTRAL HORIZONTAL AND VERTICAL DEFLECTION WITH MACHINE LOAD.

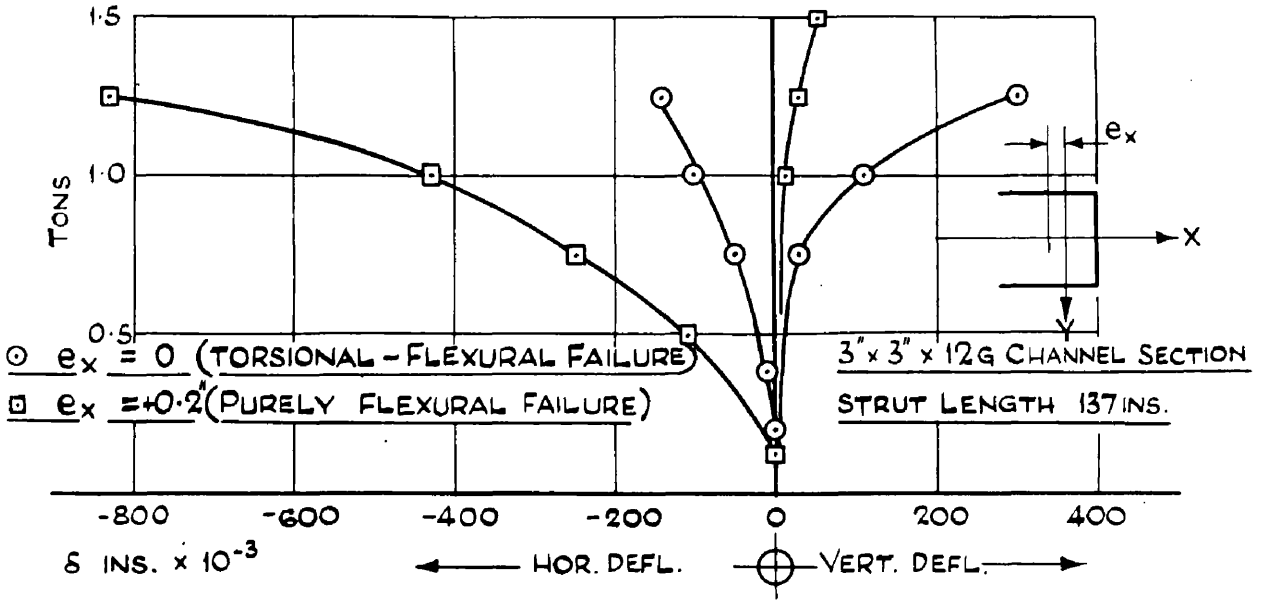

FIG. 39

VARIATION OF CENTRAL TWIST WITH MACHINE LOAD

3" x 3" x 12G CHANNEL SECTION. STRUT LENGTH 137 INS.

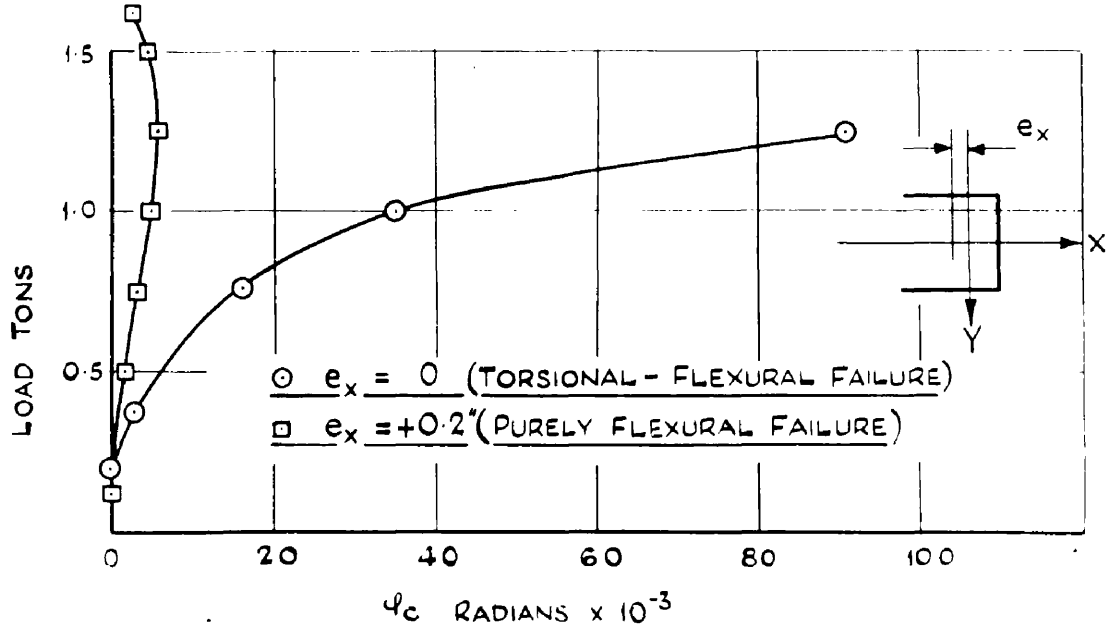

FIG. 40.

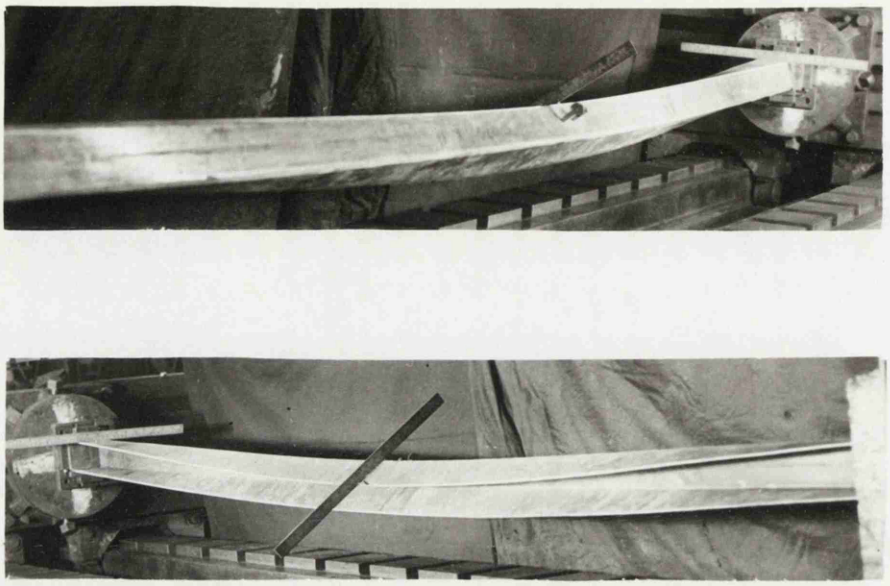

FIG. 41.

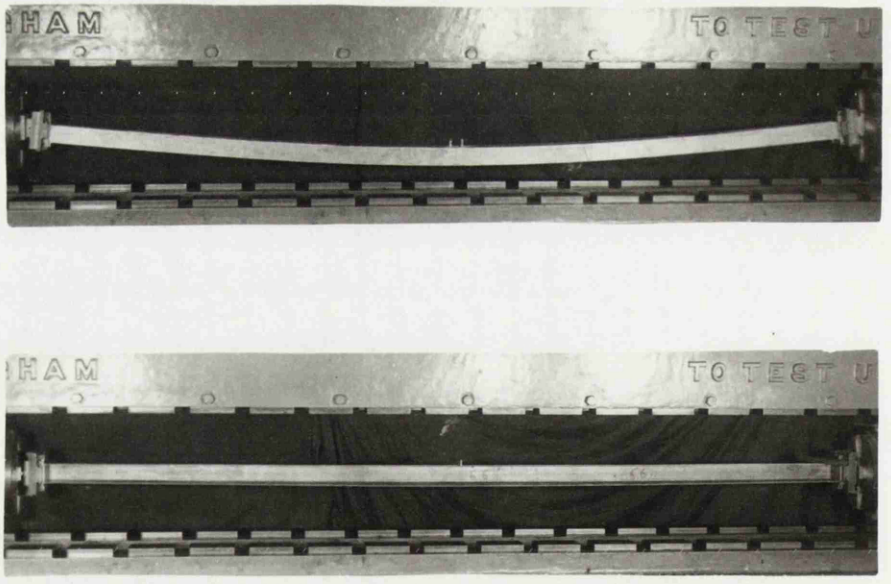

FIG. 42.

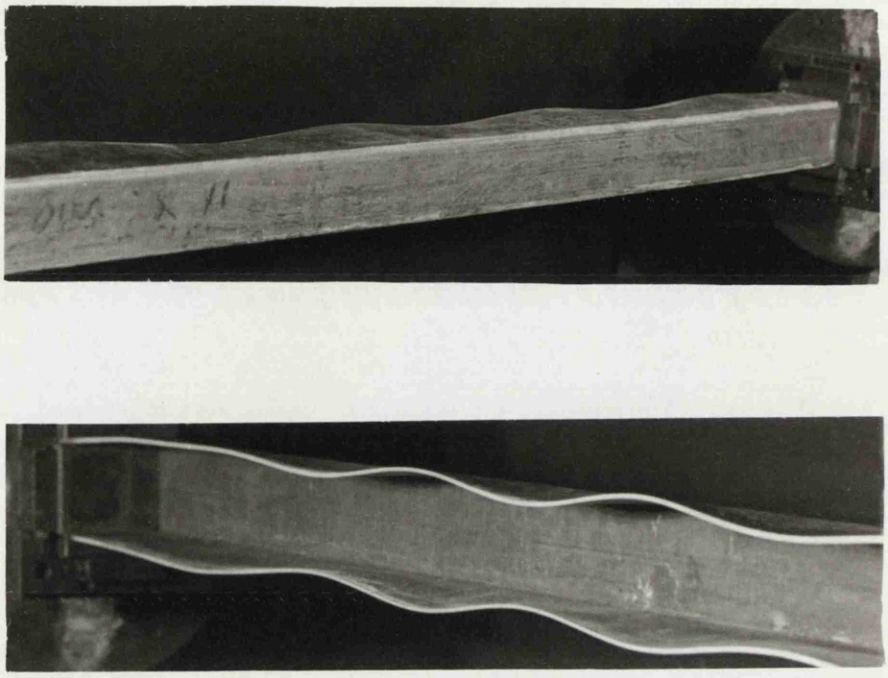

FIG. 43.

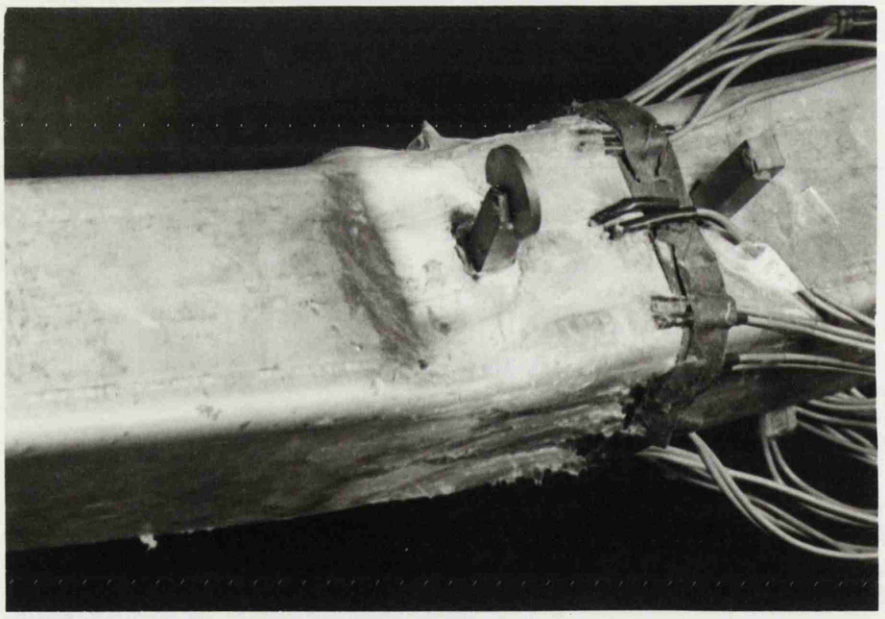

FIG. 44.

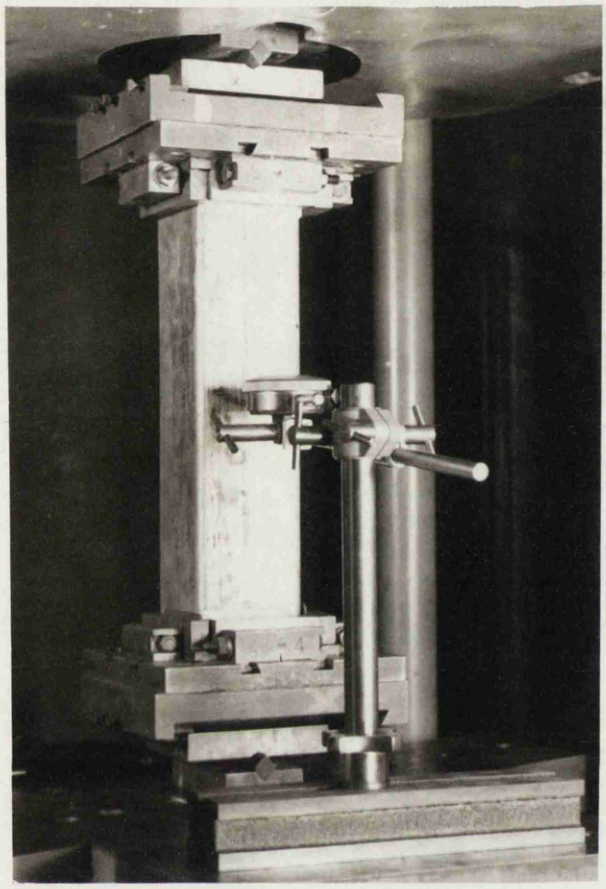

FIG. 45.

39 and 40. Figures 41 and 42 show typical examples of torsional-flexural and purely flexural failure, respectively. Plate component failure was characterised by the failure as a plate of either the flange or web components of a channel strut. Flange failure was denoted by symmetrical waving of the flanges, Figure 43, which increased with load. As the failure load was approached sudden excessive flange deflections occurred at one of the wave peaks, while the other waves were "ironed out". In some tests failure of the web suddenly occurred near the middle of the strut length. Figure 44 shows a close-up of the failed part of a web of an eccentrically loaded channel, which had deflected considerably due to relatively high eccentricity. The two different types of plate failure were readily recognised. In most cases of web failure, secondary flange failure occurred. Typical stress distribution values are shown in Figures 31 and 32.

In the tests to investigate the effect of the section profile, it was observed that the channels with broader flanges were generally more susceptible to flange plate failure than those with narrower flanges, which failed either by material failure or due to flexure, depending on the length of the specimen. Most of the 12 inch eccentrically loaded channels failed by flange failure, those with narrower flanges failed by material failure. The set-up for the 12 inch specimens in the 50 ton Denison Machine is shown in Figure 45.

All the experimental failure modes and loads are listed in Appendix 5.

PART IV.

ANALYSIS AND DISCUSSION OF EXPERIMENTAL RESULTS.

1. STRUT TESTS ON ANGLE SECTIONS.

2. STRUT TESTS ON CHANNEL SECTIONS.

   (i) Concentrically Loaded Channels.

   (ii) Eccentrically Loaded Channels.

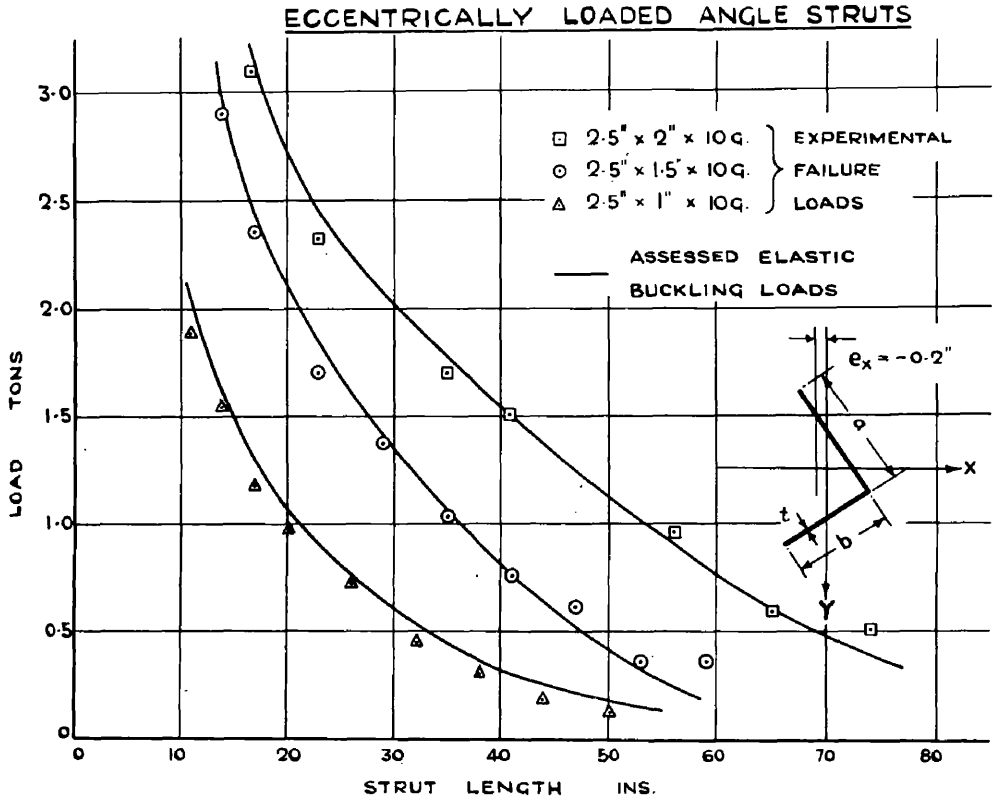
ECCENTRICALLY LOADED ANGLE STRUTS
2·5" x 2" x 10G. EXPERIMENTAL
2·5" x 1·5" x 10G. FAILURE
2·5" x 1" x 10G. LOADS
ASSESSED ELASTIC BUCKLING LOADS
e_x = -0·2"
LOAD TONS
STRUT LENGTH INS.
3·0
2·5
2·0
1·5
1·0
0·5
0
10
20
30
40
50
60
70
80
X
Y
t
b

FIG. 46.

1. STRUT TESTS ON ANGLE SECTIONS.

The modes of collapse encountered in the angle strut tests were mainly two over-all failure types - torsion combined with flexure and pure flexure. Some of the shorter specimens failed due to failure of the material. The unequal angle struts all failed by combined torsion and flexure; but the longer struts failed primarily in flexure.

The elastic critical instability loads in torsion-flexure were deduced by Southwell-Lundquist plots (32,36), of the measured angles of twist. These, as shown in Figure 46, come so close to the experimental failure loads that the latter have been used in all comparisons.

To obtain an over-all view of all the results it was essential to present the relevant theoretical results in the form of a single curve. The experimental values, including failures in both pure flexure and flexure combined with torsion, could then be represented on the same graph. This has been done by utilising the device of an equivalent slenderness ratio and a nominal stress concept.

The equivalent slenderness ratio of a strut was obtained by equating the theoretical critical load $P_{cr.}$ of the particular strut considered in torsion-flexure, to the critical load in pure flexure, of an "equivalent" strut of the same section profile, i.e.,

STRUT TESTS ON ANGLE SECTIONS - CONCENTRIC AND ECCENTRIC AXIAL LOAD

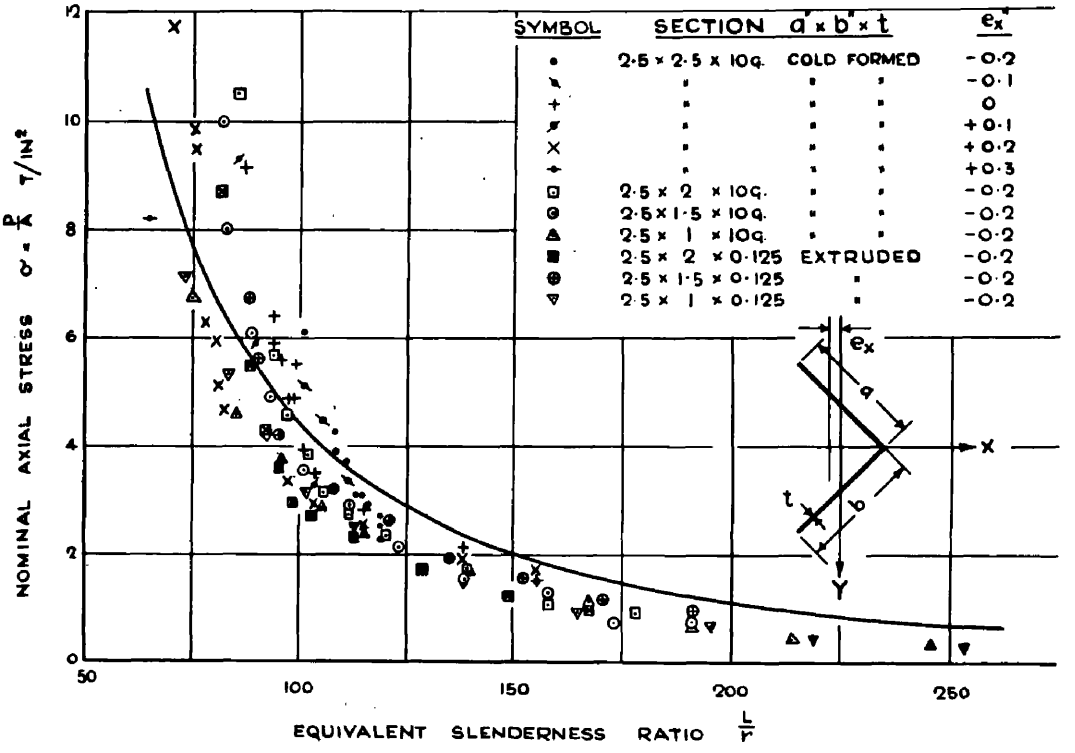

FIG. 47.

$$P_{cr.} = \frac{A\pi^2 E}{\left(\frac{L}{r}\right)^2_{eq.}}$$

$$\text{hence } \left(\frac{L}{r}\right)_{eq.} = \sqrt{\frac{A\pi^2 E}{P_{cr.}}} \qquad (97)$$

The nominal critical and nominal failure stresses $\sigma_{N.cr.}$ and $\sigma_{N.F.}$ are the averages of the critical and failure loads over the cross section, i.e.,

$$\sigma_{N.cr.} = \frac{P_{cr.}}{A} \qquad (98)$$

$$\sigma_{N.F.} = \frac{P_F}{A} \qquad (99)$$

The reduced theoretical curve and the experimental results are shown in Figure 47.

It is seen that on the whole the agreement between experimental and theoretical values is quite satisfactory. The characteristic feature of the strut instability curves, namely the tendency of the theoretical values to be slightly higher at the higher values of slenderness ratio is manifested. This is due to the increasingly greater effects of accidental eccentricities as the length of the specimen increases. In the shorter strut range, the experimental values are more evenly distributed on both sides of the theoretical curve. Taking account of these considerations, Figure 47 clearly indicates that the theoretical values obtained, using the iterative method of solution put forward in the theoretical part of the thesis, form a rational and

ECCENTRICALLY LOADED ANGLES - VARYING ECCENTRICITY

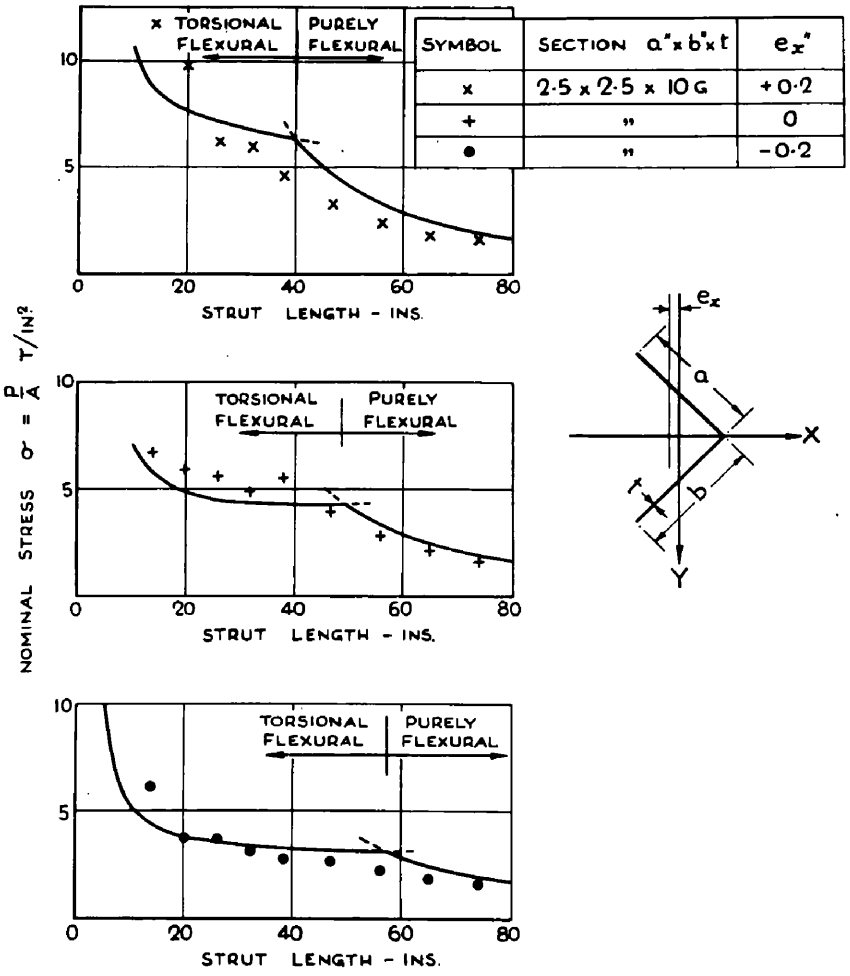

FIG. 48.

reliable basis of assessing the torsional-flexural buckling strengths of angle sections.

Figures 48 to 52 present a sample selection of the experimental results of Figure 47 in greater detail to indicate the variations corresponding to different failure modes.

The effect of different eccentricities on struts of equal angle cross section and varying length is shown in Figure 48. The following points are apparent.

(i) In the torsional-flexure failure range the nominal failure stress $\sigma_{N.F.}$ increases as the point of applied load approaches the shear centre from the direction of the centroid, i.e., eccentricity has, as indicated by the theory, a definite influence on the value of the elastic critical load.

(ii) In the pure flexural failure range it is seen that, irrespective of the applied eccentricity, the nominal failure stress $\sigma_{N.F.}$ remains sensibly constant for a given length. This is the well-known concept of over-all instability in pure flexure.

(iii) The theoretical curves indicate a sharp change over from torsional flexural failure in the shorter lengths to pure flexural failure in the longer lengths. This sharp transition could not be obtained experimentally, since at such change-over points the failure mode becomes extraordinarily sensitive to the effects of unavoidable irregularities.

(iv) Agreement between the theoretical and experimental results is

ECCENTRICALLY LOADED ANGLES - VARYING LENGTH

SYMBOL	SECTION a"x b"x t	e_x"
●	2·5 x 2·5 x 10 G	-0·2
⊡	2·5 x 2 x 10 G	-0·2
⊙	2·5 x 1·5 x 10 G	-0·2
▲	2·5 x 1 x 10 G	-0·2

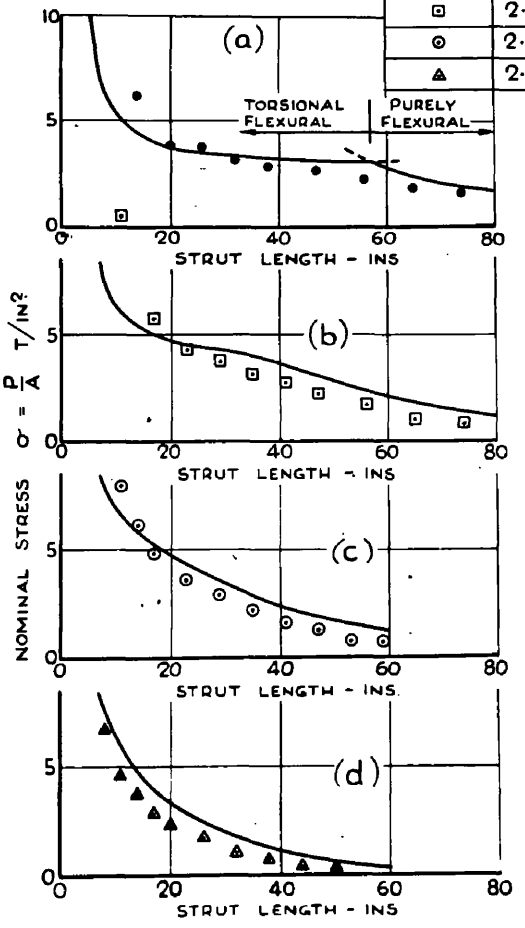

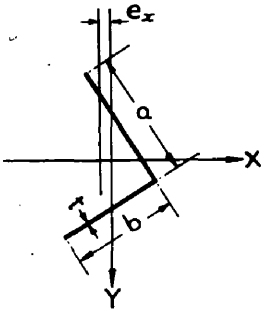

ALL FAILURES OF (b), (c) AND (d) DUE TO COMBINED TORSION AND FLEXURE

FIG. 49.

ECCENTRICALLY LOADED ANGLES VARYING LENGTH

SYMBOL	SECTION a' x b' x t	ex'
⊠	2·5 x 2 x 0·125	- 0·2
⊕	2·5 x 1·5 x 0·125	- 0·2
▽	2·5 x 1 x 0·125	- 0·2

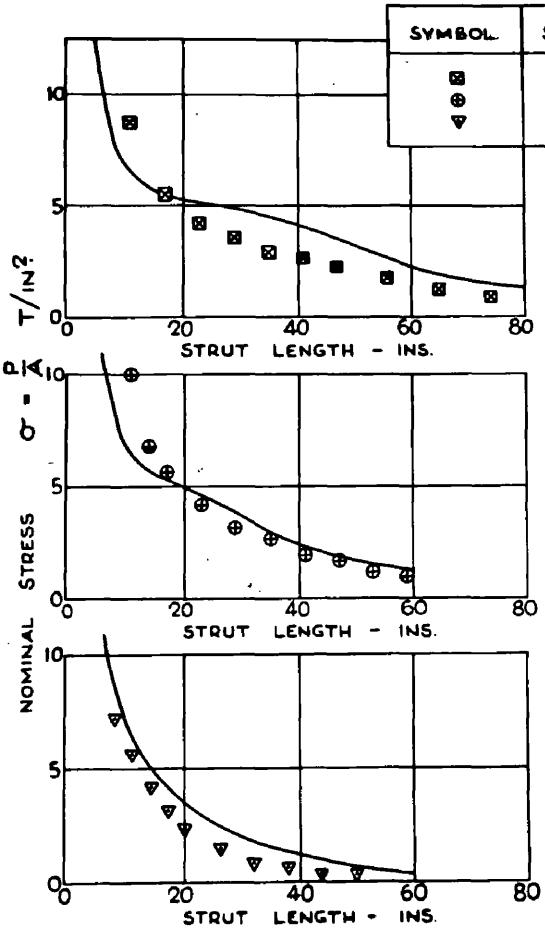

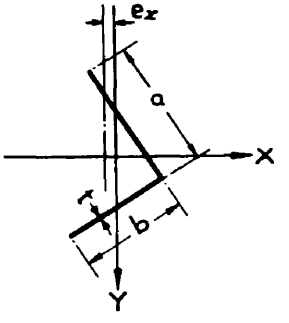

ALL FAILURES DUE TO COMBINED TORSION AND FLEXURE

FIG. 50

reasonable, keeping in mind that specific individual values rather than a range,are being compared. The tendency appears to be a slight underestimate of the torsional-flexural failure stress on short lengths. This may be due to an underestimate of the torsional stiffness of the section outline. It is significant to point out that while these separate values appear to be slightly higher than the theoretical, as can be seen in Figure 47, the distribution of the collective results show a balancing number of experimental results slightly below the theoretical values.

Figure 49 shows the effect of variation of profile at a constant eccentricity on the stress-length curve. The results generally show good agreement with the theoretically computed values. The experimental values are slightly lower than the theoretical throughout the range considered, except for the shortest struts. It is of interest to note that the curves of failure-stress versus length for equal angles show, as mentioned, a sharp change over from the torsional-flexural to the purely flexural mode of failure. This is replaced for unequal angles by a variation corresponding to torsional-flexural failure throughout, predominantly torsional in character on the shorter lengths, tending to predominantly flexural for the longer lengths.

Figure 50 shows the theoretical and experimental values corresponding to those of Figure 49, but for extruded sections of similar overall section dimensions. Agreement is again obtained between experimental and theoretical values.

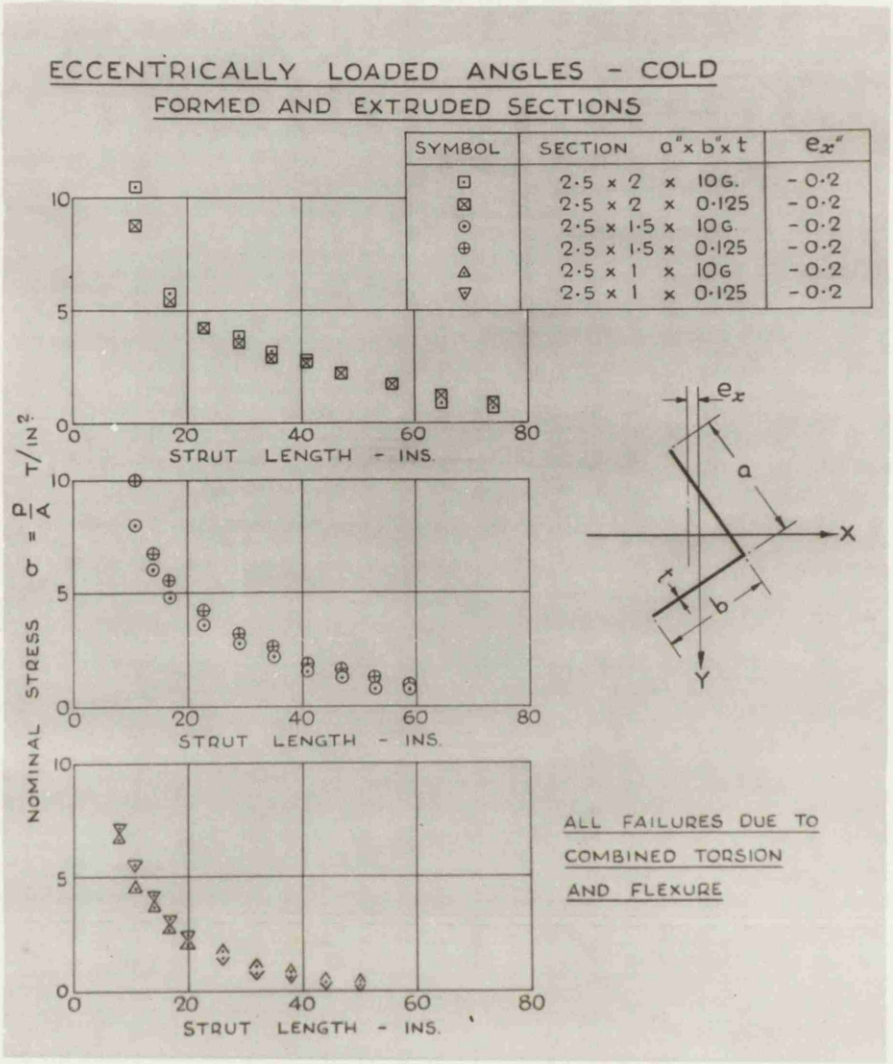
ECCENTRICALLY LOADED ANGLES - COLD FORMED AND EXTRUDED SECTIONS
SYMBOL
SECTION a"x b"x t
ex"
2·5 x 2 x 10G. - 0·2
2·5 x 2 x 0·125 - 0·2
2·5 x 1·5 x 10G. - 0·2
2·5 x 1·5 x 0·125 - 0·2
2·5 x 1 x 10G - 0·2
2·5 x 1 x 0·125 - 0·2
NOMINAL STRESS σ = P/A T/IN²
STRUT LENGTH - INS.
ex
a
b
t
X
Y
ALL FAILURES DUE TO COMBINED TORSION AND FLEXURE

FIG. 51.

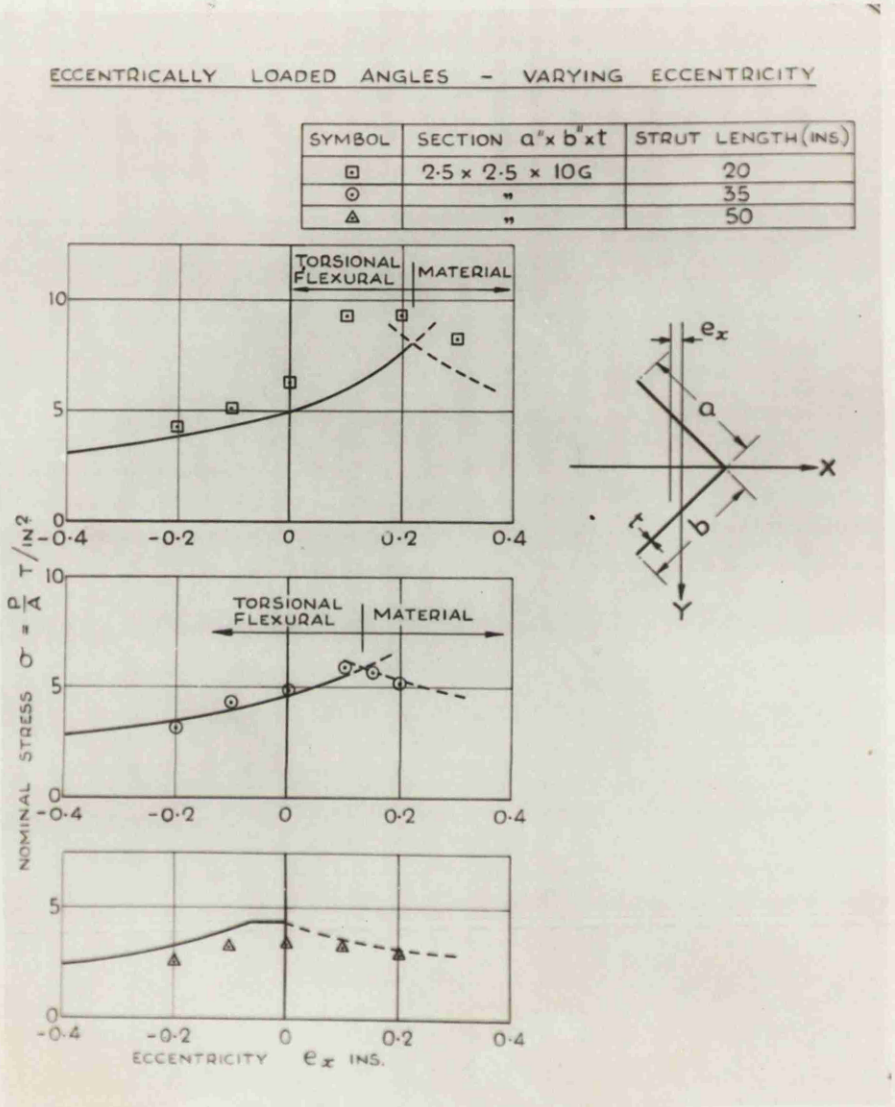
ECCENTRICALLY LOADED ANGLES - VARYING ECCENTRICITY
SYMBOL
SECTION a"x b"xt
STRUT LENGTH (INS.)
2·5 x 2·5 x 10G
20
"
35
"
50
TORSIONAL FLEXURAL
MATERIAL
NOMINAL STRESS σ = P/A T/IN²
ECCENTRICITY e_x INS.
e_x
a
b
t
X
Y

FIG. 52.

Figure 51 gives a direct comparison between equivalent cold formed and extruded section profile struts. It can be seen that there is literally no difference between the behaviour of cold formed and extruded sections under eccentric axial loads.

Figure 52 shows the effect of eccentricity on the critical stress of struts of various length. The main feature, which has already been mentioned, is a decrease or an increase from the critical load under concentric loading, depending upon whether the load point moves away or towards the shear centre from the centroid. The failure mode encountered, in the range of strut lengths considered, changes from torsional-flexural to a stable material failure in bending at the higher eccentricities when the load is between the centroid and the shear centre. Agreement between theory and experiment is again reasonable.

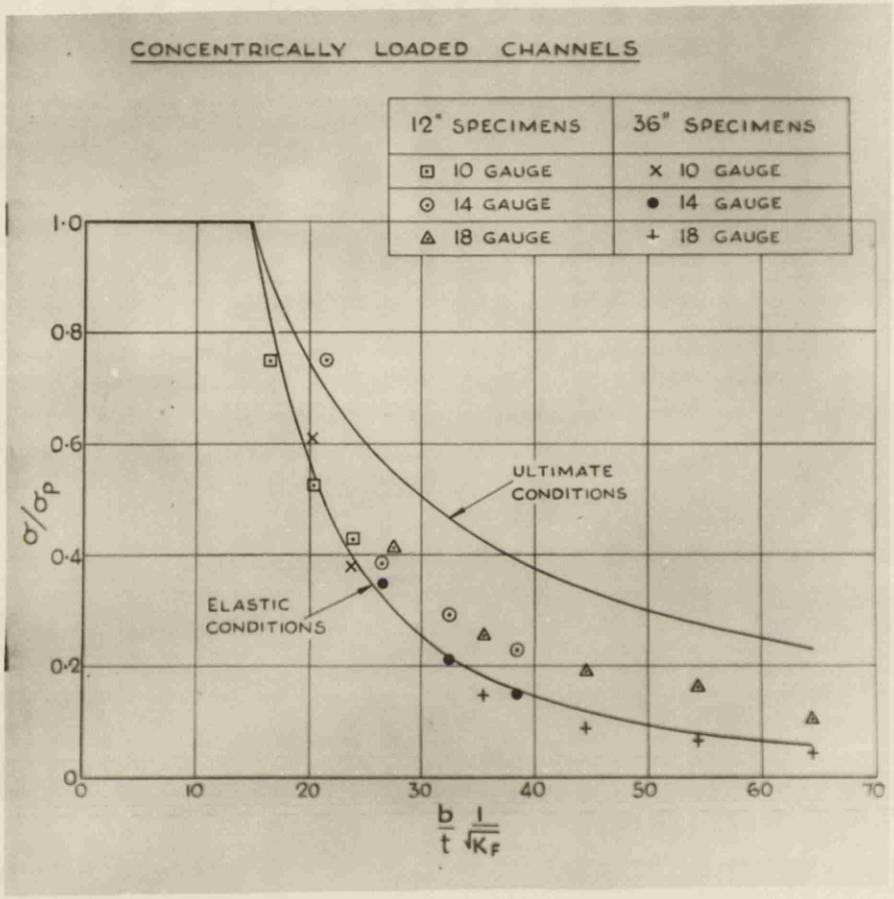
CONCENTRICALLY LOADED CHANNELS
12" SPECIMENS
36" SPECIMENS
10 GAUGE
14 GAUGE
18 GAUGE
10 GAUGE
14 GAUGE
18 GAUGE
ULTIMATE CONDITIONS
ELASTIC CONDITIONS
σ/σp
1·0
0·8
0·6
0·4
0·2
0
0
10
20
30
40
50
60
70
b/t √(l/KF)

FIG. 53.

2. STRUT TESTS ON CHANNEL SECTIONS.

The experimental work was designed to investigate local instability (i.e., flange failure) of cold formed aluminium channel struts, when the specimens were concentrically and eccentrically loaded. The eccentricities applied were along the axis of symmetry of the channels. As a further step, a preliminary investigation of the relation between direct and bending stress values, under varying eccentricity, was also included.

(i) Concentrically Loaded Channels.

Figure 53 presents a comparison of the experimental and theoretical values obtained. The theoretical curves are based on equations (11) and (12) of Part I. These define the theoretical and ultimate stresses and are restated as follows.

$$\sigma_{cr.} = K_F \frac{\pi^2 E}{12(1-\nu^2)} \left(\frac{t}{b}\right)^2 \qquad \text{(11)}$$

$$\sigma_u = \frac{\pi t \sqrt{K_F E \sigma_p}}{b\sqrt{12(1-\nu^2)}} \qquad \text{(100)}$$

replacing σ_p for σ_y in equation (12). The value of the plate constant K_F can be obtained using Figure 20.

It can be seen that, if the basis of plotting is taken as $\frac{b}{t}\frac{1}{\sqrt{K_F}}$, then single theoretical curves are obtained for channels of any cross sectional dimensions.

The stresses are presented for clearer comparison as fractions of the proof stress, i.e.,

$\frac{\sigma_{cr.}}{\sigma_p}$ and $\frac{\sigma_u}{\sigma_p}$ for the theoretical values,

and $\frac{\sigma_F}{\sigma_p}$ for the experimental results,

where σ_F is the average direct stress at failure.

The introduction of the proof stress to allow generalisation for the slightly different grades of material used, strictly speaking, upsets the single curve presentation, since there is one curve for each value of the proof stress. These differences, however, are so small for the range of proof stress values encountered, that the differences in the various curves cannot be shown up and the single curves, as indicated, are an accurate representation of both the elastic and ultimate conditions in the range considered.

The 12 inches long specimen results approximate to pure plate failure, since the lateral deflection of the edge of the flange connected to the web is negligible. The experimental values exhibit the same characteristics as those obtained for steel, Harvey(25), namely, as the width to thickness ratio of the flange increases, the post elastic load carrying capacity increases and the experimental points tend towards the ultimate curve.

In the 36 inches long specimens, this same effect is obscured by the effect of length which, by permitting lateral deflections of significant magnitude, induces a drop in plate strength. This is the reason for the apparently good agreement of the long specimens with the critical curve for elastic conditions.

(ii) Eccentrically Loaded Channels.

The iterative method, the application of which to the instability of flat plates under longitudinal compression, is presented in Part II, Section 3, of the thesis, may be generally applied to any type of longitudinal load variation. The laborious computation involved, however, precluded its application in the range of work undertaken to more than one case of load distribution. The chosen instance was that of the variation shown in Figure 18. Experimentally this was achieved for the 12 inches long specimens, by appropriately altering the load eccentricity to give the required load distribution.

The theoretical and experimental results are again presented graphically, using a single graph plot by utilising the group variable $\frac{b}{t}\frac{1}{\sqrt{K_F}}$ as before. The theoretical elastic critical stress at the free edge of the flange is given in Part II, Section 3, as

$$(N_o)_{cr.} = K_F \frac{\pi^2 D}{b^2} \qquad (74)$$

or

$$(\sigma_o)_{cr.} = K_F \frac{\pi^2 E}{12(1-\nu^2)} \left(\frac{t}{b}\right)^2 \qquad (101)$$

It is assumed that collapse of eccentrically loaded wide flanges obtains

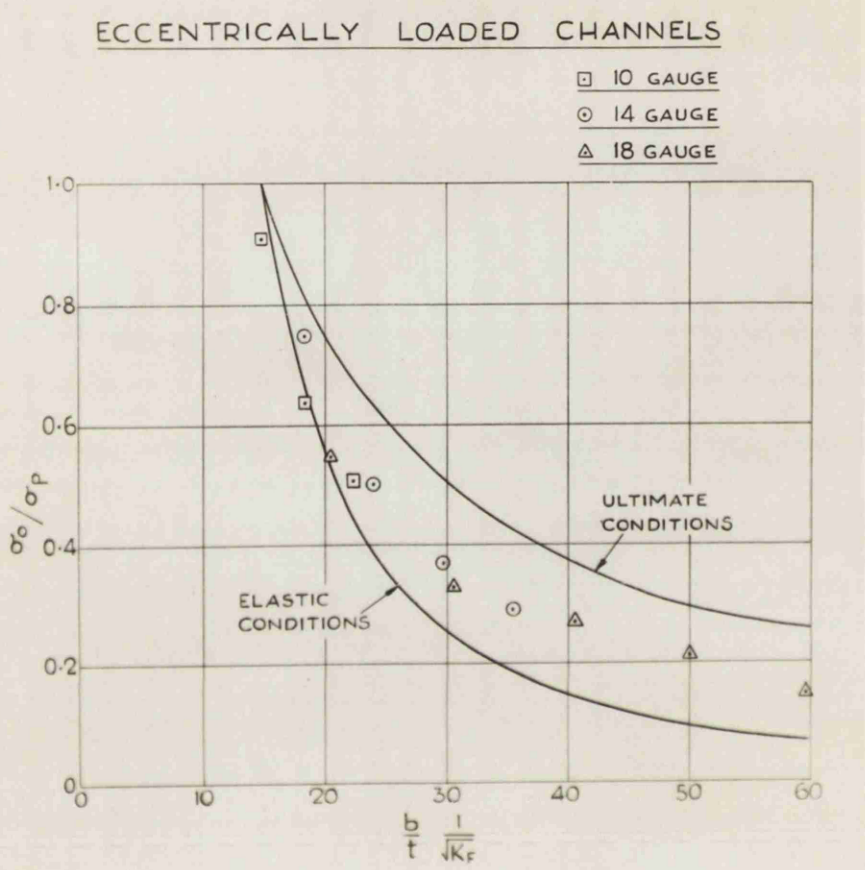
ECCENTRICALLY LOADED CHANNELS
10 GAUGE
14 GAUGE
18 GAUGE
1·0
0·8
0·6
0·4
0·2
0
σo/σp
ULTIMATE CONDITIONS
ELASTIC CONDITIONS
0
10
20
30
40
50
60
b/t √(1/Kf)

FIG. 54.

at the same load as that carried by a plate of width b_e of the same edge fixity and stress distribution as the wide flange, with a free edge stress = σ_p , i.e.,

$$\sigma_p = K_F \frac{\pi^2 E}{12(1-\nu^2)}\left(\frac{t}{b_e}\right)^2 \qquad (102)$$

hence $$b_e = \pi t \sqrt{\frac{K_F E}{12(1-\nu^2)\sigma_p}}$$

from which $$\sigma_{o_u} = \frac{b_e}{b}\sigma_p = \frac{\pi t}{b}\sqrt{\frac{K_F E \sigma_p}{12(1-\nu^2)}} \qquad (103)$$

The stresses $\sigma_{o_{cr.}}$, σ_{o_u} and σ_{o_F} , are again presented as fractions of the proof stress.

It should be noted as a matter of interest that the theoretical graphs are identical with those of the centrally loaded channels. The difference for the same channel section, between concentric and eccentric loading conditions, is manifested by a horizontal shift of the relevant point on the curve, because of the change in the K_F value.

Figure 54 shows a comparison between theoretical and experimental values obtained for the eccentrically loaded channels in the plate failure range. It can be seen that the general tendency is the same as that for concentrically loaded channels, but the experimental results in this case tend to approach the ultimate conditions more closely, within the same range of $\frac{b}{t}\frac{1}{\sqrt{K_F}}$ values. This is anticipated as a characteristic of load eccentricity and results in the relatively greater post elastic carrying capacity of an unsymmetrically loaded flange. In the stress distribution investigated, the connected edge carried

CHANNEL STRUT TESTS

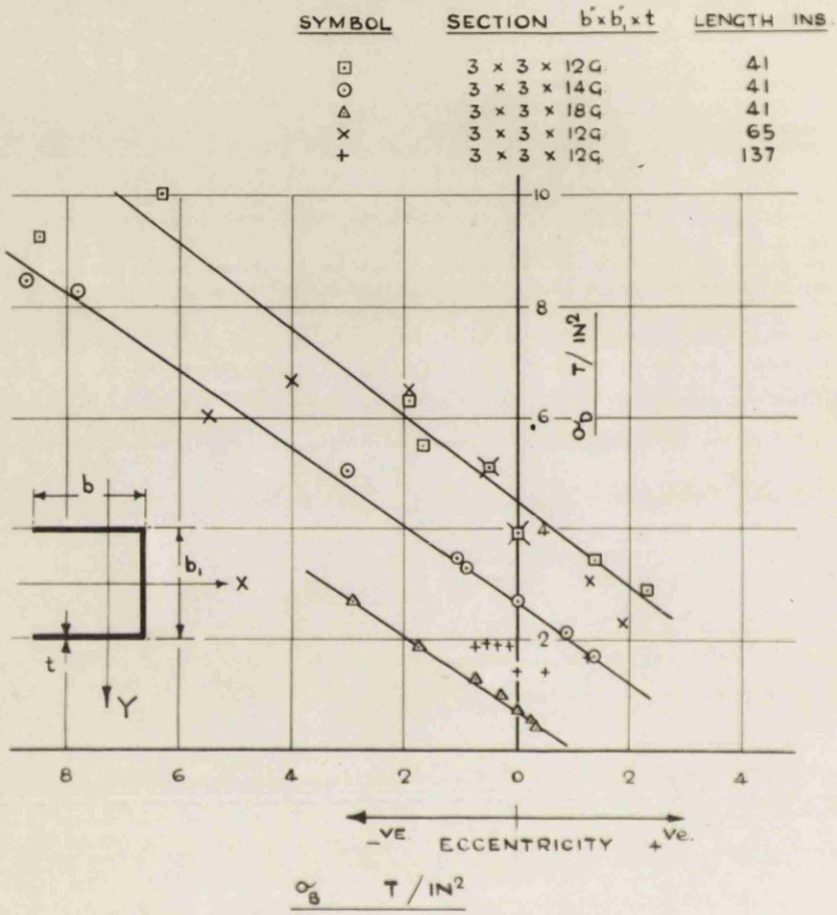

FIG. 55

$\frac{1}{4}$ of the stress at the free edge; thus, when the free edge stress reached its appropriate critical value, the connected edge was still capable of sustaining a greater amount of post critical stressing than in the concentric loaded case, where the free and connected edges are both at the same uniform stress value. Keeping this in mind, the degree of agreement obtained between the experimental and the theoretical values is comparable to that obtained in the concentrically loaded channels

The results of a set of preliminary tests into the relationship between direct and maximum free edge bending stress for channels, are presented in Figure 55. The section outline used was of square form and incorporated thickness and length variations. The investigation was not intended to be carried beyond the stage reached, i.e., tentative interaction curves. It can be seen that the bending and direct stresses corresponding to the eccentric failure loads (computed on the basis of the simple bending theory), appear to give straight lines indicating that these struts fail at some constant maximum stress. This matter forms part of future research programmes.

SUMMARY AND CONCLUSIONS.

SUMMARY AND CONCLUSIONS.

1. An iterative method of general application to problems of instability is presented.

2. This is applied to obtain:

(i) The critical load initiating over-all instability in torsion-flexure for boundary conditions corresponding to "hinged" ends in flexure accompanied by complete warping restraint at these ends.

(ii) The critical load initiating local instability in flexure of eccentrically loaded channel sections of short length.

3. The experimental work carried out consisted of strut tests to failure of aluminium alloy equal and unequal angle and channel specimens, under varying conditions of length, eccentricity, cross sectional dimensions and method of manufacture. The range investigated included failure due to over-all instability in torsion-flexure and local instability in flexure.

4. The following theoretical and/or experimental results obtained are of particular interest.

(i) Warping restraint at the ends appreciably increases the buckling strength of struts in torsion-flexure.

(ii) The buckling strength is influenced by the eccentricity of the applied load, increasing as the point of applied load approaches the shear centre from the direction of the centroid.

(iii) There appears to be no difference between the behaviour of cold formed and extruded angle section struts under eccentric axial loads.

(iv) Local buckling of channel sections under eccentric axial loads may be treated in the same manner as the buckling of uniformly compressed sections, provided the effect of eccentricity on the appropriate support conditions of the weakest plate component (in the case considered the flange), is taken into account.

5. In general the theory developed and presented in the thesis gives good agreement with the experimental results in both the over-all and local instability cases investigated.

B I B L I O G R A P H Y.

BIBLIOGRAPHY.

1. Wagner, H., "Verdrehung und Knickung von offenen Profilen", 25th Anniversary Publication, Technische Hochschule Danzig, 1904-1929. Translated in N.A.C.A. Tech. Mem. No.807, 1936.

2. Wagner, H.and W. Pretschner, "Verdrehung und Knickung von offenen Profilen", Luftfahrt-Forschung 1934. Translated in N.A.C.A. Tech. Note No.784, 1936.

3. Lundquist, E.E., and C.M.Fligg, "A Theory for Primary Failure of Straight Centrally Loaded Columns", N.A.C.A., Report No.582, 1937.

4. Kappus, R. "Drillknicken zentrisch gedrückter Stäbe mit offenem Profil im elastischen Bereich", Luftfahrt-Forschung, 1937. Translated in N.A.C.A. Tech. Mem. No.851, 1938.

5. Goodier, J.N. "The Buckling of Compressed Bars by Torsion and Flexure", Cornell University Eng. Expt. Sta. Bull. No.27, 1941.

6. Goodier, J.N. "Flexural-Torsional Buckling of Bars of Open Section, Under Bending, Eccentric Thrust or Torsional Loads", Cornell University Eng. Expt. Sta. Bull. No.28, 1942.

7. Timoshenko, S., "Theory of Bending, Torsion and Buckling of Thin-walled Members of Open Cross Section", Journal of the Franklin Institute, March, April and May, 1945.

8. Bleich, F. "Buckling Strength of Metal Structures", McGraw-Hill Book Company, Inc., 1952 Chapter III.

9. Bleich, F., and H. Bleich, "Bending Torsion and Buckling of Bars Composed of Thin Walls", Prelim. Pub. 2nd Cong. Intern. Assoc. Bridge and Structural Eng., English edition, p.871, Berlin, 1936.

10. Baker, J.F. and J.W.Roderick, "The Strength of Light Alloy Struts" The Aluminium Development Association, Research Report No.3, 1948.

11. Niles, A.S., "Experimental Study of Torsional Column Failure", N.A.C.A. Tech. Note No.733, 1939.

12. Thomas, E.W., "Torsional Instability of Thin Angle Section Struts" Structural Engr., Vol.19, No.5, 1941, p.77.

13. Ramberg, W., and S. Levy, "Instability of Extrusions under Compressive Loads", Jour. Aeronaut. Sci., 1945, p.485.

14. Timoshenko, S., "Theory of Elastic Stability", McGraw-Hill Book Co., Inc., 1936, Chapter VII,.

15. Budiansky, B., and Pai C. Hu, "The Lagrangian Multiplier Method of Finding the Upper and Lower Limits to Critical Stress of Clamped Plates", N.A.C.A., Tech. Note No.1103, 1946.

16. Budiansky, B., R.W.Connor, and Pai C. Hu, "Notes on the Lagrangian Multiplier Method in Elastic Stability Analysis" N.A.C.A. Tech.Note No.1558, 1948.

17. Lundquist, E.E., and E.Z.Stowell, "Critical Compressive Stress for Flat Rectangular Plates Supported Along all Edges and Elastically Restrained Against Rotation Along the Unloaded Edges" N.A.C.A. Report No.733, 1942.

18. Lundquist, E.E., and E.Z.Stowell, "Critical Compressive Stress for Outstanding Flanges", N.A.C.A., Report No.734, 1942.

19. Hill, N.N. "Chart for Critical Compressive Stress of Flat Rectangular Plates", N.A.C.A., Tech.Notes No.773, 1940.

20. Bryan, G.H. "On the Stability of a Plane Plate Under Thrusts in its Own Plane with Applications to the "Buckling" of Sides of a Ship". Proceedings, London Mathematical Society, Volume 22, 1891.

21. Kroll, W.D. "Tables of Stiffness and Carry-over Factor for Flat Rectangular Plates Under Compression", N.A.C.A. Wartime Report No. L-398, 1943.

22. Kroll, W.D., G.P.Fisher and G.J.Heimerl, "Charts for Calculation of the Critical Stress for Local Instability of Columns with I, Z, Channel and Rectangular Tube Section" N.A.C.A. Wartime Report No. L-429, 1943.

23. Lundquist, E.E., and E.F.Stowell, "Restraint Provided a Flat Rectangular Plate by a Sturdy Stiffener Along an Edge of the Plate", N.A.C.A. Report No.735, 1941.

24. Chilver, A.H. "Thin Walled Structural Members", Engineering, August 31st, 1951.

25. Harvey, J.M. "Structural Strength of Thin-Walled Channel Sections", Engineering, March, 6th, 1953.

26. Davidson, J.F. "Flange Buckling in a Bent I-Section Beam", Journal of the Mechanics and Physics of Solids, Vol.I, No.3, April, 1953.

27. Stowel, E.F. "TheCompressive Strength of Flanges", N.A.C.A., Tech. Note No.2020, 1950.

28. Karman, T, E.E.Sechler, and L.H.Donell, "Strength of Thin Plates in Compression", Transactions, American Society of Mechanical Engineers, Vol.54, 1932, p.53.

29. Marguerre, K., "The Apparent Width of the Plate in Compression" N.A.C.A., Tech. Mem. No.833, 1942.

30. Levy, S., "Bending of Rectangular Plates with Large Deflections", N.A.C.A. Tech. Note No.846, 1942.

31. Winter, G. "Strength of Thin Steel Compression Flanges", Proceedings, American Society of Civil Engineers, February, 1946.

32. Southwell, R.V. "On the Analysis of Experimental Observations in Problems of Elastic Stability", Proceedings, Royal Society of London, Section A, Vol.135, April, 1932.

33. Pai, C.Hu, E.E.Lundquist, and S.B.Batdorf, "Effect of Small Deviations from Flatness on Effective Width and Buckling of Plates in Compression", N.A.C.A. Tech.Note No.1124, 1946.

34. Cox, H.L., "Note on the Southwell Method of Estimating Critical Loads", N.A.C.A. Report and Mem. No.2696, 1947.

35. Heimerl, G.J., "Determination of Plate Compressive Strengths, N.A.C.A. Tech.Note No.1480, 1947.

36. Lundquist, E.E., "Generalized Analysis of Experimental Observations in Problems of Elastic Stability", N.A.C.A., Tech. Note No.658, 1938.

37. Milne-Thomson, L.M., and L.J.Comrie, "Standard Four-Figure Mathematical Tables", Macmillan and Co. Ltd., London, 1948.

38. " Aluminium and Aluminium Alloy Sections", British Standard Specification, B.S. 1161 : 1951.

39. Handbook of Aeronautics No.1, "Structural Principles and data" Pitman and Sons, Ltd., London, 1952.

40. Cullimore, M.S.G., and A.G.Pugsley, "The Torsion of Aluminium Alloy Structural Members", The Aluminium Development Association, Research Report No.9, 1951.

41. Palmer, P.J., "The Determination of Torsion Constants for Bulbs and Fillets by Means of an Electrical Potential Analyser" The Aluminium Development Association, Research Report No.22, 1953.

42. Kenedi, R.M., W.Shearer Smith, F.O. Fahmy, "Light Structures - Research and its Application to Economic Design." Institution of Engineers and Shipbuilders in Scotland, Paper No.1203, Dec. 1955.

A P P E N D I C E S.

APPENDIX I.

INFLUENCE OF THE ASSUMED POSITION OF THE MAXIMUM DEFLECTION ON THE ACCURACY OF THE ITERATIVE METHOD.

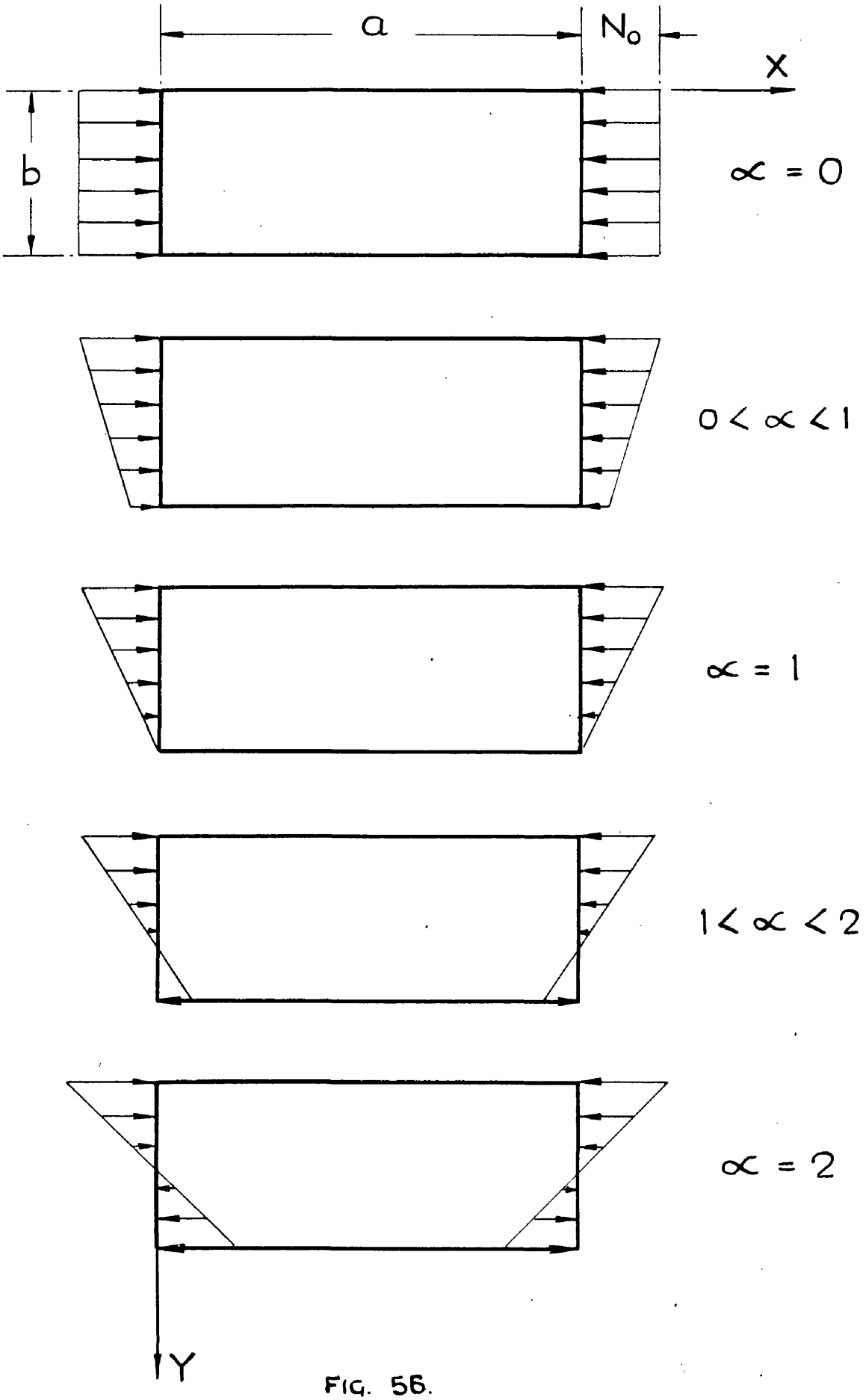

FIG. 56.

INFLUENCE OF THE ASSUMED POSITION OF THE MAXIMUM DEFLECTION ON THE ACCURACY OF THE ITERATIVE METHOD.

To demonstrate the effect of the assumed deflected form on the accuracy of the iterative method, the case of a square plate under various load conditions is considered. Two deflected forms are assumed and the plate constant K is calculated by iteration for various load conditions. The values of K calculated by the iterative method are compared with those given by Timoshenko(14) using the energy method.

The rectangular plate shown in Figure 58 is simply supported along all edges. Distributed forces, acting in the middle plane of the plate are applied along the edges $x = 0$ and $x = a$; their intensity is given by the equation

$$N_x = N_0 \left(1 - \alpha \frac{y}{b}\right) \qquad (104)$$

where N_0 is the intensity of compressive forces at the edge $y = 0$ and α is a numerical factor. By changing α various particular cases are obtained, e.g., for uniformly distributed compressive forces $\alpha = 0$ and for pure bending $\alpha = 2$. If α is between zero and two, a combination of bending and compression is present, as indicated in Figure 56.

The differential equation for the deflected form of the plate is again given by equation (14). Substituting for N_x from (104) gives

$$\frac{\partial^4 \omega}{\partial x^4} + 2\frac{\partial^4 \omega}{\partial x^2 \partial y^2} + \frac{\partial^4 \omega}{\partial y^4} = -\frac{1}{D} N_o \left(1 - \alpha \frac{y}{b}\right) \frac{\partial^2 \omega}{\partial x^2} \qquad (105)$$

The boundary conditions to be satisfied are

$$\left.\begin{aligned} &\omega = 0 \\ &\frac{\partial^2 \omega}{\partial x^2} + \nu \frac{\partial^2 \omega}{\partial y^2} = 0 \end{aligned}\right\} \text{ for } \quad x = 0 \quad \text{and} \quad x = a \qquad (106)$$

$$\left.\begin{aligned} &\omega = 0 \\ &\frac{\partial^2 \omega}{\partial y^2} + \nu \frac{\partial^2 \omega}{\partial x^2} = 0 \end{aligned}\right\} \text{ for } \quad y = 0 \quad \text{and} \quad y = b \qquad (107)$$

Conditions (106) and (107) (for minimum requirements of stability) are satisfied by taking the solution of equation (105) in the form

$$\omega = Y \sin \frac{\pi x}{a} \qquad (18)\,a$$

in which Y is a function of y only.

Substituting in equation (105) gives

$$\frac{d^4 Y}{dy^4} = A \frac{d^2 Y}{dy^2} - \left[B - Cy\right] Y \qquad (108)$$

where $A = \dfrac{2 m^2 \pi^2}{a^2}$

$$B = \frac{m^2 \pi^2}{a^2} - \frac{m^2 \pi^2}{a^2} \frac{N_o}{D}$$

$$C = -\frac{m^2 \pi^2}{a^2} \frac{N_o}{D} \frac{\alpha}{b}$$

The appropriate boundary conditions in terms of Y relevant to equation (108) are now

$$\left.\begin{aligned} Y &= 0 \\ \frac{d^2Y}{dy^2} - \nu\frac{\pi^2}{a^2}Y &= 0 \end{aligned}\right\} \text{for} \quad y=0 \quad \text{and} \quad y=b \qquad (109)$$

(i) Single Sine Wave.

The first approximation to the deflected form of the plate in the y-direction (again corresponding to the minimum requirements of stability) is assumed to be given by

$$Y_1 = \Omega \sin\frac{\pi y}{b} \qquad (110)$$

where Ω is a constant. This satisfies the boundary conditions (109).

Substituting in the right hand side of equation (108) gives

$$\frac{d^4Y_2}{dy^4} = -A\Omega\frac{\pi^2}{b^2}\sin\frac{\pi y}{b} - \left[B - Cy\right]\Omega\sin\frac{\pi y}{b} \qquad (111)$$

where Y_2 is the second approximation.

An expression for Y_2 is obtained by successive integration; the integration constants are evaluated by applying the boundary conditions (109).

The maximum deflection occurs at $y = \frac{b}{2}$. The first approximation to the critical load is obtained by equating $(Y_1)_{max.}$ to $(Y_2)_{max.}$. This, after evaluation, gives the following relationship:

$$\left(1 + \frac{a^2}{b^2}\right) - \frac{a^2 N_o}{\pi^2 D}\left(1 - \frac{\alpha}{2}\right) = 0 \qquad (112)$$

At the critical loading condition

$$\frac{N_o}{D} = \frac{K\pi^2}{b^2} \qquad (113)$$

hence

$$\left(1 + \frac{a^2}{b^2}\right) - K\frac{a^2}{b^2}\left(1 - \frac{\alpha}{2}\right) = 0 \qquad (114)$$

or for a square plate, i.e., $\frac{a}{b} = 1$

$$K = \frac{4}{1 - \frac{\alpha}{2}} \qquad (115)$$

(ii) Double Sine Wave.

The first approximation to the deflected form of the plate in the y-direction is assumed to be given by

$$Y_1 = \Omega \sin\frac{\pi y}{b} + \frac{\Omega}{2}\sin\frac{2\pi y}{b} \qquad (116)$$

where Ω is a constant. This satisfies the boundary conditions (109).

Substituting in the right hand side of equation (108) gives

$$\frac{d^4 Y_2}{dy^4} = -A\Omega\left(\frac{\pi^2}{b^2}\sin\frac{\pi y}{b} - \frac{2\pi^2}{b^2}\sin\frac{2\pi y}{b}\right) - \Omega\left[B - Cy\right]\left(\sin\frac{\pi y}{b} + \frac{1}{2}\sin\frac{2\pi y}{b}\right) \qquad (117)$$

Integrating and evaluating the integration constants as before, gives an expression for Y_2.

The maximum deflection occurs at $y = \frac{b}{3}$. Again equating $(Y_1)_{max.}$ and $(Y_2)_{max.}$ gives

$$1.299\frac{a^4}{b^4} + 2.166\frac{a^2}{b^2} + 0.894 - a^2\frac{N_0}{D}\left(0.0906 - 0.038\alpha\right) = 0 \qquad (118)$$

Using equation (113) this reduces to

$$1.299\frac{a^4}{b^4} + 2.166\frac{a^2}{b^2} + 0.894 - K\frac{a^2}{b^2}\left(0.894 - 0.375\alpha\right) = 0 \qquad (119)$$

or for a square plate, i.e., $\frac{a}{b} = 1$

$$K = \frac{4.379}{\left(0.894 - 0.375\alpha\right)} \qquad (120)$$

TABLE 2

α	K		
SQUARE PLATE $\frac{a}{b} = 1$	SINGLE SINE WAVE	DOUBLE SINE WAVE	TIMOSHENKO
2	∞	30·4	25·6
$\frac{4}{3}$	12	11·1	11·0
1	8	8·15	7·8
$\frac{2}{3}$	6	6·65	5·8
0	4	4·9	4·0

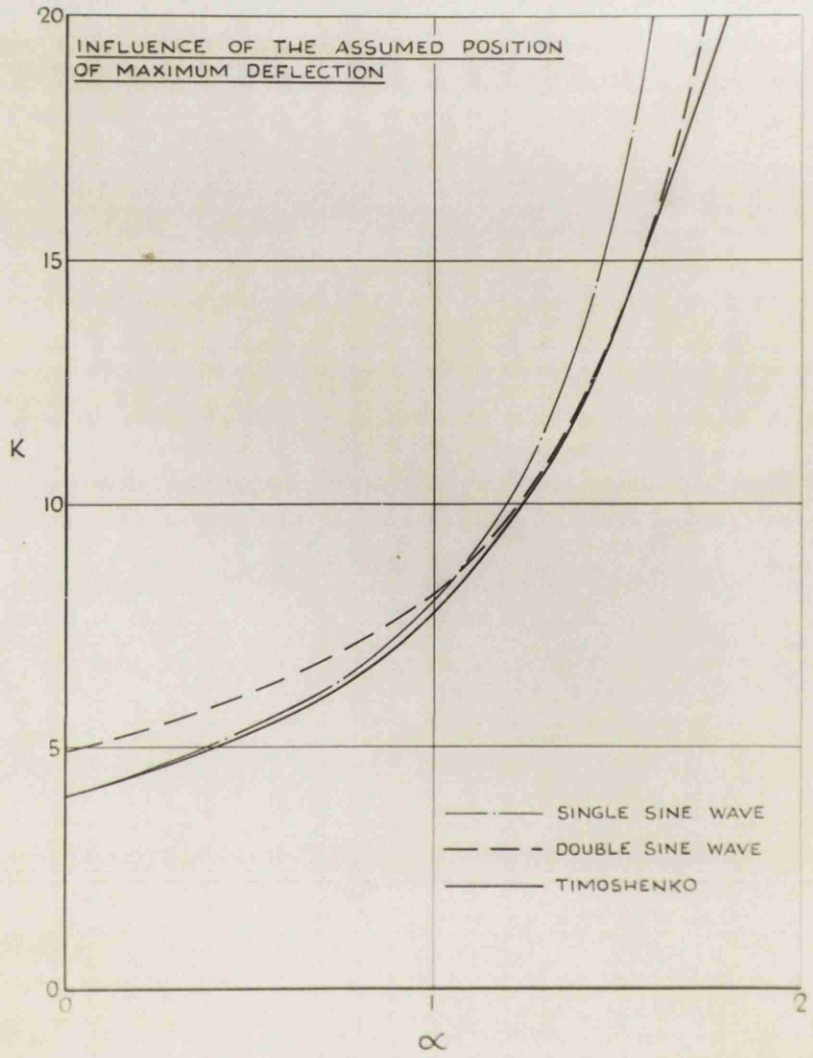
INFLUENCE OF THE ASSUMED POSITION
OF MAXIMUM DEFLECTION
20
15
10
5
0
K
0
1
2
∝
SINGLE SINE WAVE
DOUBLE SINE WAVE
TIMOSHENKO

FIG. 57.

The values of K calculated by the iterative method for several α values, and the corresponding values given by Timoshenko(14) using the energy method, are given in Table 2. For a clearer comparison a graphical presentation of results is given in Figure 57.

It can be seen that any desired degree of approximation may be obtained by the appropriate choice of the deflected form. The point of importance which has been borne out by other subsequent work is that in defining the assumed deflected form, it is of greater importance to assess, as nearly as possible, the true position of the point of maximum deflection rather than the particular type (sine , parabolic, etc.) of deflected form. This is quite strikingly demonstrated by the rapid decrease of accuracy of the single sine assumption as the applied load changes from uniform loading to pure bending. The changeover to the double sine assumption and the consequent shift of the assumed point of maximum deflection towards the position of that of the actual deflected form, substantially improves the approximation.

The full importance of this feature is realised when dealing with problems such as plates, free along one longitudinal edge, where the position of maximum deflection of the laterally deflected form is fixed by the physical conditions of the plate supports. In such cases, it is perfectly permissible to use any algebraic expression most suited to ease mathematical working, provided it gives the maximum deflection at the free edge. In the theoretical development presented in the text, polynominal expressions were found to be most suitable.

APPENDIX 2.

THE ITERATIVE METHOD - CONCENTRICALLY LOADED STRUTS.

1. First Order Approximation.

2. Second Order Approximation.

3. Comparison of Critical Load Values Obtained by the First and Second Order Approximations.

THE ITERATIVE METHOD - CONCENTRICALLY LOADED STRUTS.

1. First Order Approximation.

Restating equations (33), (34) and (35)

$$EI_y \frac{d^2u}{dz^2} = -P(u + y_o\varphi) \qquad (33)$$

$$EI_x \frac{d^2v}{dz^2} = -P(v - x_o\varphi) \qquad (34)$$

$$C_1 \frac{d^4\varphi}{dz^4} = (c - r_o^2 P)\frac{d^2\varphi}{dz^2} + P\left(x_o \frac{d^2v}{dz^2} - y_o \frac{d^2u}{dz^2}\right) \qquad (35)$$

The boundary conditions to be satisfied are

$$\left.\begin{aligned} u = v = \varphi = 0 \\ u'' = v'' = \varphi' = 0 \end{aligned}\right\} \text{ for } z = 0 \text{ and } z = L \qquad (38)$$

These conditions are satisfied by

$$\left.\begin{aligned} u_1 &= A_1 \sin\frac{\pi z}{L} \\ v_1 &= A_2 \sin\frac{\pi z}{L} \\ \varphi_1 &= A_3\left(1 - \cos\frac{2\pi z}{L}\right) \end{aligned}\right\} \qquad (39)$$

Putting $u = u_1$ and $\varphi = \varphi_1$ in the right hand side of equation (33) and integrating twice gives

$$EI_y \frac{d^2u_2}{dz^2} = -P\left[A_1 \sin\frac{\pi z}{L} + y_o A_3\left(1 - \cos\frac{2\pi z}{L}\right)\right] \qquad (40)$$

$$EI_y \frac{du_2}{dz} = -P\left[-A_1 \frac{\cos\frac{\pi z}{L}}{\left(\frac{\pi}{L}\right)} + y_o A_3\left(z - \frac{\sin\frac{2\pi z}{L}}{\left(\frac{2\pi}{L}\right)}\right)\right] + B \qquad (121)$$

$$EI_y u_2 = -P\left[-A_1 \frac{\sin\frac{\pi z}{L}}{\left(\frac{\pi}{L}\right)^2} + y_o A_3\left(\frac{z^2}{2} + \frac{\cos\frac{2\pi z}{L}}{\left(\frac{2\pi}{L}\right)^2}\right)\right] + Bz + C \qquad (41)$$

From (41): $z = 0$, $u_2 = 0$ $\qquad C = P y_o \left(\frac{L}{2\pi}\right)^2 A_3$

From (41): $z = L$, $u_2 = 0$ $\qquad B = P y_o \frac{L}{2} A_3$

Substituting for B and C in equation (41) and putting $u_2 = u_1$ at $z = \frac{L}{2}$ gives

$$EI_y A_1 = P\left(\frac{L}{\pi}\right)^2 A_1 + P y_o \frac{L^2}{8} A_3 + 2P y_o \left(\frac{L}{2\pi}\right)^2 A_3$$

Multiplying both sides by $\left(\frac{\pi}{L}\right)^2$ and grouping terms

$$\left(P - EI_y \frac{\pi^2}{L^2}\right) A_1 + 1.733\, P y_o A_3 = 0 \qquad (42)$$

Similarly, putting $v = v_1$ and $\varphi = \varphi_1$ in the right hand side of equation (34) and integrating twice gives

$$EI_x \frac{d^2 v_2}{dz^2} = -P\left[A_2 \sin\frac{\pi z}{L} - x_0 A_3\left(1 - \cos\frac{2\pi z}{L}\right)\right] \qquad (43)$$

$$EI_x \frac{dv_2}{dz} = -P\left[-A_2 \frac{\cos\frac{\pi z}{L}}{\left(\frac{\pi}{L}\right)} - x_0 A_3\left(z - \frac{\sin\frac{2\pi z}{L}}{\left(\frac{2\pi}{L}\right)}\right)\right] + D \qquad (122)$$

$$EI_x v_2 = -P\left[-A_2 \frac{\sin\frac{\pi z}{L}}{\left(\frac{\pi}{L}\right)^2} - x_0 A_3\left(\frac{z^2}{2} + \frac{\cos\frac{2\pi z}{L}}{\left(\frac{2\pi}{L}\right)^2}\right)\right] + Dz + E \qquad (44)$$

From (44): $z = 0$, $v_2 = 0$ $\qquad E = -Px_0\left(\frac{L}{2\pi}\right)^2 A_3$

From (44): $z = L$, $v_2 = 0$ $\qquad D = -Px_0 \frac{L}{2} A_3$

Substituting for D and E in equation (44) and putting $v_2 = v_1$ at $z = \frac{L}{2}$ gives

$$EI_x A_2 = P\left(\frac{L}{\pi}\right)^2 A_2 - Px_0 \frac{L^2}{8} A_3 - 2Px_0\left(\frac{L}{2\pi}\right)^2 A_3$$

Multiplying both sides by $\left(\frac{\pi}{L}\right)^2$ and grouping terms

$$\left(P - EI_4 \frac{\pi^2}{L^2}\right) A_2 - 1.733\, Px_0 A_3 = 0 \qquad (45)$$

Putting $\frac{d^2u}{dz^2} = \frac{d^2u_1}{dz^2}$, $\frac{d^2v}{dz^2} = \frac{d^2v_1}{dz^2}$ and $\frac{d^2\varphi}{dz^2} = \frac{d^2\varphi_1}{dz^2}$

in the right hand side of equation (35) gives

$$C_1 \frac{d^4\varphi_2}{dz^4} = R_1 \cos\frac{2\pi z}{L} + R_2 \sin\frac{\pi z}{L} \qquad \text{——————} \quad (46)$$

where $R_1 = \left(C - r_0^2 P\right)\left(\frac{2\pi}{L}\right)^2 A_1$

and $R_2 = P\left[x_0\left(\frac{\pi}{L}\right)^2 A_3 + y_0\left(\frac{\pi}{L}\right)^2 A_1\right]$

Integrating

$$C_1 \frac{d^3\varphi_2}{dz^3} = R_1 \frac{\sin\frac{2\pi z}{L}}{\left(\frac{2\pi}{L}\right)} - R_2 \frac{\cos\frac{\pi z}{L}}{\left(\frac{\pi}{L}\right)} + F \qquad \text{——————} \quad (123)$$

$$C_1 \frac{d^2\varphi_2}{dz^2} = -R_1 \frac{\cos\frac{2\pi z}{L}}{\left(\frac{2\pi}{L}\right)^2} - R_2 \frac{\sin\frac{\pi z}{L}}{\left(\frac{\pi}{L}\right)^2} + Fz + G \qquad (124)$$

$$C_1 \frac{d\varphi_2}{dz} = -R_1 \frac{\sin\frac{2\pi z}{L}}{\left(\frac{2\pi}{L}\right)^3} + R_2 \frac{\cos\frac{\pi z}{L}}{\left(\frac{\pi}{L}\right)^2} + F\frac{z^2}{2} + Gz + H \qquad (125)$$

$$C_1 \varphi_2 = R_1 \frac{\cos\frac{2\pi z}{L}}{\left(\frac{2\pi z}{L}\right)^4} + R_2 \frac{\sin\frac{\pi z}{L}}{\left(\frac{\pi}{L}\right)^4} + F\frac{z^3}{6} + G\frac{z^2}{2} + Hz + K$$

——————— (47)

To evaluate the constants of integration, the boundary conditions used are

$$\left.\begin{aligned} \varphi &= A_3\left(1-\cos\frac{2\pi z}{L}\right) = 0 \\ \varphi' &= A_3\left(\frac{2\pi}{L}\right)\sin\frac{2\pi z}{L} = 0 \end{aligned}\right\} \text{for} \quad z=0 \qquad (38)$$

$$\left.\begin{aligned} \varphi' &= A_3\left(\frac{2\pi}{L}\right)\sin\frac{2\pi z}{L} = 0 \\ \varphi''' &= -A_3\left(\frac{2\pi}{L}\right)^3\sin\frac{2\pi z}{L} = 0 \end{aligned}\right\} \text{for} \quad z=\frac{L}{2} \qquad (48)$$

The additional boundary conditions (48) are selected to conform to the conditions which prevail in the experimental work

From (123) $\quad z=\frac{L}{2}\,,\ \varphi'''=0 \quad F=0$

From (125) (i) $\quad z=0\,,\ \varphi'=0 \quad H=-R_2\left(\frac{L}{\pi}\right)^3$

(ii) $\quad z=\frac{L}{2}\,,\ \varphi'=0 \quad G=R_3\frac{2}{L}\left(\frac{L}{\pi}\right)^3$

From (47) $\quad z=0\,,\ \varphi=0 \quad K=-R_1\left(\frac{L}{2\pi}\right)^4$

Equation (47) now can be rewritten

$$C_1\varphi_2 = R_1\frac{\cos\frac{2\pi z}{L}}{\left(\frac{2\pi}{L}\right)^4} + R_2\frac{\sin\frac{\pi z}{L}}{\left(\frac{\pi}{L}\right)^4} + R_2\frac{1}{L}\left(\frac{L}{\pi}\right)^3 z^2 - R_2\left(\frac{L}{\pi}\right)^3 z - R_1\left(\frac{L}{2\pi}\right)^4 \qquad (49)$$

Putting $\varphi_2 = \varphi_1$ at $z = \frac{L}{2}$ in equation (49) and collecting terms

$$2 C_1 A_3 = -2 R_1 \left(\frac{L}{2\pi}\right)^4 - R_2 \left(\frac{L}{4}\right)\left(\frac{L}{\pi}\right)^3 + R_2 \left(\frac{L}{\pi}\right)^4$$

substituting for R_1 and R_2

$$2 C_1 A_3 = -2 \left(C - r_o^2 P\right)\left(\frac{L}{2\pi}\right)^2 A_3 + P x_o \frac{L}{4}\left(\frac{L}{\pi}\right) A_2 - P y_o A_1 \left(\frac{L}{4}\right)\left(\frac{L}{\pi}\right)$$
$$- P x_o \left(\frac{L}{4}\right)\left(\frac{L}{\pi}\right) A_1 + P y_o \left(\frac{L}{\pi}\right)^2 A_1$$

Multiplying both sides by $\left(\frac{\pi}{L}\right)^2$ and collecting terms

$$0.215\, P y_o A_1 - 0.215\, P x_o A_2 + \left[-2 C_1 \left(\frac{\pi}{L}\right)^2 - \frac{1}{2} C + \frac{1}{2} r_o^2 P\right] = 0 \qquad (50)$$

To simplify the writing, the following notations are used.

$$P_1 = E I_y \frac{\pi^2}{L^2} \quad , \quad P_2 = E I_x \frac{\pi^2}{L^2} \quad , \quad P_3 = \frac{1}{r_o^2}\left(C + C_1 \frac{4\pi^2}{L^2}\right) \qquad (51)$$

Equations (42) , (45) and (50) can be rewritten

$$\left(P - P_1\right) A_1 + 1.733\, P y_o A_3 = 0 \qquad (52)$$

$$\left(P - P_2\right) A_2 - 1.733\, P x_o A_3 = 0 \qquad (53)$$

$$0.215\, P y_o A_1 - 0.215\, P x_o A_2 + 0.5\, r_o^2 \left(P - P_3\right) A_3 = 0 \qquad (54)$$

Equating to zero the determinant of equations (52), (53) and (54), gives the following cubic equation for calculating the critical value of P :

$$r_o^2(P-P_1)(P-P_2)(P-P_3) - 0.744P^2y_o^2(P-P_2) - 0.744P^2x_o^2(P-P_1) = 0 \qquad (55)$$

2. Second Order Approximation. (In abbreviated form).

The values of u_2, v_2 and φ_2, derived in Part II, Section 2, are taken as the solutions of equations (33), (34) and (35), satisfying the boundary conditions (38).

Where

$$u_2 = -\frac{P}{EI_y}\left[-A_1\frac{\sin\frac{\pi z}{L}}{\left(\frac{\pi}{L}\right)^2} + y_0 A_3\frac{\cos\frac{2\pi z}{L}}{\left(\frac{2\pi}{L}\right)^2} + y_0 A_3\frac{z^2}{2} - y_0 A_3 L\frac{z}{2} - y_0 A_3\left(\frac{L}{2\pi}\right)^2\right] \quad (59)$$

$$v_2 = -\frac{P}{EI_x}\left[-A_2\frac{\sin\frac{\pi z}{L}}{\left(\frac{\pi}{L}\right)^2} - x_0 A_3\frac{\cos\frac{2\pi z}{L}}{\left(\frac{2\pi}{L}\right)^2} - x_0 A_3\frac{z^2}{2} + x_0 A_3 L\frac{z}{2} + x_0 A_3\left(\frac{L}{2\pi}\right)^2\right] \quad (60)$$

$$\varphi_2 = \frac{R_1}{C_1}\frac{\cos\frac{2\pi z}{L}}{\left(\frac{2\pi}{L}\right)^4} + \frac{R_2}{C_1}\frac{\sin\frac{\pi z}{L}}{\left(\frac{\pi}{L}\right)^4} + \frac{R_2}{C_1}\frac{1}{L}\left(\frac{L}{\pi}\right)^3 z^2 - \frac{R_2}{C_1}\left(\frac{L}{\pi}\right)^3 z - \frac{R_1}{C_1}\left(\frac{L}{2\pi}\right)^4 \quad (61)$$

where $R_1 = \left(C - r_0^2 P\right)\left(\frac{2\pi}{L}\right)^2 A_3$

and $R_2 = P\left[-x_0\left(\frac{\pi}{L}\right)^2 A_3 + y_0\left(\frac{\pi}{L}\right)^2 A_1\right]$

Proceeding, as in (i) by putting $u_1 = u_2$, $v_1 = v_2$, $\varphi_1 = \varphi_2$, $\frac{d^2u_1}{dz^2} = \frac{d^2u_2}{dz^2}$, $\frac{d^2v_1}{dz^2} = \frac{d^2v_2}{dz^2}$ and $\frac{d^2\varphi_1}{dz^2} = \frac{d^2\varphi_2}{dz^2}$ in the right hand side of equation (33), (34) and (35), integrating and evaluating the constants of integration from the boundary conditions, the following expressions are obtained.

$$EI_y u_3 = -P\left\{-\frac{P}{EI_y}\left[A_1\frac{\sin\frac{\pi z}{L}}{\left(\frac{\pi}{L}\right)^4} - y_o A_3\frac{\cos\frac{2\pi z}{L}}{\left(\frac{2\pi}{L}\right)^4} + y_o A_3\frac{z^4}{24} - y_o A_3 L\frac{z^3}{12} - y_o A_3\left(\frac{L}{\pi}\right)^2\frac{z^2}{8}\right]\right.$$

$$\left. + \frac{y_o}{C_1}\left[-R_2\frac{\sin\frac{\pi z}{L}}{\left(\frac{\pi}{L}\right)^6} - R_1\frac{\cos\frac{2\pi z}{L}}{\left(\frac{2\pi}{L}\right)^6} + R_2\frac{1}{L}\left(\frac{L}{\pi}\right)^3\frac{z^4}{12} - R_2\left(\frac{L}{\pi}\right)^3\frac{z^3}{6} - R_1\left(\frac{L}{\pi}\right)^4\frac{z^2}{32}\right]\right\}$$

$$+ Pz\left\{-\frac{P}{EI_y}\left[-y_o A_3\frac{L^3}{24} - y_o A_3\left(\frac{L}{\pi}\right)^2\frac{L}{8}\right] + \frac{y_o}{C_1}\left[-R_1\left(\frac{L}{\pi}\right)^4\frac{L}{32} - R_2\left(\frac{L}{\pi}\right)^3\frac{L^2}{12}\right]\right\}$$

$$+ \frac{P^2}{EI_y} y_o A_3\left(\frac{L}{\pi}\right)^4\frac{1}{16} - \frac{P}{C_1} y_o R_1\left(\frac{L}{\pi}\right)^6\frac{1}{64} \qquad (126)$$

$$EI_x v_3 = -P\left\{-\frac{P}{EI_x}\left[A_2\frac{\sin\frac{\pi z}{L}}{\left(\frac{\pi}{L}\right)^4} + x_o A_3\frac{\cos\frac{2\pi z}{L}}{\left(\frac{2\pi}{L}\right)^4} - x_o A_3\frac{z^4}{24} + x_o A_3 L\frac{z^3}{12} + x_o A_3\left(\frac{L}{\pi}\right)^2\frac{z^2}{8}\right]\right.$$

$$\left. - \frac{x_o}{C_1}\left[-R_2\frac{\sin\frac{\pi z}{L}}{\left(\frac{\pi}{L}\right)^6} - R_1\frac{\cos\frac{2\pi z}{L}}{\left(\frac{2\pi}{L}\right)^6} + R_2\frac{1}{L}\left(\frac{L}{\pi}\right)^3\frac{z^4}{12} - R_2\left(\frac{L}{\pi}\right)^3\frac{z^3}{6} - R_1\left(\frac{L}{\pi}\right)^4\frac{z^2}{32}\right]\right\}$$

$$+ Pz\left\{-\frac{P}{EI_x}\left[x_o A_3\frac{L^3}{24} + x_o A_3\left(\frac{L}{\pi}\right)^2\frac{L}{8}\right] - \frac{x_o}{C_1}\left[-R_1\left(\frac{L}{\pi}\right)^4\frac{L}{32} - R_2\left(\frac{L}{\pi}\right)^3\frac{L^2}{12}\right]\right\}$$

$$- \frac{P^2}{EI_x} x_o A_3\left(\frac{L}{\pi}\right)^4\frac{1}{16} + \frac{P}{C_1} x_o R_1\left(\frac{L}{\pi}\right)^6\frac{1}{64} \qquad (127)$$

$$C_1 \varphi_3 = (C - r_o^2 P)\left\{ -\frac{R_2}{C_1}\frac{\sin\frac{\pi z}{L}}{\left(\frac{\pi}{L}\right)^6} - \frac{R_1}{C_1}\frac{\cos\frac{2\pi z}{L}}{\left(\frac{2\pi}{L}\right)^6} + \frac{R_2}{C_1}\frac{1}{L}\left(\frac{L}{\pi}\right)^3\frac{z^4}{12}\right\}$$

$$+ P x_o\left\{ -\frac{P}{EI_x}\left[A_2\frac{\sin\frac{\pi z}{L}}{\left(\frac{\pi}{L}\right)^4} + x_o A_3\frac{\cos\frac{2\pi z}{L}}{\left(\frac{2\pi}{L}\right)^4} - x_o A_3\frac{z^4}{24}\right]\right\}$$

$$- P y_o\left\{ -\frac{P}{EI_y}\left[A_1\frac{\sin\frac{\pi z}{L}}{\left(\frac{\pi}{L}\right)^4} - y_o A_3\frac{\cos\frac{2\pi z}{L}}{\left(\frac{2\pi}{L}\right)^4} + y_o A_3\frac{z^4}{24}\right]\right\}$$

$$+ \frac{z^3}{6}\left\{ A_2\frac{(C - r_o^2 P)}{C_1}\left(\frac{L}{\pi}\right) P x_o - A_1\frac{(C - r_o^2 P)}{C_1}\left(\frac{L}{\pi}\right) P y_o \right.$$

$$\left. - A_3\frac{L}{2}\left(\frac{P^2 x_o^2}{EI_x} + \frac{P^2 y_o^2}{EI_y}\right)\right\}$$

$$+ \frac{z^2}{2}\left\{ A_1 P y_o\left(\frac{L}{\pi}\right)^2\left[\frac{\pi}{6}\frac{(C - r_o^2 P)}{C_1} - \frac{2}{\pi}\frac{(C - r_o^2 P)}{C_1} + \frac{2}{\pi}\frac{P}{EI_y}\right]\right.$$

$$- A_2 P x_o\left(\frac{L}{\pi}\right)^2\left[\frac{\pi}{6}\frac{(C - r_o^2 P)}{C_1} - \frac{2}{\pi}\frac{(C - r_o^2 P)}{C_1} + \frac{2}{\pi}\frac{P}{EI_x}\right]$$

$$\left. + A_3\frac{L^2}{12}\left[\frac{P^2 x_o^2}{EI_x} + \frac{P^2 y_o^2}{EI_y}\right]\right\}$$

$$+ z\left\{ A_1 P y_o\left(\frac{L}{\pi}\right)^3\left[\frac{(C - r_o^2 P)}{C_1} - \frac{P}{EI_y}\right]\right.$$

$$\left. - A_2 P x_o\left(\frac{L}{\pi}\right)^3\left[\frac{(C - r_o^2 P)}{C_1} - \frac{P}{EI_x}\right]\right\}$$

$$+ A_3\left(\frac{L}{\pi}\right)^4\frac{1}{16}\left[\frac{(C - r_o^2 P)^2}{C_1} + \frac{P^2 x_o^2}{EI_x} + \frac{P^2 y_o^2}{EI_{y_o}}\right] \qquad (128)$$

Putting $u_3 = u_2$, $v_3 = v_2$ and $\phi_3 = \phi_2$ at $z = \frac{L}{2}$ in equations (126) (127) and (128), these finally reduce to

$$A_1\left(P - P_1 + 0.193\,\frac{P y_0^2 E I_y}{C_1}\right) - A_2\, 0.193\,\frac{P y_0 x_0 E I_y}{C_1} + A_3\left[1.696\,P y_0 - 0.433\left(C - r_0^2 P\right)\frac{y_0 E I_y}{C_1} - 1.73\,P_1 y_0\right] = 0 \qquad (129)$$

$$-A_1\, 0.193\,\frac{P x_0 y_0 E I_x}{C_1} + A_2\left(P - P_2 + 0.193\,\frac{P x_0^2 E I_x}{C_1}\right) - A_3\left[1.696\,P x_0 - 0.433\left(C - r_0^2 P\right)\frac{x_0 E I_x}{C_1} - 1.73\,P_2 x_0\right] = 0 \qquad (130)$$

$$-A_1\left[0.054\,P y_0\,\frac{\left(C - r_0^2 P\right)}{C_1} + 2.12\,\frac{P y_0}{L^2} - 0.215\,\frac{P^2 y_0}{E I_y}\right] + A_2\left[0.054\,P x_0\,\frac{\left(C - r_0^2 P\right)}{C_1} + 2.12\,\frac{P x_0}{L^2} - 0.215\,\frac{P^2 x_0}{E I_x}\right] + A_3\left[0.125\,\frac{\left(C - r_0^2 P\right)^2}{C_1} + 4.93\,\frac{\left(C - r_0^2 P\right)}{L^2} + 0.378\,\frac{P^2 x_0^2}{E I_x} + 0.378\,\frac{P^2 y_0^2}{E I_x}\right] = 0 \qquad (131)$$

where $P_1 = \frac{\pi^2 E I_y}{L^2}$ and $P_2 = \frac{\pi^2 E I_x}{L^2}$

To satisfy equations (129), (130) and (131) for a buckled form of equilibrium, their determinant must equal zero. This gives an equation for calculating the critical value of P.

For a cross section with the x-axis an axis of symmetry $y_o = 0$ and the determinant reduces to:

$$\begin{vmatrix} (P-P_1) & 0 & 0 \\ 0 & \left(P-P_2+0.193\frac{Px_o^2EI_x}{C_1}\right) & -\left(1.696Px_o-0.433\frac{(C-r_o^2P)}{C_1}x_oEI_x - 1.73P_2x_o\right) \\ 0 & \left(0.054Px_o\frac{(C-r_o^2P)}{C_1}+2.12\frac{Px_o}{L^2} - 0.215\frac{P^2x_o}{EI_x}\right) & \left(0.125\frac{(C-r_o^2P)^2}{C_1}+4.93\frac{(C-r_o^2P)}{L^2} + 0.378\frac{P^2x_o^2}{EI_x}\right) \end{vmatrix} = 0$$

Hence

$$(P-P_1)\left(P-P_2+0.193\frac{Px_o^2EI_x}{C_1}\right)\left(0.125\frac{(C-r_o^2P)^2}{C_1}+4.93\frac{(C-r_o^2P)}{L^2}+0.378\frac{P^2x_o^2}{EI_x}\right)$$
$$+(P-P_1)\left(0.054Px_o\frac{(C-r_o^2P)}{C_1}+2.12\frac{Px_o}{L^2}-0.215\frac{P^2x_o}{EI_x}\right)$$
$$\left(1.696Px_o-0.433\frac{(C-r_o^2P)}{C_1}x_oEI_x-1.73P_2x_o\right)=0 \qquad (132)$$

3. Comparison of Critical Load Values Obtained by the First and Second Order Approximations.

The case of a centrally loaded, 40 inches long, aluminium strut having a 2.5" x 2·5" x 10G. angle cross section is considered.

(1) First Approximation.

The critical load is obtained from equation (56), namely,

$$(P-P_1)\left[r_o^2(P-P_2)(P-P_3) - 0.744\,P^2x_o^2\right] = 0 \qquad \text{——— (56)}$$

$$P_1 = \frac{\pi^2 E I_y}{L^2} = \frac{\pi^2 \times 4470 \times 0.141}{40^2} = 3.88 \quad T$$

$$P_2 = \frac{\pi^2 E I_x}{L^2} = \frac{\pi^2 \times 4470 \times 0.615}{40^2} = 16.95 \quad T$$

$$P_3 = \frac{1}{r_o^2}\left(C + C_1 \frac{4\pi^2}{L^2}\right) = \frac{1}{2.05}\left(5.6 + 8.11 \frac{4\pi^2}{40^2}\right) = 2.83 \quad T$$

The smallest root of equation (56) gives

$$P_{cr.} = 2.68 \quad T$$

(ii) Second Approximation.

The critical load is obtained by trial and error from equation (132) of this Appendix.

Taking the critical load $P_{cr.} = 2.68\,T$, the following computations are made:

$$0.193\,\frac{P x_o^2 E I_x}{C_1} = \frac{0.193 \times 2.68 \times 0.894^2 \times 4470 \times 0.615}{8.11} = 140$$

$$0.125\,\frac{(C - r_o^2 P)^2}{C_1} = \frac{0.125\,(5.6 - 2.05 \times 2.68)^2}{8.11} = 0.000154$$

$$4.93\,\frac{(C - r_o^2 P)}{L^2} = \frac{4.93 \times 0.1}{40^2} = 0.000308$$

$$0.378\,\frac{P^2 x_o^2}{E I_x} = \frac{0.378 \times 2.68^2 \times 0.894^2}{4470 \times 0.615} = 0.00079$$

$$0.54\,P x_o\,\frac{(C - r_o^2 P)}{C_1} = \frac{0.54 \times 2.68 \times 0.894 \times 0.1}{8.11} = 0.001595$$

$$2.12\,\frac{P x_o}{L^2} = \frac{2.12 \times 2.68 \times 0.894}{40^2} = 0.00318$$

$$0.215\,\frac{P^2 x_o}{E I_x} = \frac{0.215 \times 2.68^2 \times 0.894}{4470 \times 0.615} = 0.000502$$

$$1.696\,P x_o = 1.696 \times 2.68 \times 0.894 = 4.06$$

$$0.433\,\frac{(C-r_0^2P)}{C_1}\,x_0 EI_x = \frac{0.433\times 0.1\times 0.894\times 4470\times 0.615}{8.11} = 13.1$$

$$1.73\,P_2 x_0 = 1.73\times 16.95\times 0.894 = 26.2$$

Again $P_1 = 3.88$ T

and $P_2 = 16.95$ T

Substituting in equation (132) gives

$$(2.68-16.95+140)(0.000154+0.000308+0.00079)$$
$$+(0.001595+0.00318-0.000502)(4.06-13.1-26.2)$$
$$= 125.73\times 0.001252 + 0.004273\times(-35.24)$$
$$= 0.157-0.151 = 0.006 \cong 0$$

Hence $P_{cr} = 2.68$ T

It is seen that the effect of the second approximation is negligible.

APPENDIX 3.

THE ITERATIVE METHOD - ECCENTRICALLY LOADED STRUTS.

First Order Approximation.

THE ITERATIVE METHOD - ECCENTRICALLY LOADED STRUTS.

First Order Approximation.

Restating equations (62), (63) and (64)

$$EI_y \frac{d^4u}{dz^4} = -P\frac{d^2u}{dz^2} - P(y_o - e_y)\frac{d^2\varphi}{dz^2} \qquad (62)$$

$$EI_x \frac{d^4v}{dz^4} = -P\frac{d^2v}{dz^2} + P(x_o - e_x)\frac{d^2\varphi}{dz^2} \qquad (63)$$

$$C_1 \frac{d^4\varphi}{dz^4} = \left(C - Pe_y\beta_1 - Pe_x\beta_2 - Pr_o^2\right)\frac{d^2\varphi}{dz^2} - P(y_o - e_y)\frac{d^2u}{dz^2} + P(x_o - e_x)\frac{d^2v}{dz^2} \qquad (64)$$

where $$\beta_1 = \frac{\int_A y^3 dA + \int_A x^2 y\, dA}{I_x} - 2y_o$$

and $$\beta_2 = \frac{\int_A x^3 dA + \int_A x y^2 dA}{I_y} - 2x_o$$

The boundary conditions to be satisfied are

$$\left.\begin{aligned} u = v = \varphi = 0 \\ u'' = v'' = \varphi' = 0 \end{aligned}\right\} \text{ for } z = 0 \text{ and } z = L \qquad (38)$$

These conditions are satisfied by

$$\left.\begin{aligned} u_1 &= A_1 \sin\frac{\pi z}{L} \\ v_1 &= A_2 \sin\frac{\pi z}{L} \\ \varphi_1 &= A_3\left(1 - \cos\frac{2\pi z}{L}\right) \end{aligned}\right\} \qquad (39)$$

Putting $\frac{d^2u}{dz^2} = \frac{d^2u_1}{dz^2}$ and $\frac{d^2\varphi}{dz^2} = \frac{d^2\varphi_1}{dz^2}$ in the right hand side of equation (62) gives

$$EI_y \frac{d^4u_2}{dz^4} = P\left(\frac{\pi}{L}\right)^2 A_1 \sin\frac{\pi z}{L} - P\left(y_o - e_y\right)\left(\frac{\pi}{L}\right)^2 4A_3 \cos\frac{2\pi z}{L} \qquad (133)$$

successive integration leads to

$$EI_y u_2 = PA_1 \frac{\sin\frac{\pi z}{L}}{\left(\frac{\pi}{L}\right)^2} - P\left(y_o - e_y\right)A_3 \frac{\cos\frac{2\pi z}{L}}{\left(\frac{2\pi}{L}\right)^2} + B\frac{z^3}{6} + C\frac{z^2}{2} + Dz + E \qquad (134)$$

To evaluate the constants of integration, the boundary conditions used are

$$\left.\begin{aligned} u &= A_1 \sin\frac{\pi z}{L} = 0 \\ u'' &= -A_1\left(\frac{\pi}{L}\right)^2 \sin\frac{\pi z}{L} = 0 \end{aligned}\right\} \text{for} \quad z = 0 \qquad (38)$$

$$\left.\begin{aligned} u' &= A_1\left(\frac{\pi}{L}\right)\cos\frac{\pi z}{L} = 0 \\ u''' &= -A_1\left(\frac{\pi}{L}\right)^3 \cos\frac{\pi z}{L} = 0 \end{aligned}\right\} \text{for} \quad z = \frac{L}{2} \qquad (135)$$

The constants of integration are obtained as

$$B = 0$$

$$C = -P(y_o - e_y) A_3$$

$$D = P(y_o - e_y) \frac{L}{2} A_3$$

$$E = P(y_o - e_y) \left(\frac{L}{\pi}\right)^2 \frac{1}{4} A_3$$

Equation (134) now can be written

$$EI_y u_2 = PA_1 \frac{\sin \frac{\pi z}{L}}{\left(\frac{\pi}{L}\right)^2} - P(y_o - e_y) A_3 \frac{\cos \frac{2\pi z}{L}}{\left(\frac{2\pi}{L}\right)^2} - P(y_o - e_y) A_3 \frac{z^2}{2}$$
$$+ P(y_o - e_y) \frac{L}{2} A_3 z + P(y_o - e_y) \left(\frac{L}{\pi}\right)^2 \frac{1}{4} A_3 \qquad \text{(136)}$$

Putting $u_2 = u_1$ at $z = \frac{L}{2}$ in equation (136) and collecting terms

$$EI_y A_1 = P\left(\frac{L}{\pi}\right)^2 A_1 + P(y_o - e_y) \left(\frac{L}{\pi}\right)^2 \frac{1}{2} A_3 + P(y_o - e_y) \frac{L^2}{8} A_3$$

Multiplying both sides by $\left(\frac{\pi}{L}\right)^2$ and regrouping

$$\left(P - EI_y \frac{\pi^2}{L^2}\right) A_1 + 1.733\, P(y_o - e_y) A_3 = 0 \qquad \text{(137)}$$

Similarly, putting $\frac{d^2v}{dz^2} = \frac{d^2v_1}{dz^2}$ and $\frac{d^2\varphi}{dz^2} = \frac{d^2\varphi_1}{dz^2}$ in the right hand side of equation (63) gives

$$EI_x \frac{d^4 v_2}{dz^4} = P\left(\frac{\pi}{L}\right)^2 A_2 \sin\frac{\pi z}{L} + P\left(x_o - e_x\right)\left(\frac{\pi}{L}\right)^2 4 A_3 \cos\frac{2\pi z}{L} \qquad (138)$$

Successive integration leads to

$$EI_x v_2 = PA_2 \frac{\sin\frac{\pi z}{L}}{\left(\frac{\pi}{L}\right)^2} + P\left(x_o - e_x\right) A_3 \frac{\cos\frac{2\pi z}{L}}{\left(\frac{2\pi}{L}\right)^2} + F\frac{z^3}{6} + G\frac{z^2}{2} + Hz + K \qquad (139)$$

To evaluate the constants of integration, the boundary conditions used are

$$\left.\begin{aligned} v &= A_2 \sin\frac{\pi z}{L} = 0 \\ v'' &= -A_2\left(\frac{\pi}{L}\right)^2 \sin\frac{\pi z}{L} = 0 \end{aligned}\right\} \text{ for } z = 0 \qquad (38)$$

$$\left.\begin{aligned} v' &= A_2\left(\frac{\pi}{L}\right)\cos\frac{\pi z}{L} = 0 \\ v''' &= -A_2\left(\frac{\pi}{L}\right)^3 \cos\frac{\pi z}{L} = 0 \end{aligned}\right\} \text{ for } z = \frac{L}{2} \qquad (140)$$

The constants of integration are obtained as

$$F = 0$$

$$G = P\left(x_o - e_x\right) A_3$$

$$H = -P\left(x_o - e_x\right)\frac{L}{2} A_3$$

$$K = -P\left(x_o - e_x\right)\left(\frac{L}{\pi}\right)^2 \frac{1}{4} A_3$$

Equation (139) now can be written

$$EI_x v_2 = PA_2 \frac{\sin \frac{\pi z}{L}}{\left(\frac{\pi}{L}\right)^2} + P\left(x_o - e_x\right) A_3 \frac{\cos \frac{2\pi z}{L}}{\left(\frac{2\pi}{L}\right)^2} + P\left(x_o - e_x\right) A_3 \frac{z^2}{2}$$
$$- P\left(x_o - e_x\right) \frac{L}{2} A_3 z - P\left(x_o - e_x\right) \left(\frac{L}{\pi}\right)^2 \frac{1}{4} A_3 \qquad (141)$$

Putting $v_2 = v_1$ at $z = \frac{L}{2}$ in equation (141) and collecting terms

$$EI_x A_2 = P\left(\frac{L}{\pi}\right)^2 A_2 - P\left(x_o - e_x\right)\left(\frac{L}{\pi}\right)^2 \frac{1}{2} A_3 - P\left(x_o - e_x\right) \frac{L^2}{8} A_3$$

Multiplying both sides by $\left(\frac{\pi}{L}\right)^2$ and regrouping

$$\left(P - EI_x \frac{\pi^2}{L^2}\right) A_1 - 1.733\, P\left(x_o - e_x\right) A_3 = 0 \qquad (142)$$

Putting $\frac{d^2u}{dz^2} = \frac{d^2u_1}{dz^2}$, $\frac{d^2v}{dz^2} = \frac{d^2v_1}{dz^2}$ and $\frac{d^2\varphi}{dz^2} = \frac{d^2\varphi_1}{dz^2}$ in the right hand side of equation (64) gives

$$C_1 \frac{d^4\varphi_2}{dz^4} = N\left(\frac{\pi}{L}\right)^2 4A_3 \cos \frac{2\pi z}{L} + P\left(y_o - e_y\right)\left(\frac{\pi}{L}\right)^2 A_1 \sin \frac{\pi z}{L}$$
$$- P\left(x_o - e_x\right)\left(\frac{\pi}{L}\right)^2 A_2 \sin \frac{\pi z}{L} \qquad (143)$$

where $N = \left(C - Pe_y\beta_1 - Pe_x\beta_2 - Pr_o^2\right)$

Successive integration leads to

$$C_1 \varphi_2 = N A_3 \frac{\cos \frac{2\pi z}{L}}{\left(\frac{2\pi}{L}\right)^2} + P\left(y_o - e_y\right) A_1 \frac{\sin \frac{\pi z}{L}}{\left(\frac{\pi}{L}\right)^2} - P\left(x_o - e_x\right) A_2 \frac{\sin \frac{\pi z}{L}}{\left(\frac{\pi}{L}\right)^2}$$
$$+ Q\frac{z^3}{6} + R\frac{z^2}{2} + Sz + T \qquad (144)$$

To evaluate the constants of integration, the boundary conditions used are

$$\left.\begin{aligned} \varphi &= A_3\left(1 - \cos\tfrac{2\pi z}{L}\right) = 0 \\ \varphi' &= A_3\left(\tfrac{2\pi}{L}\right)\sin\tfrac{2\pi z}{L} = 0 \end{aligned}\right\} \text{for} \quad z = 0 \qquad (38)$$

$$\left.\begin{aligned} \varphi' &= A_3\left(\tfrac{2\pi}{L}\right)\sin\tfrac{2\pi z}{L} = 0 \\ \varphi''' &= -A_3\left(\tfrac{2\pi}{L}\right)^3\sin\tfrac{2\pi z}{L} = 0 \end{aligned}\right\} \text{for} \quad z = \frac{L}{2} \qquad (145)$$

The constants of integration are obtained as

$$Q = 0$$

$$R = P\left(y_o - e_y\right)\frac{2}{\pi}A_1 - P\left(x_o - e_x\right)\frac{2}{\pi}A_2$$

$$S = -P\left(y_o - e_y\right)\left(\frac{L}{\pi}\right)A_1 - P\left(x_o - e_x\right)\left(\frac{L}{\pi}\right)A_2$$

$$T = -N A_3 \left(\frac{L}{\pi}\right)^2 \frac{1}{4}$$

Equation (142) now can be written

$$C_1\varphi_2 = NA_3\frac{\cos\frac{2\pi z}{L}}{\left(\frac{2\pi}{L}\right)^2} + P(y_o-e_y)A_1\frac{\sin\frac{\pi z}{L}}{\left(\frac{\pi}{L}\right)^2} - P(x_o-e_x)A_2\frac{\sin\frac{\pi z}{L}}{\left(\frac{\pi}{L}\right)^2}$$
$$+P(y_o-e_y)\frac{2}{\pi}A_1\frac{z^2}{2} - P(x_o-e_x)\frac{2}{\pi}A_2\frac{z^2}{2} - P(y_o-e_y)\left(\frac{L}{\pi}\right)A_1 z$$
$$+P(x_o-e_x)\left(\frac{L}{\pi}\right)A_2 z - N\left(\frac{L}{\pi}\right)\frac{1}{4}A_3 \qquad (146)$$

Putting $\varphi_2 = \varphi_1$ at $z=\frac{L}{2}$ in equation (146) and collecting terms

$$C_1 2A_3 = -N\left(\frac{L}{\pi}\right)^2\frac{1}{2}A_3 + P(y_o-e_y)\left(\frac{L}{\pi}\right)^2A_1 - P(y_o-e_y)\left(\frac{L}{\pi}\right)\frac{L}{4}A_1$$
$$-P(x_o-e_x)\left(\frac{L}{\pi}\right)^2A_2 + P(x_o-e_x)\left(\frac{L}{\pi}\right)\frac{L}{4}A_2$$

Multiplying both sides by $\left(\frac{\pi}{L}\right)^2$ and regrouping

$$0.215\,P(y_o-e_y)A_1 - 0.215\,P(x_o-e_x)A_2$$
$$+0.5\,r_o^2\left[P\left(1+\frac{e_y\beta_1+e_x\beta_2}{r_o^2}\right)-\frac{1}{r_o^2}\left(C+C_1\frac{4\pi^2}{L^2}\right)\right]A_3 = 0 \qquad (147)$$

Equations (137), (142) and (147) can be rewritten

$$(P-P_1)A_1 + 1.733\,P(y_o-e_y)A_3 = 0 \qquad (148)$$

$$(P-P_2)A_2 - 1.733\,P(x_o-e_x)A_3 = 0 \qquad (149)$$

$$0.215\,P(y_o-e_y)A_1 - 0.215\,P(x_o-e_x)A_2$$
$$+0.5\,r_o^2\left[P\left(1+\frac{e_y\beta_1+e_x\beta_2}{r_o^2}\right)-P_3\right]A_3 = 0 \qquad (150)$$

where $P_1 = \dfrac{EI_y \pi^2}{L^2}$, $P_2 = \dfrac{EI_x \pi^2}{L^2}$,

and $P_3 = \dfrac{1}{r_o^2}\left(C + C_1 \dfrac{4\pi^2}{L^2}\right)$

Equating to zero the determinant of equations (148) , (149) and (150) ,

$$\begin{vmatrix} (P - P_1) & 0 & 1.733\,P(y_o - e_y) \\ 0 & (P - P_2) & -1.733\,P(x_o - e_x) \\ 0.215\,P(y_o - e_y) & -0.215\,P(x_o - e_x) & 0.5\,r_o^2\left[P\left(1 + \dfrac{e_y\beta_1 + e_x\beta_2}{r_o^2}\right) - P_3\right] \end{vmatrix} = 0$$

which, after evaluation, gives the following cubic equation for calculating the critical value of P .

$$r_o^2(P-P_1)(P-P_2)\left[P\left(1 + \frac{e_y\beta_1 + e_x\beta_2}{r_o^2}\right) - P_3\right] - 0.744P^2(y_o - e_y)^2(P-P_2) - 0.744P^2(x_o - e_x)^2(P-P_1) = 0 \qquad (151)$$

If the xz-plane is a plane of symmetry and the thrust P acts in that plane, the general equation (151) reduces to

$$(P-P_1)\left\{r_o^2(P-P_2)\left[P\left(1 + \frac{e_x\beta_2}{r_o^2}\right) - P_3\right] - 0.744P^2(x_o - e_x)^2\right\} = 0 \qquad (152)$$

APPENDIX 4.

TYPICAL EVALUATION OF THE DIMENSION RATIO H CORRESPONDING TO A GIVEN RESTRAINT FOR FLANGE BUCKLING OF AN ECCENTRICALLY LOADED CHANNEL SECTION STRUT.

TYPICAL EVALUATION OF THE DIMENSION RATIO H CORRESPONDING TO A GIVEN RESTRAINT FOR FLANGE BUCKLING OF AN ECCENTRICALLY LOADED SECTION STRUT.

The equation defining the elastic edge restraint provided by the web, during buckling of the flange of an eccentrically loaded channel section strut, similar to that described in Part II, Section 3, is given by

$$r = \frac{\alpha_1^2 + \beta_1^2}{\alpha_1 \tanh H\alpha_1 \frac{b}{2} + \beta_1 \tan H\beta_1 \frac{b}{2}} \qquad (96)$$

where $H = \frac{b_1}{b}$

$$\alpha_1^2 = \frac{m^2\pi^2}{a^2} + \left[\left(\frac{N_o}{4D}\right)\left(\frac{m^2\pi^2}{a^2}\right)\right]^{\frac{1}{2}}$$

and $$\beta_1^2 = -\frac{m^2\pi^2}{a^2} + \left[\left(\frac{N_o}{4D}\right)\left(\frac{m^2\pi^2}{a^2}\right)\right]^{\frac{1}{2}}$$

Taking $m=1$ and substituting $\frac{K_F\pi^2}{b^2}$ for $\frac{N_o}{D}$, the following expressions for α_1 and β_1 are obtained:

TABLE 3

r b	K(min.)	a/b CORRESPONDING TO K(min.)
8	1·26	2·3
4	1·15	2·4
3	1·12	2·45
2	1·04	2·5
1·75	1·02	2·525
1·5	0·995	2·55

$$\alpha_1 = \frac{\pi}{b}\sqrt{\left(\frac{b}{a}\right) + \frac{b}{2a}\sqrt{K_F}}$$

$$\beta_1 = \frac{\pi}{b}\sqrt{-\left(\frac{b}{a}\right)^2 + \frac{b}{2a}\sqrt{K_F}}$$

The $\frac{a}{b}$ ratios corresponding to various minimum values of K_F are obtained from Figure 19 and presented in Table 3.

The values of H for various values of rb can be obtained from equation (96) as illustrated in the following example.

For $rb = 4$ and $m = 1$, $K_{(min.)}$ is 1.15 corresponding to $\frac{a}{b} = 2.4$, Figure 19. Hence

$$\alpha_1 = \frac{\pi}{b}\sqrt{0.1735 + 0.208\sqrt{1.15}} = \frac{1.98}{b}$$

and $$\beta_1 = \frac{\pi}{b}\sqrt{-0.1735 + 0.208\sqrt{1.15}} = \frac{0.7}{b}$$

Substituting in equation (96)

$$\frac{4}{b} = \frac{\left(\frac{1.98}{b}\right)^2 + \left(\frac{0.7}{b}\right)^2}{\frac{1.98}{b}\tanh H\frac{1.98}{2} + \frac{0.7}{b}\tan H\frac{0.7}{2}}$$

$$\tan 0.37H + 2.83 \tanh 0.99H = 1.575$$

which gives $H = 0.54$

The values of H for various values of $K_{(min.)}$ are presented in graphical form in Figure 20.

APPENDIX 5.

TABLES OF FAILURE MODES AND LOADS FOR ANGLE AND CHANNEL SECTION STRUTS TESTED.

TABLE 4

SERIES	SPEC. No.	SECTION	LENGTH OF SPEC. (IN.)	ECCTY e_x (IN.)	FAILURE LOAD (TON)	MODE OF FAILURE ※	GERERAL DESCRIPTION
1.a	1	2·5"x 2·5"x 10G.	45	-0·2	1·525	T.F.	CONSTANT LENGTH
	2	ANGLE	45	-0·1	2·05	T.F.	
	3	(COLD FORMED)	45	0	2·1	P.F.	VARYING ECCENTRICITY
	4		45	+0·1	1·975	P.F.	
	5		45	+0·2	1·8	P.F.	
1.b.	6		30	-0·2	1·875	T.F.	
	7		30	-0·1	2·68	T.F.	
	8		30	0	2·925	T.F.	
	9		30	0	2·95	T.F.	
	10		30	+0·1	3·575	T.F.	
	11		30	+0·15	3·375	P.F.	
	12		30	+0·2	3·125	P.F.	
1.c.	13		15	-0·2	2·575	T.F.	
	14		15	-0·1	3·125	T.F.	
	15		15	0	3·875	T.F.	
	16		15	+0·1	5·625	T.F.	
	17		15	+0·2	5·75	M.F.	
	18		15	+0·3	4·975	M.F.	
2.a	19	2·5"x 2·5"x 10G	69	-0·2	0·925	P.F.	CONSTANT ECCENTRICITY
	20	ANGLE	60	-0·2	1·125	P.F.	
	21	(COLD FORMED)	51	-0·2	1·375	T.F.	VARYING LENGTH
	22		42	-0·2	1·625	T.F.	
	23		33	-0·2	1·775	T.F.	
	24		27	-0·2	1·85	T.F.	
	25		21	-0·2	2·2	T.F.	
	26		15	-0·2	2·35	T.F.	
	27		9	-0·2	3·7	T.F.	

※ T.F. = TORSIONAL - FLEXURAL

P.F. = PURELY FLEXURAL

M.F. = MATERIAL FAILURE

TABLE 4 (CONTD)

SERIES	SPEC. No.	SECTION	LENGTH OF SPEC. (IN.)	ECCTY e_x (IN.)	FAILURE LOAD (TON)	MODE* OF FAILURE	GENERAL DESCRIPTION
2.b.	28	2·5" x 2·5" x 10 G.	69	0	0·925	P.F.	CONSTANT ECCENTRICITY VARYING LENGTH
	29	ANGLE	60	0	1·25	P.F.	
	30	(COLD FORMED)	51	0	1·7	P.F.	
	31		42	0	2·4	P.F.	
	32		33	0	3·325	T.F.	
	33		27	0	2·95	T.F.	
	34		21	0	3·4	T.F.	
	35		15	0	3·6	T.F.	
	36		9	0	5·55	T.F.	
2.c.	37		69	+0·2	1·0	P.F.	
	38		60	+0·2	1·25	P.F.	
	39		51	+0·2	1·475	P.F.	
	40		42.	+0·2	2·025	P.F.	
	41		33	+0·2	2·8	P.F.	
	42		27	+0·2	3·625	P.F.	
	43		21	+0·2	3·8	T.P.	
	44		15	+0·2	5·95	M.F.	
	45		9	+0·2	7·125	M.F	
3.a.	19	2·5" x 2·5" x 10 G	69	-0·2	0·925	P.F.	SELECTED ECCENTRICITY VARYING LENGTH
	20	ANGLE	60	-0·2	1·125	P.F	
	21	(COLD FORMED)	51	-0·2	1·375	T.F.	
	22		42	-0·2	1·625	T.F.	
	23		33	-0·2	1·775	T.F.	
	24		27	-0·2	1·87	T.F.	
	25		21	-0·2	2·2	T.F.	
	26		15	-0·2	2·35	T.F.	
	27		9	-0·2	3·7	T.F.	

*T.F. = TORSIONAL - FLEXURAL
P.F. = PURELY FLEXURAL
M.F. = MATERIAL FAILURE

TABLE 4 (CONT^D)

SERIES	SPEC. No.	SECTION	LENGTH OF SPEC. (IN.)	ECC^TY e_x (IN.)	FAILURE LOAD (TON)	MODE* OF FAILURE	GENERAL DESCRIPTION
3.b.	46	2·5" x 2" x 10 G	69	-0·2	0·5	T. F.	SELECTED ECCENTRICITY VARYING LENGTH
	47	ANGLE	60	-0·2	0·575	T. F.	
	48	(COLD FORMED)	51	-0·2	0·95	T. F.	
	49		42	-0·2	1·25	T. F.	
	50		36	-0·2	1·5	T. F.	
	51		30	-0·2	1·7	T. F.	
	52		24	-0·2	2·075	T. F.	
	53		18	-0·2	2·325	T. F.	
	54		12	-0·2	3·1	T. F.	
	55		6	-0·2	5·7	M.F.	
3.c.	56	2·5" x 1·5" x 10 G.	54	-0·2	0·35	T. F.	
	57	ANGLE	48	-0·2	0·35	T. F.	
	58	(COLD FORMED)	42	-0·2	0·6	T. F.	
	59		36	-0·2	0·75	T. F.	
	60		30	-0·2	1·025	T. F.	
	61		24	-0·2	1·375	T. F.	
	62		18	-0·2	1·7	T. F.	
	63		12	-0·2	2·35	T. F.	
	64		9	-0·2	2·9	T. F.	
	65		6	-0·2	3·825	M.F.	
3.d.	66	2·5" x 1" x 10.G.	45	-0·2	0·125	T. F.	
	67	ANGLE	39	-0·2	0·175	T. F.	
	68	(COLD FORMED)	33	-0·2	0·3	T. F.	
	69		27	-0·2	0·45	T. F.	
	70		21	-0·2	0·725	T. F.	
	71		15	-0·2	0·975	T. F.	
	72		12	-0·2	1·175	T. F.	
	73		9	-0·2	1·55	T. F.	
	74		6	-0·2	1·9	M.F.	
	75		3	-0·2	2·8	M.F.	

* T. F. = TORSIONAL - FLEXURAL

M.F. = MATERIAL FAILURE

TABLE 4 (CONTD)

SERIES	SPEC. No.	SECTION	LENGTH OF SPEC. (IN.)	ECCTY e_x (IN.)	FAILURE LOAD (TON)	MODE* OF FAILURE	GENERAL DESCRIPTION
4.a	76	2·5" x 2" x 0·125"	69	-0·2	0·55	T. F.	SELECTED ECCENTRICITY VARYING LENGTH
	77	ANGLE	60	-0·2	0·675	T. F.	
	78	(EXTRUDED)	51	-0·2	0·975	T. F.	
	79		42	-0·2	1·275	T. F.	
	80		36	-0·2	1·5	T. F.	
	81		30	-0·2	1·65	T. F.	
	82		24	-0·2	2	T. F.	
	83		18	-0·2	2·375	T. F.	
	84		12	-0·2	3·05	T. F.	
	85		6	-0·2	4·875	M.F.	
4.b.	86	2·5" x 1·5" x 0·125"	54	-0·2	0·475	T. F.	
	87	ANGLE	48	-0·2	0·575	T. F.	
	88	(EXTRUDED)	42	-0·2	0·725	T. F.	
	89		36	-0·2	0·95	T. F.	
	90		30	-0·2	1·3	T. F.	
	91		24	-0·2	1·6	T. F.	
	92		18	-0·2	2·1	T. F.	
	93		12	-0·2	2·8	T. F.	
	94		9	-0·2	3·375	T. F.	
	95		6	-0·2	5	M.F.	
4.c.	96	2·5" x 1" x 0·125"	45	-0·2	0·125	T. F.	
	97	ANGLE	39	-0·2	0·175	T. F.	
	98	(EXTRUDED)	33	-0·2	0·275	T. F.	
	99		27	-0·2	0·4	T. F.	
	100		21	-0·2	0·65	T. F.	
	101		15	-0·2	1·075	T. F.	
	102		12	-0·2	1·35	T. F.	
	103		9	-0·2	1·8	T. F.	
	104		6	-0·2	2·45	M.F.	
	105		3	-0·2	3·125	M.F.	

* T.F. = TORSIONAL - FLEXURAL
M.F. = MATERIAL FAILURE

TABLE 4. (CONTD)

SERIES	SPEC. No.	SECTION	LENGTH OF SPEC. (IN.)	ECC TY e_x (IN.)	FAILURE LOAD (TON)	MODE OF FAILURE ※	GENERAL DISCRIPTION
5.a.	106	3" x 3" x 12G.	132	-0·4	1·5	T.F.	CONSTANT LENGTH
	107	CHANNEL	132	-0·2	1·25	T.F.	
	108	(COLD FORMED)	132	0	1·25	T.F.	VARYING
	109		132	+0·05	1·65	T.F.	ECCENTRICITY
	110		132	+0·1	1·725	T.F.	
	111		132	+0·15	1·75	T.F.	
	112		132	+0·2	1·65	P.F.	
5.b.	113		60	-0·4	2·1	F.F.	
	114		60	-0·2	2·75	F.F.	
	115		60	0	3·5	F.F.	
	116		60	+0·05	4·625	F.F.	
	117		60	+0·15	5·8	F.F.	
	118		60	+0·3	5·925	W.F.	
5.c.	119		36	-0·4	2·6	F.F.	
	120		36	-0·2	3·1	F.F.	
	121		36	0	3·5	F.F.	
	122		36	+0·05	4·575	F.F.	
	123		36	+0·15	4·9	F.F.	
	124		36	+0·15	5·7	F.F.	
	125		36	+0·3	9·2	W.F.	
	126		36	+0·45	8·35	W.F.	
6.a	119	3" x 3" x 12G.	36	-0·4	2·6	F.F.	SELECTED LENGTH
	120	CHANNEL	36	-0·2	3·1	F.F.	
	121	(COLD FORMED)	36	0	3·5	F.F.	VARYING
	122		36	+0·05	4·575	F.F.	ECCENTRICITY
	123		36	+0·15	4·9	F.F.	
	124		36	+0·15	5·7	F.F.	
	125		36	+0·3	9·2	W.F.	
	126		36	+0·45	8·35	W.F.	

※ T.F. = TORSIONAL-FLEXURAL F.F. = FLANGE FAILURE
P.F. = PURELY FLEXURAL W.F. = WEB FAILURE

TABLE 4. (CONTD)

SERIES	SPEC. No.	SECTION	LENGTH OF SPEC. (IN.)	ECCTY e_x (IN.)	FAILURE LOAD (TON)	MODE OF FAILURE ※	GENERAL DESCRIPTION
6.b.	127	3" x 3" x 14 G.	36	-0·4	1·2	F. F.	SELECTED LENGTH VARYING ECCENTRICITY
	128	CHANNEL	36	-0·2	1·5	F. F.	
	129	(COLD FORMED)	36	0	1·875	F. F.	
	130	"	36	+0·15	2·3	F. F.	
	131		36	+0·15	2·375	F. F.	
	132		36	+0·3	3·5	F. F.	
	133		36	+0·45	5·8	W.F.	
	134		36	+0·5	5·85	W.F.	
6.c.	135	3" x 3" x 18G.	36	-0·4	0·18	F. F.	
	136	CHANNEL	36	-0·2	0·225	F. F.	
	137	(COLD FORMED)	36	0	0·325	F. F.	
	138		36	+0·15	0·425	F. F.	
	139		36	+0·3	0·55	F. F.	
	140		36	+0·45	0·8	F. F.	
	141		36	+0·55	1·125	F. F.	
7.a.	142	3" x 3" x 10 G.	36	0	7·7	F. F.	CONCENTRICALLY LOADED CHANNELS
	143	"	12	0	8·7	F. F.	
	144	3" x 2·5" x 10 G.	36	0	10·925	F. F.	
	145	"	12	0	9·25	F. F.	
	146	3" x 2" x 10 G	36	0	8·775	P. F.	
	147	"	12	0	11·4	M.F.	
	148	3" x 1·5" x 10 G.	36	0	3·775	P. F.	
	149	"	12	0	11·0	M.F.	
	150	3" x 1" x 10 G.	36	0	0·975	P. F.	
	151	" CHANNELS (COLD FORMED)	12	0	6·75	M.F.	

※ P.F. = PURELY FLEXURAL F. F. = FLANGE FAILURE
M.F. = MATERIAL FAILURE W.F. = WEB FAILURE

TABLE 4. (CONTD)

SERIES	SPEC. No.	SECTION	LENGTH OF SPEC. (IN.)	ECCTY e_x (IN.)	FAILURE LOAD (TON)	MODE OF FAILURE ※	GENERAL DESCRIPTION
7.b.	152	3" x 3" x 14 G.	36	0	1·875	F. F.	CONCENTRICALLY
	153		12	0	2·9	F. F.	LOADED
	154	3" x 2·5" x 14 G.	36	0	2·375	F. F.	CHANNELS
	155		12	0	3·25	F. F.	
	156	3" x 2" x 14 G	36	0	3·575	F. F.	
	157		12	0	3·7	F. F.	
	158	3" x 1·5" x 14 G.	36	0	2·525	P. F.	
	159		12	0	6·1	F. F.	
	160	3" x 1" x 14 G.	36	0	0·625	P. F.	
	161		12	0	6·1	M.F.	
7.c.	162	3" x 3" x 18 G.	36	0	0·325	F. F.	
	163		12	0	0·74	F. F	
	164	3" x 2·5" x 18 G.	36	0	0·42	F. F	
	165		12	0	1·05	F. F	
	166	3" x 2" x 18 G.	36	0	0·475	F. F.	
	167		12	0	1·11	F. F.	
	168	3" x 1·5" x 18 G.	36	0	0·7	F. F.	
	169		12	0	1·23	F. F.	
	170	3" x 1" x 18 G.	36	0	0·3	P. F	
	171		12	0	1·66	F. F.	
		CHANNELS (COLD FORMED)					
8.a	172	3" x 3" x 10. G	12	-0·458	5·3	F. F.	ECCENTRICALLY LOADED CHANNELS
	173	3" x 2·5" x 10.G.	12	-0·388	5·75	F. F.	
	174	3" x 2" x 10. G.	12	-0·314	6·86	F. F.	THE ECCENTRICITY e_x CHOSEN SUCH
	175	3" x 1·5" x 10.G.	12	-0·23	6·2	M.F.	THAT THE RATIO
	176	3" x 1" x 10.G.	12	-0·141	3·92	M.F.	OF STRESS AT THE FREE EDGE OF THE FLANGE TO THE STRESS IN THE WEB EQUALS 4
		CHANNELS (COLD FORMED)					

※ P.F. = PURELY FLEXURAL F.F. = FLANGE FAILURE

M.F. = MATERIAL FAILURE

TABLE 4 (CONTD)

SERIES	SPEC. No.	SECTION	LENGTH OF SPEC. (IN.)	ECCTY e_x (IN.)	FAILURE LOAD (TON)	MODE OF FAILURE*	GENERAL DESCRIPTION
8.b.	177	3" x 3" x 14 G.	12	-0.474	1.9	F. F.	
	178	3" x 2.5" x 14G.	12	-0.405	2.02	F. F.	
	179	3" x 2" x 14G	12	-0.327	2.3	F. F.	
	180	3" x 1.5" x 14G	12	-0.238	2.79	F. F.	
	181	3" x 1" x 14G.	12	-0.15	2.48	M.F.	
8.c.	182	3" x 3" x 18G.	12	-0.485	0.55	F. F.	
	183	3" x 2.5" x 18G.	12	-0.413	0.7	F. F.	
	184	3" x 2 x 18 G.	12	-0.337	0.74	F. F.	
	185	3" x 1.5" x 18 G.	12	-0.256	0.72	F. F.	
	186	3" x 1" x 18 G	12	-0.157	0.93	F. F.	
		CHANNELS (COLD FORMED)					
9.a.	187	2.5" x 2.5" x 10.G.	30	0	3.875	T. F.	CONSTANT LENGTH VARYING ECCENTRICITY
	188		30	+0.228	3.375	P. F.	
		ANGLES (COLD FORMED)					
9.b	189	3" x 3" x 12G.	60	0	3.5	F. F.	STRESS INVESTIGATION TESTS
	190		60	+0.45	5.375	W.F.	
		CHANNELS (COLD FORMED)					

* P.F. = PURELY FLEXURAL F.F. = FLANGE FAILURE
M.F. = MATERIAL FAILURE W.F. = WEB FAILURE

APPENDIX 6.

MATERIAL CHARACTERISTICS OF SPECIMENS CUT FROM SECTIONS USED IN THE EXPERIMENTAL WORK.

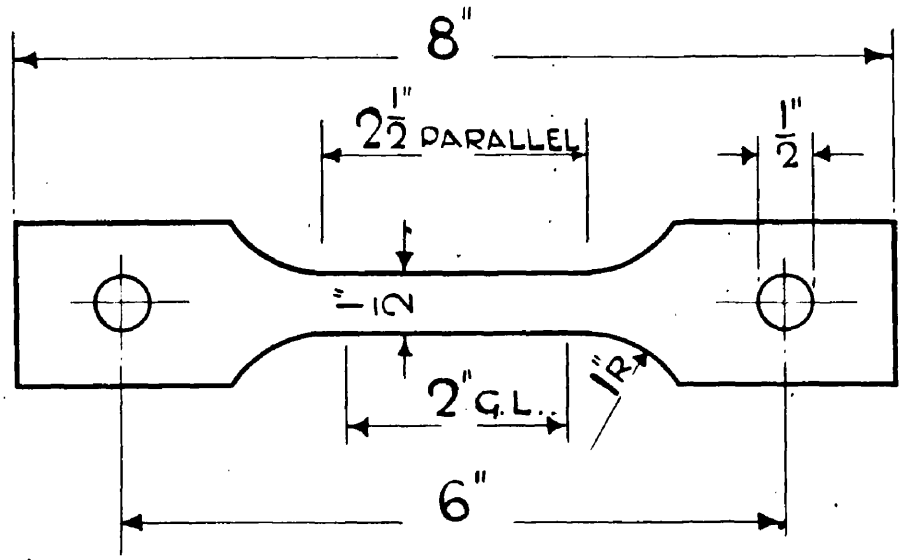

FIG. 58.

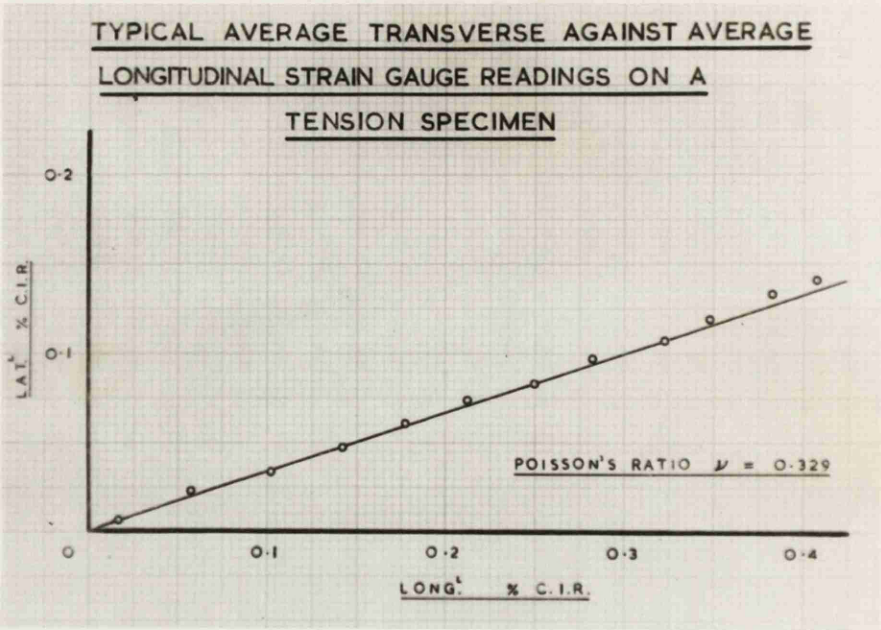
TYPICAL AVERAGE TRANSVERSE AGAINST AVERAGE
LONGITUDINAL STRAIN GAUGE READINGS ON A
TENSION SPECIMEN
LAT.L % C.I.R.
0·2
0·1
0
0·1
0·2
0·3
0·4
LONG.L % C.I.R.
POISSON'S RATIO ν = 0·329

FIG. 59.

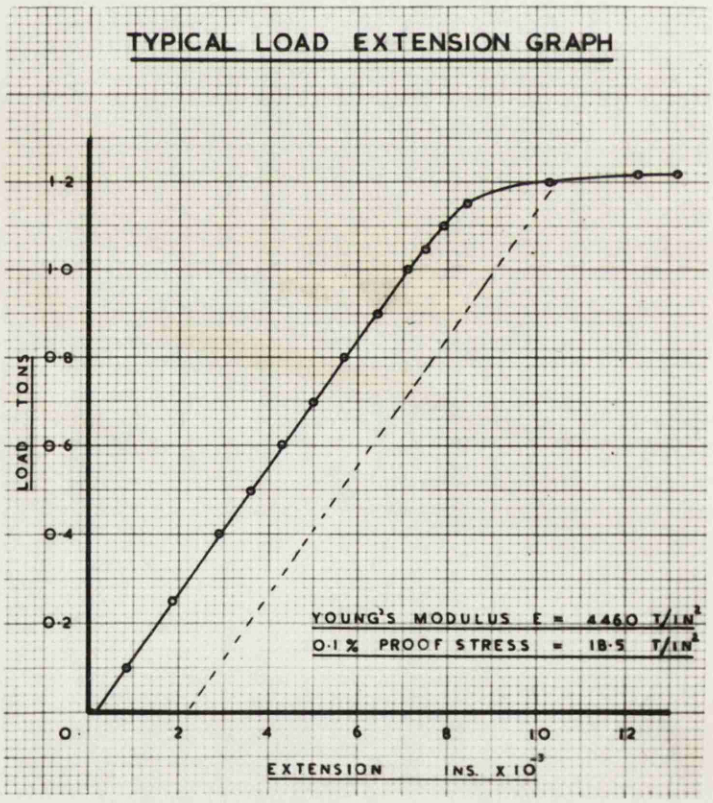
TYPICAL LOAD EXTENSION GRAPH
LOAD TONS
1·2
1·0
0·8
0·6
0·4
0·2
0
2
4
6
8
10
12
EXTENSION INS. X 10⁻³
YOUNG'S MODULUS E = 4460 T/IN²
0·1 % PROOF STRESS = 18·5 T/IN²

FIG. 60.

MATERIAL CHARACTERISTICS OF SPECIMENS CUT FROM SECTIONS USED IN THE EXPERIMENTAL WORK.

(i) Experimental Appliances.

The material characteristics were determined from tensile tests carried out on specimens cut from a selected number of struts after failure. The specimens were tested in a 30 ton Avery Universal Testing Machine, Figure 23. The dimensions of typical tensile specimens are given in Figure 58.

A Hounsfield extensometer with a 2 inches gauge length was used to measure longitudinal strains. Poisson's Ratio was determined by using electrical resistance strain gauges to measure longitudinal and transverse strains on both sides of tension specimens.

(ii) Typical Experimental Results.

The results of typical tensile tests on two specimens cut from a 2.5" x 2.5" x 10 G. angle section are presented in graphical form. Young's Modulus (E) and the 0.1% Proof stress (σ_p) are obtained from the load-extension graph shown in Figure 60. Poisson's Ratio (ν) is obtained from the straight line of Figure 59.

TABLE 5

NOMINAL THICKNESS	YOUNG'S MODULUS E T/IN.^{2}	0·1% PROOF STRESS σ_p T/IN^2	POISSON'S RATIO ν
10 GAUGE	4490	18·5	0·32
12 GAUGE	4490	17·07	—
14 GAUGE	4490	17·85	—
18 GAUGE	4420	17·35	—
0·125 IN.	4470	17·98	—

(iii) Summary of Tensile Tests.

The average results of not less than 10 tensile tests per gauge thickness for (E) and (σ_p) are given in Table 5. The average value of (ν) is determined from tests on 4 specimens.

The values used in calculations presented in the test are:

Young's Modulus (E) = 4470 $T/IN.^2$

Torsion Modulus (G) = 1690 $T/IN.^2$

Poisson's Ratio (ν) = 0.32